Microarray analysis of chromosome 14 congenic strains in the SHRSP

Wendy Crawford BSc (Hons)

Submitted in fulfilment of the requirements for the degree of Master of Science (by Research)

University of Glasgow
School of Medicine

Abstract

The stroke-prone spontaneously hypertensive rat (SHRSP) is an excellent inbred model of cardiovascular disease. Previous work in our laboratory utilising chromosome 14 congenic strains confirmed a quantitative trait locus for left ventricular mass index. The aims of this project were to use gene expression profiling in the heart during the development of left ventricular hypertrophy (LVH) to identify positional candidate genes within the congenic interval. Exon analysis identified significant differential expression of Chemokine ligand 13 (*Cxcl13*) in 5 week old SHRSP, WKY and respective chromosome 14 congenic strains. After validation by qRT-PCR, DNA sequencing and Transfac analysis implicated the loss of Hepatocyte Nuclear Factor 4 in the SHRSP. Illumina analysis identified differential expression of Osteopontin (*Spp1*) in neonatal hearts of the SHRSP versus WKY and respective chromosome 14 congenic strains as a positional candidate gene. The identification of these positional genes prior to the onset of hypertension may identify novel mechanisms in the development of LVH in the SHRSP.

Table of Contents

List of Tables

List of Figures

Acknowledgements

I would like to thank Dr Martin McBride for his supervision and guidance throughout the project. Thanks also to Professor Anna Dominiczak, not only in support, but also in helping to finance the registration fees. A special thanks to Dr Delyth Graham for taking her own time to proofread the script, and Dr John McClure for his assistance in the understanding of the statistics involved.

To my mum, Ian, David, Kate, Stuart, Noelle, and also Ruth, MaryAlice and Julie-Ann, thank you so much for your support, through phone calls and visits which helped me through everything, and to stay positive throughout. I know you didn't always know what I was talking about, but you never failed to encourage me, or to keep my spirits up.

To my amazing friends Nina, Marion, Helen, Jen, Helen, Joanne, Richard, Emma, Lynn, Martin, Michael, Jenny and Monica, who have understood everytime I've missed dinner, drinks, gigs, or just been plain unsociable – at least you had Facebook to see a picture of me! Your support and friendship - as well as knowing the right time to crack open a bottle (Nina especially!) has seen me through this. A special thank you to Andy for the cups of tea, back rubs and french toast, and being so understanding and patient – now you get the benefit of me being your girlfriend!

My friends, work colleagues and office mates at the BHF who have not only provided valuable insights into the world of science, but gave such cracking support and advice too, screened phone calls, listened to my moans over drinks in the pub, and on many occasions, have kept me sane. Gregor, Willie, Carol, Debbie, Aiste, Claire, Ruth, Amanda, Laura, Lynsey, Emily, Margaret, Lynda and Carolyn, a massive thank you.

Author's Declaration

I declare that this thesis has been written entirely by myself and has not been submitted previously for a higher degree. The work recorded has been carried out by myself under the supervision of Dr Martin McBride, unless stated otherwise here. The phenotype data was collected by Dr's Delyth Graham & Kirsten Gilday. The Affymetrix exon array was executed by Dr's Klio Maratou & Tim Aitman (EuRatools). The Affymetrix microarray data was analysed by, Drs Martin McBride and John McClure and Illumina data analysed by myself and Drs Martin McBride and John McClure.

…….

Wendy Crawford

Summary

Left ventricular hypertrophy (LVH) is accepted as an important independent predictor of adverse cardiovascular outcome; the aetiology includes a number of well-recognized causes but there is considerable interest in the genetics underlying cardiac hypertrophy. The stroke-prone spontaneously hypertensive rat (SHRSP) is an excellent inbred model of cardiovascular disease. Previous work within the laboratory identified a quantitative trait locus (QTL) for left ventricular mass index (LVMI) on chromosome 14, and congenic strains (SP.WKYGla14a & WKY.SPGla14a) on both the SHRSP and WKY genetic backgrounds were constructed. SNP genotyping in the SHRSP and WKY strains confirmed the microsatellite genotyping data and identified SNP's principally to a 29Mbp region (between 5-34Mbp) on chromosome 14 confirming the LVMI QTL data. The remaining region of chromosome 14 was identical by descent in the SHRSP and WKY.

Affymetrix exon array was carried out in collaboration with Klio Maratou & Tim Aitman using RNA from the 5 week old hearts in the SHRSP, WKY and chromosome 14a congenic (SP.WKYGla14a & WKY.SPGla14a) strains. A number of analysis strategies were implemented including exon level, gene level and alternate splicing. Genome-wide analysis did not yield any significant differences across all 4 strains at the exon or the gene level analyses. However, filtering the analysis specifically to the 29Mbp minimum congenic interval of chromosome 14 identified 59 exons, representing 14 annotated genes in the exon analysis, and 2 genes (*Cxcl13* & *Abcg3*) in the gene level analysis. Furthermore alternative splicing implicated 6 genes including the *Clock* gene. The exon array identified the *Clock* gene as a potential candidate, but it was suggested that a SNP in the open reading frame had led to the difference in signal intensity in the array, as the probe was not able to hybridize to the cRNA on the chip efficiently.

Gene level analysis identified *Cxcl13* and *Abcg3* as positional candidate genes, and analysis using qRT-PCR confirmed *Cxcl13* as being differentially expressed across the 4 strains. Further analysis utilising PCR and sequencing has identified a SNP in the 5' promoter region and 2 SNP's in the 3' UTR. Transcription factor analysis of the 5' promoter region SNP implicated the loss of Hepatocyte Nuclear Factor 4 (HNF4) in the SHRSP. We extended the analysis on the Illumina

platform to include neonatal, 5 week and 16 week old parental and chromosome 14a congenic animals. This allowed for the identification of positional candidate genes, prior to the onset of hypertension and cardiac hypertrophy. Genome-wide gene expression profiling on the Illumina platform was generated using neonatal, 5 week & 16 week old animals. Focus was placed on the neonatal time point, and analysis identified 4 differentially expressed genes including Osteopontin (*Spp1*) as a positional candidate gene in neonatal hearts of the SHRSP vesus WKY and the reciprocal chromosome 14a congenic strains. This was validated by qRT-PCR, and further analysis of the gene through DNA sequencing identified 2 SNP's in the 5' promoter region and 2 SNP's in the ORF. Primer design of the poorly annotated 5' upstream region of *Spp1* in the rat was enabled by the alignment of 7 other mammalian strains to identify areas of homology.

Primary cardiomyocytes and fibroblasts were isolated for functional analysis of hypertrophy and migration/proliferation in the cells. Cardiomyocytes were identified as the source of increased expression of *Spp1*. ANG II stimulation of cardiomyocytes led to an increase in cell size in the SHRSP and WKY, but did not significantly increase *Spp1* expression levels in these strains. Migration assay implicated the WKY.SPGla14a cardiac fibroblasts as having an increased migration potential compared with WKY cardiac fibroblasts, which may indicate their role in fibrosis of the heart. The results were validated by performing an MTT assay to measure proliferation of the cells, to ensure it is migration, not proliferation which is causing this effect.

This highlights *Spp1's* potential for further work as an excellent positional candidate gene.

List of abbreviations

α-MHC	α-Myosin Heavy chain
Abcg3	ATP binding cassette gene
ACE	Angiotensin converting enzyme
ACTH	Adrenocorticotropic hormone
ADH	Anti diuretic hormone
AME	Apparent mineralocorticoid excess
ANG I	Angiotensin I
ANG II	Angiotensin II
ANP	Atrial natriuretic peptide
ATP	Adenosine triphosphate
ß-MHC	ß-Myosin Heavy chain
BCA	Bicinchoninic acid assay
BLC	B-Lymphocyte chemoattractant
BN	Brown norway
BNP	Brain natriuretic peptide
BP	Blood Pressure
cDNA	Complementary DNA
cRNA	Complementary RNA
CF	Cystic fibrosis
CK	Creatine kinase
Clock	Circadian locomotor output cycles kaput gene
CO	Cardiac Output
CHD	Coronary heart disease
CVD	Cardiovascular disease
Cxcl13	Chemokine ligand 13
DMSO	Dimethylsulphoxide
DNA	Deoxyribonucleic acid
ECG	Echocardiograph
EDTA	Ethylenediamine tetra-acetic acid
ENaC	Epithelial sodium channel
ET	Ejection time
EtOH	Ethanol
FCS	Foetal calf serum
FDR	False discovery rate
Fzd2	Frizzled-2
GRA	Glucocorticoid-remediable aldosteronism
GWAS	Genome wide association studies
HS	Heterogeneous stock
HTNB	Hypertension with Brachydactyly
HNF4	Hepatocyte nuclear factor 4

IL-6	Interleukin 6
IVCT	Isolvolumetric contraction time
IVRT	Isovolumetric relaxation time
IVT	In Vitro Transcription
LOD	Logarithm of the odds
LV	Left ventricular
LVH	Left Ventricular Hypertrophy
LVMI	Left Ventricular Mass Index
MI	Myocardial Infarction
MMP2	Matrix metalloprotease 2
MMP14	Matrix metalloprotease 14
MPI	Myocardial Perfusion Imaging
MR	Mineralocorticoid receptor
mRNA	Messenger RNA
MTAB	Minimally invasive transverse aortic banding
MTT	3-(4,5-dimethythiazol- 2-yl)-2,5-diphenyl tetrazolium bromide
MT-TI	Mitochondrial tRNA
NaCl	Sodium Chloride
NaOH	Sodium Hydroxide
NCC	Na-Cl co-transporter
ORF	Open reading frame
PBS	Phosphate buffered saline
PCA	Principal component analysis
PCR	polymerase chain reaction
PFA	Paraformaldehyde
PHA II	Pseudohypoaldosteronism type II
PTH	Parathyroid hormone
PVR	Peripheral vascular resistance
QE	Quilty effect
qRT-PCR	Quantitative real time PCR
QTL	Quantitative Trait Loci
RFLP	Restriction-fragment length polymorphisms
RA	Rheumatoid arthritis
RI	Recombinant inbred
RIN	RNA integrity number
RNA	Ribonucleic acid
RWT	Right Wall Thickness
RQ	Relative quantification
SBP	Systolic Blood Pressure
SDS	Sodium dodecyl sulphate
SHR	Spontaneously Hypertensive Rat
SHRSP	Spontaneously Hypertensive Rat Stroke Prone
SNP	Single nucleotide polymorphisms

snRNP's	Small nuclear ribonucleproteins
Spp1	Secreted phosphoprotein-1 gene
SSLP	Simple sequence length polymorphisms
SV	Stroke Volume
SVR	Systemic vascular resistance
TGF ß-1	Transforming growth factor ß-1
tRNA	Transfer RNA
TNF-α	Tumour Necrosis Factor-α
UTR	Untranslated repeat
VDRE	Vitamin D response element
WNK	With no lysine (K)
WKY	Wistar Kyoto

1 Introduction

Cardiovascular Disease

1.1 Human Cardiovascular Disease

Cardiovascular disease (CVD), also known as heart and circulatory disease, is the biggest killer in the UK, and is responsible for 38% of all deaths. It includes conditions such as coronary heart disease (CHD) - angina and heart attack, and stroke. Approximately half of all deaths from CVD in the UK are from CHD and about a quarter are from stroke, around 53,000 every year. Stroke is second only to coronary heart disease as the biggest killer in the UK and is also a major cause of premature mortality, responsible for over 9,500 deaths every year in people under the age of 75, about one in twenty of all deaths in this age group. The incidence of stroke increases rapidly with increasing age. (British Heart Foundation statistics, 2010).

1.1.1 Blood Pressure control

Blood pressure is the force which allows blood to flow through the arteries, capillaries, reaching all the organs, before returning to the heart via the veins. It is of great importance that it is finely regulated, as the blood is relied on to deliver oxygen, nutrients and hormones, all within acceptable rates, and to subsequently clear the waste products generated by body's normal processes. Blood pressure (or mean arterial blood pressure) is defined as the rate of blood flow produced by the heart (cardiac output) multiplied by the resistance of the blood vessels to blood flow (vascular resistance). This resistance is produced mainly in the arterioles and is known as the systemic vascular resistance (SVR) or the peripheral vascular resistance (PVR), hence, mean arterial blood pressure.

Mean arterial blood pressure requires a number of physiological mechanisms to maintain a normal blood pressure, which ensures an adequate perfusion to the body tissues, and incorporates a number of integrated systems within the body for this function. The main organ used is the kidney, as it regulates blood volume by controlling salt and water levels.

1.1.1.1 The renin angiotensin aldosterone system

The renin angiotensin aldosterone system is the major mechanism responsible for blood pressure control. It requires a number of hormones, and the most studied elements of this system are the angiotensin converting enzyme (ACE), and angiotensin II (ANG II). When a fall in blood pressure, or decrease in serum sodium chloride (NaCl) is detected, the juxtaglomerular cells of the kidney secrete renin. Angiotensinogen, is an inactive α-2-globulin produced by the liver, which is produced constitutively, and released into plasma circulation. It is converted to Angiotensin I (ANG I) by the cleavage of the peptide bond between the leucine and valine residue, mediated by the enzyme renin. ANG I has no other biological activity, other than to act as a precursor for ANG II. The conversion of ANG I to ANG II is mediated by ACE, which is found predominantly in the capillaries of the lung. ANG II is a vasoconstrictor which results in increased blood pressure. It also stimulates the release of aldosterone from the adrenal cortex, which leads to sodium and chloride re-absorption and water retention. It also stimulates the release of anti-diuretic hormone (argenine vasopressin ADH), a vasoconstrictor, which leads to an increase in water retention in the collecting ducts (Figure 1.1). ANG II is also involved in other mechanisms, such as decreasing medullary flow which lowers the NaCl and urea washout, facilitating increased re-absorption. It also stimulates renal hypertrophy, which leads to further sodium re-absorption (reviewed by Paul M *et al*, 2006).

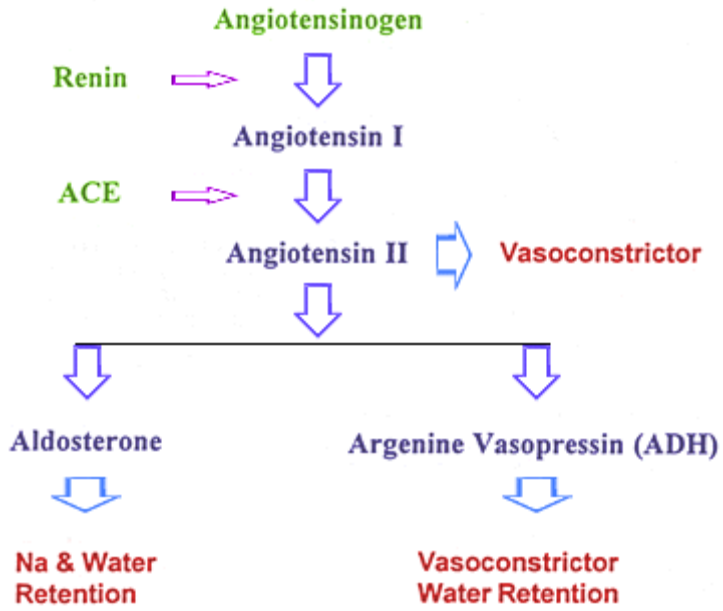

Figure 1.1 The renin angiotensin aldosterone system
The mechanism whereby blood pressure is regulated by hormones and enzymes to maintain pressure within normal physiological limits.

1.1.1.2 Other mechanisms of Blood Pressure control

The autonomic nervous system is also involved in the control of blood pressure, and is the most rapid in responding to the fall in pressure as it receives information from the baroreceptors which relays to the vasomotor centre. A fall in pressure causes the activation of the sympathetic nervous system, which leads to vasoconstriction of arteries and veins (α adrenoreceptors) and an increase in contracting of the heart (ß adrenoreceptors) (Julius S, 1993).

The capillary fluid shift mechanism is the exchange of fluid which occurs across the capillary membrane between the blood and the interstitial fluid. The fluid movement is controlled by the capillary blood pressure, the interstitial fluid pressure and the osmotic pressure of the plasma. Low blood pressure results in fluid moving from the interstitial space into the circulation in a bid to restore blood volume and blood pressure.

1.1.2 Mendelian forms of inheritance

The multifactorial nature of essential hypertension and blood pressure variation can lead to complications in understanding how many genes are involved in having an effect on the trait loci, and how they impart an influence on the

overall increase in BP. Mendelian inheritance is also known as a monogenic form of inheritance, and molecular genetics has identified rare mutations in 8 genes which cause this form of hypertension. It focuses on rare mutations in single genes which lead to a great influence on BP. The mutated gene products act on the same physiologic pathway in the kidney, affecting renal salt absorption. A form of aldosteronism which, as yet, has not had disease causing mutations identified, is also described (Geller DS *et al*. 2008).

1.1.2.1 Glucocorticoid-remediable aldosteronism

Glucocorticoid-remediable aldosteronism (GRA) is an autosomal dominant trait which displays signs of early onset hypertension with normal or elevated aldosterone levels despite suppressed plasma rennin activity (Sutherland DJ *et al*. 1996). Features of this syndrome include variations in hypokalaemia (low serum potassium levels) and metabolic acidosis (increased blood pH) (Rich GM *et al*. 1992). The defining feature of this disease is that exogenous glucocorticoids completely suppress endogenous secretion of aldosterone. Duplication in genes caused by unequal crossover brings about GRA. The genes encode for rate-limiting enzymes for aldosterone biosynthesis in the adrenal glomerulosa, aldosterone synthase (*CYP11B2*), and the enzyme involved in cortisol biosynthesis in the adrenal fasciulata, steroid 11 ß-hydroxylase (*CYP11B1*). *CYP11B1's* expression is regulated by adrenocorticotropic hormone (ACTH). The duplication leads to a chimeric gene which encodes for a protein with aldosterone synthase enzymatic activity. ACTH regulates expression of the chimeric gene in the adrenal fasciulata, rather than the normal hormonal regulator, ANG II, which leads to aldosterone secretion, and therefore artificially high aldosterone synthase activity. This results in expanded volume of plasma, which suppresses renin secretion, but does not reduce aldosterone secretion. The reabsorption of Na^+ increases K^+ and H^+ secretion, which leads to the development of hypokalaemia and metabolic acidosis.

1.1.2.2 Syndrome of apparent mineralocorticoid excess

Syndrome of apparent mineralocorticoid excess (AME) is an autosomal recessive disease which displays symptoms of early onset hypertension, coupled with hypokalaemia and metabolic acidosis. Mutations occur in the *HSD11B2* gene, which codes for 11 ß-hydroxysteroid dehydrogenase, a kidney isozyme. The isozyme converts circulating cortisol to cortisone, and as such, the mutation in this gene leads to increased levels of cortisol in the kidney. Without the protective mechanism of *HSD11B2* gene, which acts indirectly on the specific mineralocorticoid receptor (MR) for aldosterone, the excess of cortisol activates the MR, and leads to hypertension (Funder JW *et al*. 1988; Stewart PM *et al*. 1987).

1.1.2.3 Mutations in mineralocorticoid receptor – Hypertension exacerbated in pregnancy

This is an autosomal dominant form of hypertension which has been identified in pregnancy (Geller DS *et al*. 2000). It is caused by a mis-sense mutation in the MR, S810L in the ligand binding domain of MR (annotated as MR-L810). Investigation of the patient's close family shows that carriers of the MR-L810 gene all developed hypertension before the age of 20. Further investigation of this MR mutant receptor indicated partial activation when starved of steroids, and normal activation in the presence of aldosterone. Steroids such as progesterone which normally bind, but have no influence on MR, are all strong agonists on the mutant MR. Progesterone levels normally rise by about 100 fold during pregnancy, and may have an influence on patients with MR-L810 to develop severe hypertension, associated with complete suppression of the renin-angiotensin system. Molecular modeling of L810 demonstrated that the binding domain in helix 5 forms a new van der waals interaction with the A773 in helix 3, which eliminates the need for the hydroxyl group of aldosterone to interact with the N770 on helix 3. This indicates the importance of the role of this interaction in the activation of nuclear receptors (Rafestin-Oblin, ME *et al*. 2003).

1.1.2.4 Liddle syndrome

Liddle syndrome is an autosomal dominant disease, which is identified by early onset hypertension, which is characterized by hypokalaemic alkalosis, suppressed renin activity and lower levels of plasma aldosterone. The disease is caused by a mutation in either the ß or γ subunits of ENaC (epithelial sodium channel). This mutation leads to a deletion of the cytoplasmic Carboxyl termini, and displays a premature stop codon in the gene (Shimkets RA *et al*. 1994). The mutation leads to an increase in ENaC activity due to an increased number of channels at the cell surface of the distal nephrons (Snyder PM *et al*. 1995). This larger number of channels is due to a reduction in their clearance, and also a longer half-life (Shimkets RA *et al*. 1997). This leads to a volume expansion, low-renin form of hypertension.

1.1.2.5 Mutations in peroxisome proliferator-activated receptor-γ

Peroxisome proliferator-activated receptor gamma (PPARγ) is a nuclear hormone receptor which has been identified as a key regulator of adipocyte differentiation (Tontonoz P *et al*. 1994). Mutations in the gene have been found in conjunction with syndromes of insulin resistance, diabetes mellitus and hypertension (Barroso I *et al*. 1999). Thiazolidinedione is an anti-diabetic medication which improves insulin sensitivity, has hypotensive effects on BP and also reduces blood sugar levels. It is thought that this drug binds to PPARγ, and indeed, 2 mutations in the ligand binding domain leads to severe insulin resistance, diabetes mellitus and hypertension at a very young age (Barroso I *et al*. 1999).

1.1.2.6 Syndrome of hypertension, hypercholesterolaemia and hypomagnesaemia

This syndrome is manifested through mitochondrial inheritance, and is caused by a mis-sense mutation on the mitochondrial tRNA (*MT-TI*) gene. This was identified through passage of the syndrome through the maternal lineage. The

mutation leads to a cytidine residue in place of the highly conserved uridine residue, which impairs ribosome binding (Ashraf SS *et al*. 1999).

1.1.2.7 Hypertension with Brachydactyly

Hypertension with Brachydactyly (HTNB) is a severe autosomal dominant disease which is associated with short stature and shortened finger bones. It develops with age, and progresses into severe hypertension. HTNB is one of the only forms of mendelian hypertension which closely resembles essential hypertension. This is due to the responses to renin, aldosterone, and norepinephrine appearing to be normal, and no salt sensitivity (Schuster H *et al*. 1996). Studies on the autonomic nervous system revealed decreased baroreflex sensitivity with significantly impaired blood pressure buffering, which suggests that hypertension in the patients may be related to an abnormality in the baroreceptor reflex function (Jordan J *et al*. 2000).

1.1.2.8 Nonglucocorticoid-remediable Aldosteronism

This is a familial form of GRA as previously described (1.1.2.1), but differs to it in that it does not respond to glucacorticoid dexamethasone treatment. Patients may present with symptoms of bilateral adrenal hyperplasia or unilateral adenoma, and also will develop hypertension in adulthood (Stowasser M *et al*. 1992). Primary studies of a large kindred have suggested a link to chromosome 7p22. However, mutations causing the disease are yet to be identified (Jeske Y *et al*. 2008).

1.1.2.9 Pseudohypoaldosteronism type II

Pseudohypoaldosteronism type II (PHA II) is an autosomal dominant disease, also known as Gordon's Syndrome. Characteristics include familial hypertension with hyperkalaemia, a slight increase in hypercholaemic metabolic acidosis, and thiazide sensitivity, but otherwise, relatively normal renal function. WNK kinases (With No K (lysine)) are the genes responsible for PHA II. Mutations occur in *WNK1* and *WNK4*, which are normally expressed in the distal nephrons of the kidney (specifically the distal convoluted tubules and cortical collecting tubes). A deletion in the large first intron of *WNK1* (serine-threonine kinase)

causes the mutation, and has a cysteine in place of the lysine residue, leading to increased *WNK1* expression. Four mis-sense mutations cause the change in the *WNK4* gene, 3 of which are charge changing substitutions, clustered in a span of 4 amino acids (Wilson FH *et al*. 2001). The fourth mutation is also charge changing substitution. A target for the WNK kinases is the thiazide sensitive Na-Cl co-transporter (NCC), which mediates reabsorption of Na^+ with Cl^- and is expressed mainly in the distal convoluted tubule. The normal *WNK4* kinase is a negative regulator of the NCC, and PHA II *WNK4* mutations negate this inhibitory function, and lead to the physiologic effects seen in this form of hypertension. However, *WNK1* mutations prevent *WNK4*'s suppression of the NCC (Wilson FH *et al*. 2003).

1.2 Essential Hypertension

Essential Hypertension is defined as a rise in blood pressure of unknown cause, which can increase the risk of cerebral, cardiac and renal events (Carretero OA & Oparil S. 2000). In industrialised countries, it is the most common form of hypertension, affecting more than 95% of hypertensive patients. This may be influenced by both genetic and environmental factors (such as obesity, insulin resistance, high alcohol intake, high salt intake (in salt-sensitive patients), increasing age, lack of exercise, stress, low potassium intake, and low calcium intake). It is a complex polygenic disorder, which affects more than 25% of the adult population (Dominiczak AF *et al*. 2005). This has a direct impact on the health care system, due to the cost of treatments, hospital admissions and care required. A positive diagnosis is usually made when the average of 2 or more diastolic blood pressure (BP) readings is ≥90 mm Hg, or when the average of 2 or more systolic BP readings is consistently ≥140 mmHg. Although it is said to be of unknown cause, it is usually found in association with other cardiovascular risk factors, such as ageing, obesity, diabetes, high alcohol consumption, high salt consumption, stress, lack of exercising and hyperlipidaemia, which are all factors which increase BP. Early events in the course of hypertensive cardiovascular disease include subtle target-organ damage, such as left ventricular hypertrophy (LVH), microalbuminuria and cognitive dysfunction. If allowed to continue untreated for a long period, events such as stroke, heart attack, renal failure and dementia can occur (Messerli FH *et al*. 2007).

Blood pressure (BP) and hypertension show a high degree of genetic heritability (Lifton RP. 1996). The genetic contribution to the development of hypertension is complicated by many factors. BP is phenotypically determined by cardiac output and total peripheral resistance, which are in turn controlled by intermediary phenotypes, such as the autonomic nervous system, vasodepressor/vasopressor hormones, cardiovascular system structure, body fluid volume and renal function. The intermediary phenotypes add to the complexity as they are also controlled by a variety of mechanisms, including BP (Williams RR *et al*. 1994). Family studies, involving biological children, adopted children, identical and non-identical twins, and siblings show that there is a higher correlation of BP between parents and biological offspring than with adopted offspring. Identical twins show a higher correlation in BP than non-identical twins (Feinleib M *et al*. 1977). There is also a higher correlation in BP within families than between families (Longini IM *et al*. 1984). This suggests that there is a familial correlation, which results from a genetic influence on blood pressure. BP is a quantitative trait which is normally distributed in the general population, and is a significant determinant of ischemic heart disease, cerebrovascular disease, atrial fibrillation, and heart failure (MacMahon S *et al*. 1990). In the past 15 years, many genomic locations contributing to hypertension in rodent models have been mapped (Rapp JP. 2000, Dmitrieva RI *et al*. 2009).

1.3 Left Ventricular Hypertrophy

LVH is the thickening of the myocardium of the left ventricle of the heart. Ventricular hypertrophy can occur naturally as a reaction to aerobic exercise and strength training, but it is most frequently a pathological reaction to cardiovascular disease or high blood pressure. Although directly related to systolic blood pressure, other factors including age, sex, race, body mass index and stimulation of the renin-angiotensin-aldosterone and sympathetic nervous systems play an important role in the pathogenesis of LVH. Understanding of the genetic control and molecular mechanisms of LVH are relatively recent developments. It is known that ANG II is involved in the up-regulation of transforming growth factor ß1 (*TGF ß-1*) expression and the downregulation of the expression of the Wnt transmembrane receptor frizzled-2 (*Fzd2*) on smooth muscle cells which is relevant for ß-catenin signaling and other intracellular

signal transduction pathways (Berk BC *et al* 2007; Castoldi G *et al* 2005). Gene expression of matrix metalloprotease 14 (*MMP14)* was down regulated in LVH tissue. This may have an impact on blood vessel formation and capillary supply in LVH (Ridinger H *et al* 2009). Matrix metalloprotease 2 (*MMP2)* is involved in vascular remodelling of hypertrophied hearts, and is co-expressed with *MMP14* (Friehs I *et al* 2006; Seeland U *et al* 2007). Ridinger H et al have also shown that *MMP2* gene expression is down-regulated in their disease model.

LVH itself is not classified as a disease, it is a feature of hypertensive heart disease, and can be used as a marker for disease involving the heart (Messerli FH *et al*. 2007). LVH can reflect the hearts' physiological adaptation (or physiological remodelling) to the increase in workload of the heart after heavy exercise/physical training (Kahan T & Bergfeldt L. 2005). However, it can also develop as an adaptive response to an overload in pressure or volume associated with hypertension, which results in the reduction of stress in the cardiac wall (Grossman W *et al*. 1975). It is also considered to be an important predictor of the high incidence of cardiovascular complications, such as myocardial infarction (MI), congestive heart failure and cardiovascular mortality (Levy D *et al*. 1990). Following an acute MI, myocardial hypertrophy is a part of the pathological remodelling process, and is also a common finding in patients with congestive heart failure. Remodelling refers to the change in size, shape or function of the heart after an injury to the ventricles. It may also be caused by chronic hypertension and valvular heart disease. In pathological remodelling, volume overload causes ventricular dilation, where new sarcomeres are added in-series, to existing ones, which increases the overall volume of the ventricle. This is known as eccentric hypertrophy (Vinereanu D *et al*. 2002). Pressure overload leads to a substantial increase in systolic blood pressure, and the heart responds by adding new sarcomeres in-parallel to existing ones, which increases the overall wall thickness. This is known as concentric hypertrophy (Kasikcioglu E *et al*. 2004) (Figure 1.2).

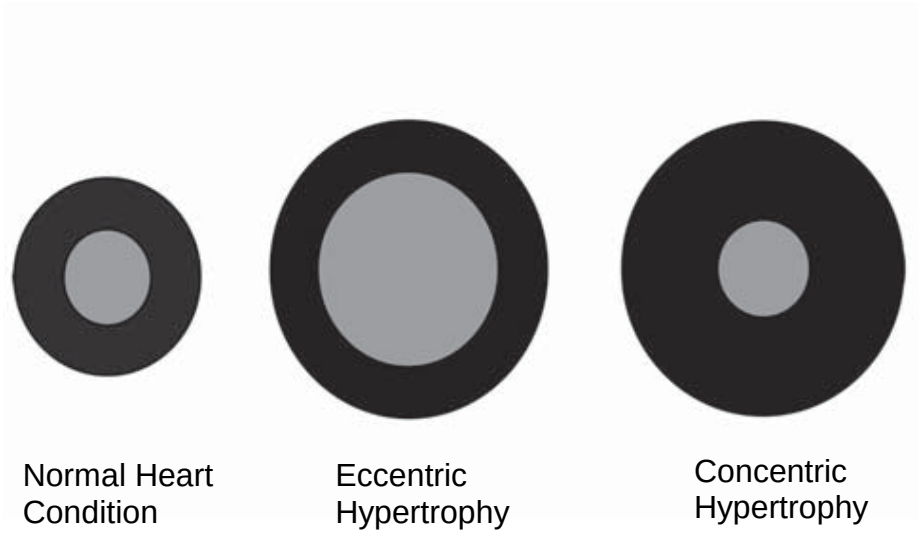

Figure 1.2 Schematic of the events involved in pathological heart remodelling
The geometric effects on the cardiac cells following the pathological events leading to hypertrophy. Blood volume overload leads to eccentric hypertrophy. Blood pressure overload leads to concentric hypertrophy.

Cardiomyocytes are the major source of remodelling in the heart, however, to a lesser extent, the fibroblasts, collagen, interstitium and coronary vessels also play a role. Dilation of the chamber arises from the infarct region. Initially, the remodelling process may be seen as beneficial, as there is improvement in LV function and cardiac output. However, over time the heart shape becomes more elliptical, and ventricular mass and volume increase, which affects cardiac function. This may eventually lead to an impairment in the heart's ability to relax between contractions.

There is also an increased risk for sudden cardiac death in subjects with LVH. In order to understand the development of LVH, the structure of the myocardium, which has three morphological compartments, is detailed as follows:

1) The muscular compartment: consists of myocytes which is the dominant cell type in a normal heart. It comprises 30% of the myocardial cells and is 70% of cardiac tissue volume;

2) The interstitial compartment, which is comprised of fibroblasts and collagen;

3) The vascular compartment, with smooth muscle and endothelial cells.

Remodelling of the myocardium, with an increase in fibrous tissue can come about following an increase in LV wall stress. This LV wall stress can stimulate

myocyte hypertrophy, collagen formation and fibroblasts. These changes will subsequently reduce LV compliance, which in turn leads to diastolic dysfunction. An increase in LV wall stress is the principal mechanical factor in the development of LV hypertrophy, and blood pressure the most powerful determinant of LV mass (Kahan T. 1998).

Recent developments in Cardiomyocyte research, involving micro-RNA's have led to, amongst others, the identification of miR-208, which is encoded by an intron of the α-Myosin Heavy Chain (*aMHC*) gene. It has been found that this cardiac specific gene is necessary for cardiomyocyte hypertrophy, fibrosis, and also expression of ß-Myosin Heavy Chain (*ßMHC*), (which is in response to stress and hyperthyroidism) (Rooji EV *et al*. 2007). miR-21 has been shown to be up-regulated through cardiac remodelling of fibroblasts. It is thought to regulate the ERK-MAP kinase signaling pathway in cardiac fibroblasts, which in turn has an impact on total cardiac structure and function, thus allowing cardiac hypertrophy and fibrosis in response to pressure overload (Thum T *et al*. 2008). However, further work on miR-21 has suggested that it doesn't have a role in cardiac remodelling, as miR-21-null mice have been identified as having similar traits of cardiac stress, hypertrophy, fibrosis, up-regulation of stress-response genes, and loss of cardiac contractility, when compared to wild-type mice (Patrick DM *et al*. 2010).

1.4 Animal Models

The use of animals as experimental models has been essential to human understanding of our own diseases. In cardiovascular disease especially, animal models allow us to study the disease in the early stages, the mechanisms of the pathogenesis, and also the effects of drug therapies (Doggrell SA. & Brown L. 1998). The ideal model should have the following characteristics:

1) The animal model should mimic the human disease;

2) Should allow studies in a chronic but stable disease;

3) Should produce symptoms which are predictable and controllable;

4) Will easily meet economical, technical and animal welfare considerations;

5) Will allow for relevant cardiac, biochemical, molecular and haemodynamic measurements to be taken.

The rat, mouse and human genomes encode for a similar number of genes. Almost all human genes have orthologues within the rat genome, and roughly 40% of the rat genome has eutherian homology with the mouse and human genome (Rat Genome Sequencing Project Consortium. 2004). This, along with the development of the rat genome sequencing, and developments in software for the analysis has allowed for translational studies to occur between humans and rats.

1.4.1 Mouse

Until recently, the mouse remained the dominant model for mammalian genetics, and was the preferred system for genetic manipulation. 90% of the mouse and human genome shows conserved regions of synteny, at the nucleotide level; about 40% of the human genome can be aligned with the mouse genome (Mouse Genome Sequencing Consortium. 2002).

A surgical method for intervention of pressure overloaded hypertrophy, which is widely used in the mouse, is aortic banding. This is an excellent model for evaluating how left ventricular hypertrophy develops in response to haemodynamic stress. With the use of this technique, a mouse model was produced which could be quickly and reproducibly banded in the transverse aorta, but which also had a low surgical morbidity and mortality. Minimally invasive transverse aortic banding (MTAB) allowed acute and chronic increase in the LV systolic pressure, increased the heart weight-to-body weight ratio, and also induced myocardial fibrosis (Hu P *et al*. 2003).

However, the mouse has several disadvantages in studies of cardiovascular disease, due to their small size and increased heart rate. A few models of spontaneous hypertension and LVH are in existence, but these have never been developed as an inbred model of human hypertension due to the need to be stimulated or surgically prepared. Although mice have been used widely in identifying structural and functional genes, these approaches cannot be utilised in finding new genetic pathways or variances which lead to hypertension.

1.4.2 Rat

The use of rats in laboratories originated in Asia, and *R. Norvegicus* was the first to be domesticated for such a purpose. Over 234 inbred strains of *R. Norvegicus* have been selectively bred, and to become 'fixed' for disease alleles for particular strains or colonies (Greenhouse DD *et al*. 1990). Because of the complexities of human essential hypertension, a large number of rats have been bred to provide an animal model of the disease (Rapp JP. 2000). The use of the Rat as a model of hypertension allows us to overcome restrictive factors, such as cost, breeding and lengthy generation time. This is essential, as these are factors which are just not feasible or ethical in human studies. Rats have many advantages over mice as models of hypertension, as physiologically they are closer to the human condition. Their larger size allows for easier handling, performance of surgical procedures, is anatomically more proportional in substructures of the organs, and taking physiological measurements. Also, many inbred models have been established for research in to other common human diseases, such as diabetes, breast cancer and cognitive behaviour. Selective breeding of specific strains of known aetiology allows production of inbred genetically homogenous models. Brother-sister mating of 20 generations is normally required to acquire a homozygous strain.

Recombinant Inbred (RI) strains provide an excellent resource for genetic mapping, which allows the opportunity to accumulate a large volume of genetic and physiological data over a period of time. RI strains provide us with the ability to study genetically identical biological replicates. This increases trait heritability by reducing environmental variance. The SHR strain has been crossed with the normotensive Brown Norway (BN) strain to generate the BXH/HXB panel of RI strains. Integrated gene expression profiling and linkage is applied, and it is found that these RI strains are a suitable genetic system for large-scale identification of positional candidates and regulatory pathways for previously mapped physiological QTLs. Comparative mapping has led to a compiled data set of candidate genes which are suitable for investigating the molecular basis of human hypertension (Hubner N *et al*. 2005).

Genetically heterogeneous stocks (HS) applied a strategy which was developed in the mouse which allows for the combination of identification and fine-mapping of QTL's in a single population in the rat (Mott R et al. 2000; Valdar W *et al*. 2006). This method exploits the recombinants which have accumulated over numerous generations of out-breeding in genetically HS, derived from inbred strains. In theory, having the HS makes genome-wide genetic association studies possible, as shown in the mouse, where 843 QTLs with an average 95% confidence interval of 2.8 Mb were identified for 97 phenotypes (Valdar W *et al*. 2006). However, for the HS to be suitable in the analysis of complex traits, it depends not only on its genetic constitution, but also on the quality and nature of the phenotypes that it can deliver (Solberg LC *et al*. 2006). The HS phenotype must correspond to that found of the standard laboratory strains, to allow for the measurement of many phenotypes on one animal, and to reduce the costs of genotyping incurred in genome wide studies. Obtaining multiple phenotypes from each animal may raise an issue of interaction between phenotypes (particularly for behavioral assays) and may limit the total amount of information that can be obtained from this stock.

Genome wide association studies (GWAS) are the study of all or most of the genes of different individuals within a species to identify variation of genes occurring within the species. The identification of the variants, genes and pathways involved in diseases could lead to potential route to new therapies, better diagnosis and improved prognosis. It is hoped that the findings from GWAS will provide this. To date, studies have been carried out in Human populations. However, The STAR consortium undertook an extensive study on the inbred laboratory rat which analysed 167 distinct strains, two recombinant inbred panels, and an F_2 intercross. They reported 20,328 single nucleotide polymorphisms (SNP's), and used the majority of them, constructed a high-density genetic map, characterizing disease, and also allowing for identification of potential QTL's. DNA from the $SHRSP_{Gla}$ and WKY_{Gla} was submitted for analysis, and identified the 5-34Mb region of chromosome 14 as having a high density of SNP's (Saar K *et al*. 2008). A major strategy for gene identification are genome wide studies, as these can lead to identification of quantitative trait loci (QTL), which is the underlying premise of the congenic breeding programme.

1.4.3 SHRSP

The spontaneously hypertensive rat (SHR) strain was developed by Okamoto and Aoki in 1963 by selective inbreeding from the WKY, and is relevant to stroke research and used widely to investigate hypertension, and its' related complications, such as LVH, stroke and renal-failure (Ginsberg MM and Busto R. 1989; Yamori Y. 1991). The WKY strain was selectively bred to produce the SHR strain. The SHRSP is a sub strain of SHR which has exceptionally high BP, and is found to be more prone to stroke than the other SHR sub strains. The SHRSP strain is derived from the A sub strain of SHR, and has been selectively bred. The B and C sub strains are stroke resistant (Takaba H *et al*. 2004). SHRSP displays the onset of spontaneous hypertension between 8-12 weeks of age, and is found to be more prevalent in males than in females, with high BP being fully established at 12 weeks of age, at approximately 180 mmHg in males and 150 mmHg in females. At the same age, WKY rats show a BP reading of 130 mmHg, found in both males and females (Davidson AO *et al*. 1995). The SHRSP shares pathophysiological similarities in hypertensive CVD between SHRSP and humans, including LVH and endothelial dysfunction.

1.5 Identification of Quantitative Trait Loci

Polygenic inheritance is the inheritance of a phenotypic characteristic which is linked to two or more genes and their interaction with the environment. Unlike the monogenic traits, polygenic traits do not follow the patterns of Mendelian inheritance. Polygenic phenotypes vary along a continuous gradient. Quantitative trait loci (QTL) refers to the stretches of DNA which are closely linked to genes which underlie a particular trait, e.g, essential hypertension, and may be used to identify the candidate genes underlying the trait. A genome wide linkage study was carried out to map QTL's, and the genome wide scan of an F2 cross between SHRSP and WKY, the QTL for LVMI was identified on chromosome 14 (Clark JS *et al*. 1996). Other QTL's of associated interest were identified on chromosome 2 and 3 (McBride MW *et al*. 2003). Chromosome 2 QTL's include systolic and diastolic BP (in both non-salt and salt-loaded animals), which is also seen in the male F_2 hybrids only. Chromosome 3 analysis indicated QTL's for pulse pressure (in both non-salt and salt-loaded animals) and systolic

and diastolic BP (salt-loaded animals only). Radiotelemetry was used to measure the phenotype haemodynamic parameters of systolic, diastolic and mean arterial pressure, heart rate and motor activity, to confirm the genotype of the strains (Davidson AO *et al*. 1995, Clark JS *et al*. 1996). The SHRSP and WKY parental strains were bred to generate heterozygous F_1 offspring. The F_1 offspring undergo brother-sister mating to give F_2 generation, which contain a random genetic compliment of the parental strains. The F_2 generation was then genotyped, using PCR amplification, with polymorphic microsatellite markers which span the genome. Phenotypic data is also collected for this generation from non-salt and salt-loaded, in both male and female rats. This data is then merged using computer software (MAPMAKER/EXP 3.0 and MAPMAKER/QTL 1.1), and the probability (which is presented as a LOD value) of for each trait is set against the genomic positions. The LOD is a statistical test in linkage analysis which compares the likelihood of obtaining the test data if the two loci are indeed linked, to the likelihood of observing the same data purely by chance. Positive LOD score favor the presence of linkage, whereas negative LOD scores indicate that linkage is less likely. By convention, a LOD score greater than 3.0 is considered evidence for linkage, and a LOD score less than -2.0 is considered evidence to exclude linkage (Figure 1.3).

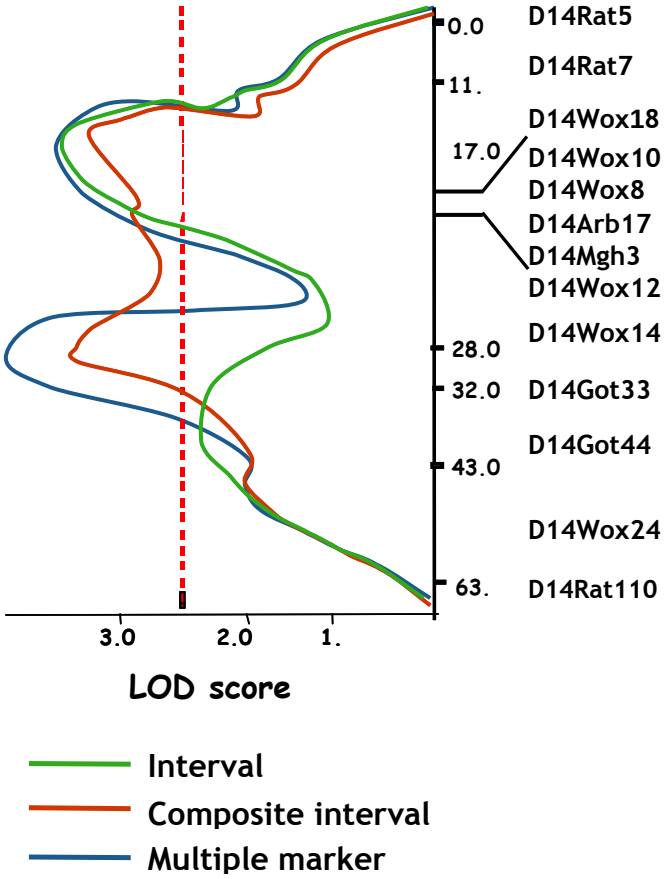

Figure 1.3 Rat chromosome 14 linkage map and LVMI localisation.
The genome wide linkage analysis shows the LOD scores in relation to the genotyping markers. Distances between the markers are shown in cM. The red broken line denotes a significant LOD threshold, determined by 10,000 permutations of the data. LVMI QTL is confirmed using simple interval mapping analysis (green line), LVMI QTL analysed using composite interval mapping (red line), LVMI QTL identified using multiple marker analysis (blue line). The QTL for LVMI is located between D14Mgh3 (marked on the linkage map) and R58 (not marked on the linkage map) markers, which are approximately 12.3 cM apart.

1.5.1 Congenic Strains

Congenic strains are constructed to confirm the existence of QTLs, and to begin narrowing the region for gene identification (Zhang QY *et al*. 1997). Congenic breeding was initiated to bring about strains of animals which receive a homologous region containing the QTL of interest, which has been selected from a donor animal which displays the quantitative trait. If the congenic interval lacks a gene (or genes), which is imperative to the genotype, then this should show a phenotypic difference between the strains. Reciprocal congenic strains have previously been constructed to identify genetic dissection of a BP QTL on chromosome 1 (Clemitson JR *et al*. 2007). There are 2 methods for the production of the congenic strain. The traditional method involves serially back-

crossing the donor strain with the recipient strain. With each back cross, the offspring are genotyped only in the region of interest until the strain has been fixed. However, this may allow for a crossover in other regions which will remain undetected. The back-crosses are performed between 8-12 times to ensure >99% of the genetic background from the donor strain has been replaced by the recipient. The second method, "Speed congenics" is applied by using a marker-directed breeding programme in conjunction with genetic linkage maps, to achieve the congenic strain in 3-4 generations (Jeffs B *et al*. 2000). After the fourth backcross generation, <1% of contamination is predicted (Figure 1.4). The polymorphic markers used to screen the region of interest, and also the entire background of the genome, and are spaced approximately 25 cM apart. The males are genotyped, and the best males are chosen with the least heterozygosity in the background to continue the speed congenic breeding.

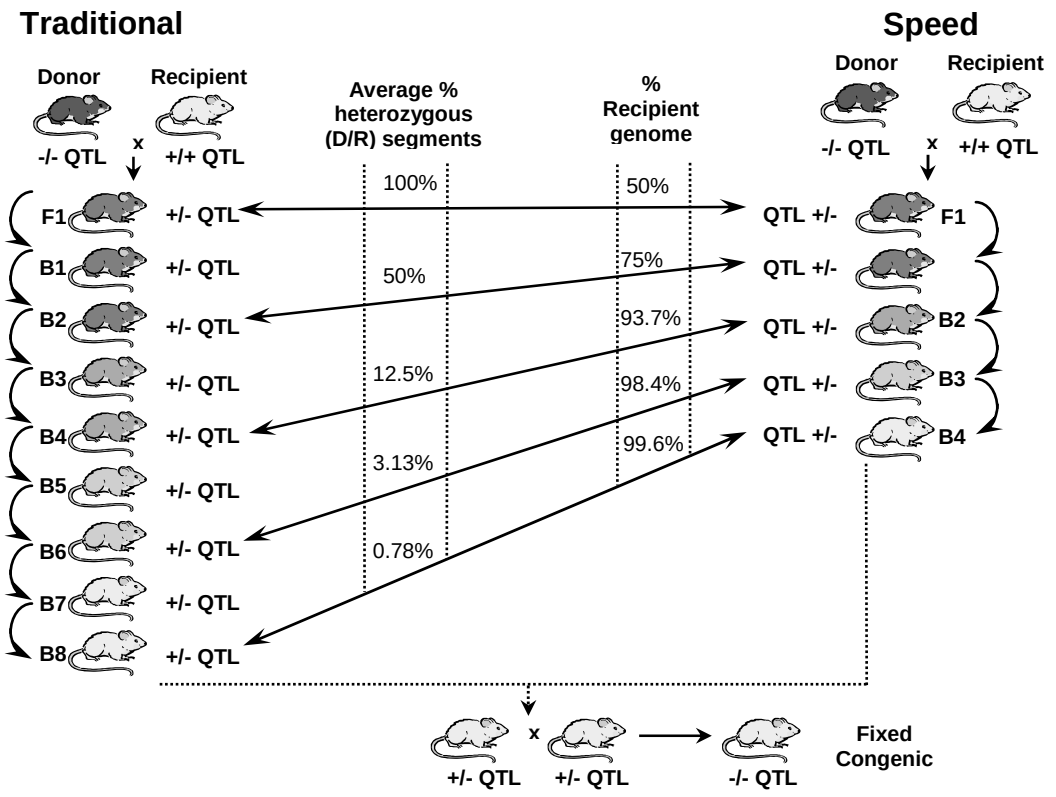

Figure 1.4 Traditional breeding v Speed congenics
The change in shading, from grey to white represents the increasing dilution of the donor genome in the genetic background. F = first filial generation, B = backcross.

1.6 Chromosome 14a

The chromosome 14a congenic strain has been generated to identify and confirm the quantitative trait loci (QTL) for Left Ventricular Mass Index (LVMI), which can be regarded as an indicator for LVH, and is a clinically important marker of cardiovascular disease (Antoniucci D *et al*. 1997). The chromosome 14a congenic breeding strategy introgressed segments of spontaneously hypertensive rat stroke prone (SHRSP) strain onto a Wistar Kyoto (WKY) background, to give the WKY.SPGla14a strain, and WKY strain onto the SHRSP background to give the SP.WKYGla14a strain (Figure 1.5). The strains were confirmed through genotyping.

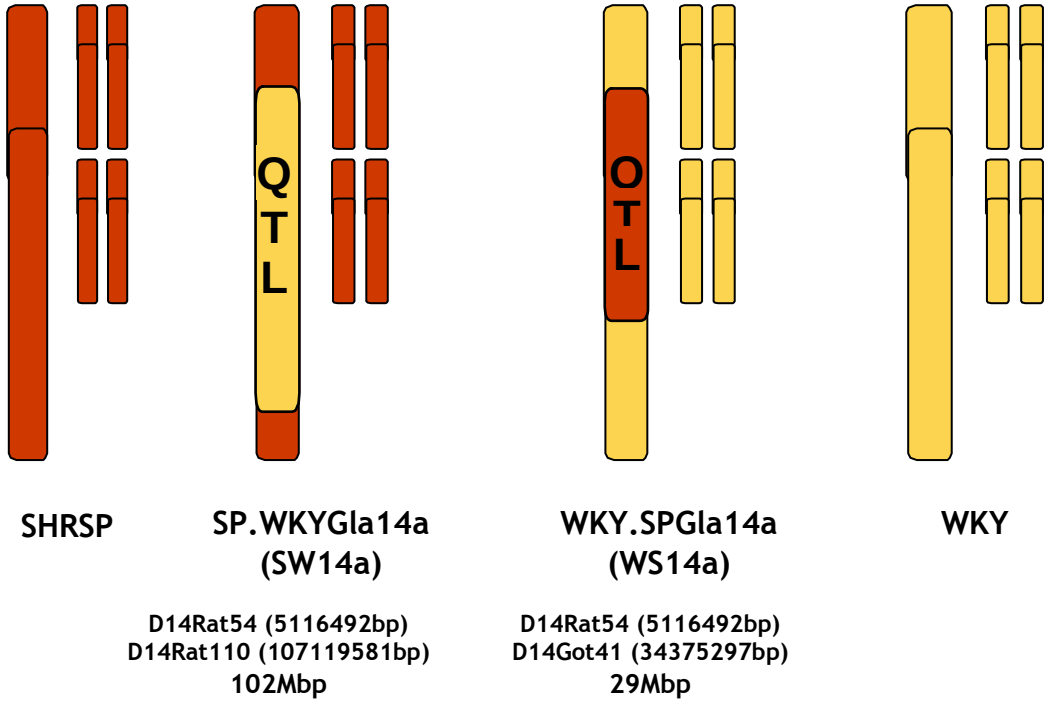

Figure 1.5 Schematic of the SHRSP, WKY and the chromosome 14 congenic strains using microsatellite markers.
Shows the positioning and size of the congenic region of the chromosome 14a congenic strains. The genotyping markers used indicate the location of the crossover regions, integrating WKY onto SHRSP background to give SP.WKYGla14a strain, and integrating SHRSP onto WKY background to give WKY.SPGla14a strain.

1.6.1 Phenotype data

A variety of echocardiographic techniques were carried out in parental and congenic rats at 5 week and 16 week time points which measured LVMI and

systolic BP, and were analysed by comparing between the parental strains (SHRSP and WKY) and their congenic strain. Echocardiograph (ECG) is a useful method to use, as it provides results in a non-invasive manner, allowing longditudinal studies in the same animal. LVMI is significantly increased in the WKY.SPgla14a at both the 5 and 16 week time point, compared to WKY, and is significantly decreased in the SP.WKYgla14a at both the 5 and 16 week time point, compared to SHRSP (Figure 1.6A). This result confirms the capture of the LVMI QTL in both congenic strains.

The systolic BP measurements were obtained using the radiotelemetry method, over a period of weeks. The same rats were used from the strains along the time course of data collection, and this allows the change in BP readings to be observed. The SHRSP and the SP.WKYGla14a strains both display hypertensive systolic measurements. The WKY and WKY.SPGla14a strains both show normotensive systolic measurements. However, there is a significant difference between the strains, which suggests the WKY.SPGla14a strain is showing SHRSP qualities in BP control (Figure 1.6B). This also indicates BP independent cardiac hypertrophy events are occurring.

The myocardial performance index (MPI) was used to assess LV function. It relies on the pulse wave Doppler measurements taken throughout specific parts of systole and diastole of the beating process. Consecutive beats are measured and then averaged to assess each parameter. The timed intervals are measured from the mitral inflow and LV outflow velocity time intervals. Isovolumetric relaxation time (IVRT) is classified as the interval between mitral valve closing and opening. Isovolumetric contraction time (IVCT) is classified as the time during early systole when the ventricles contract, with no corresponding change in volume. MPI is significantly reduced in the WKY when compared with WKY.SPgla14a at both 5 and 16 week time points. MPI is significantly reduced in the SP.WKYgla14a when compared with SHRSP at both 5 and 16 week time points (Figure 1.6C & D). This result confirms that there is correlation between LV function in the strains, and the confirmation of the LVMI QTL. This is important as it justifies the effort to identify the genes underlying LVMI through the construction of the congenic strains.

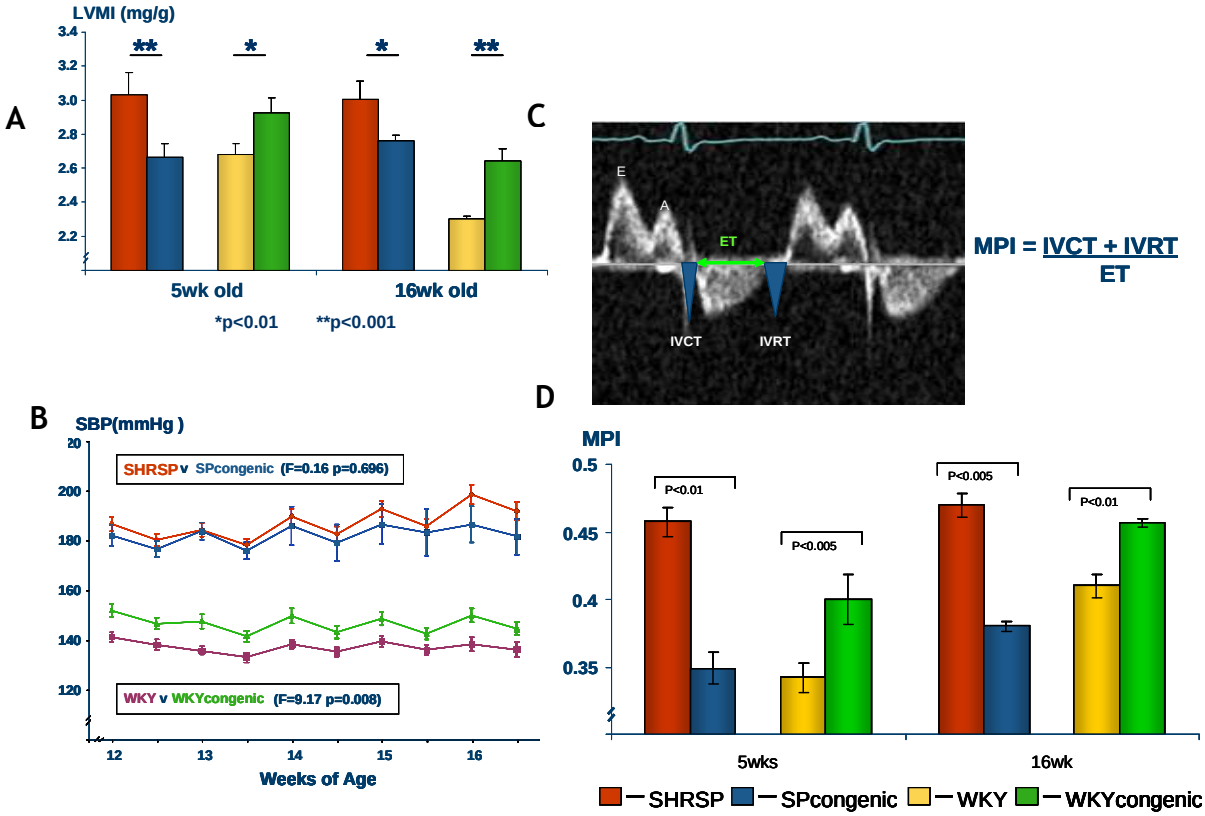

Figure 1.6 Graph showing the ECG measurements in SHRSP, WKY, SP.WKYGla14a and WKY.SPGla14a at 5 and 16 weeks of age.

The graph shows significant difference in the LVMI (mg/g), when comparing the SHRSP with the SP.WKYGla14a congenic strain, and the WKY with the WKY.SPGla14a congenic strain at both time points (Figure 1.6A). The line graph shows the BP measurements, taken over a time period (Figure 1.6B). The picture shows MPI output, as measured using the Doppler pulse wave method, by IVCT, IVRT and ET (Figure 1.6C). The graph shows statistical difference in MPI, when comparing the SHRSP with the SP.WKYGla14a congenic strain, and when comparing the WKY with the WKY.SPGla14a congenic strain at both time points (Figure 1.6 D).

Objectives

Previous work involved the generation of chromosome 14 congenic strains in both the SHRSP and WKY genetic backgrounds confirming the QTL for left ventricular mass index in the SHRSP. Using a combination of congenic strains and microarray gene expression profiling the aim of this work was to identify and validate positional candidate genes within the transferred congenic interval.

Aims

- To use Affymetrix exon array to identify differentially expressed genes in hearts isolated from 5 week old SHRSP, SP.WKYGla14a, WKY.SPGla14 and WKY animals. The analysis will focus specifically on the minimally transferred congenic interval (29Mbp).

- To extend this analysis in all four strains using Illumina genome-wide expression profiling in neonatal, 5 week and 16 week old animals. This analysis will prioritise the neonatal time point prior to the onset of hypertension and cardiac hypertrophy in the SHRSP.

- To validate selected positional candidate genes and identify putative causative SNP's in the regulatory and coding regions of the target genes.

- To investigate the functional role of cardiomyocytes and fibroblasts in hypertrophy and fibrosis in the WKY and WKY.SPGla14a strains.

2. Materials and methods

2.1 General Laboratory Practice

This chapter outlines general laboratory practises and laboratory methods that are common to more than one chapter. Laboratory equipment and reagents were of the highest commercially available grades. A laboratory coat and latex or non-latex powder-free gloves were worn during all procedures. Hazardous reagents were handled appropriately as described in the Control of Substances Hazardous to Health regulations, using laboratory spectacles or facemask and/or a fume hood where appropriate.

Laboratory glassware was cleaned in Decon 75 detergent, rinsed with distilled water and dried in a 37°C cabinet. Otherwise, sterile disposable plastic ware was used, including 0.5 ml, 1.5 ml and 2 ml microcentrifuge tubes (Greiner Bio-one) 15 ml and 50 ml Corning centrifuge tubes and 5 ml and 20 ml 'Universal' containers (Sterilin). Reagents were weighed using an Ohaus Portable Advanced balance (sensitive to 0.01 g), or a Mettler HK160 balance (sensitive to 0.0001 g). Solutions were pH'd using a Mettler Toledo digital pH meter calibrated with pH 4.0, 7.0 and 10.0 standards (Sigma). Volumes from 0.1 µl to 1,000 µl were dispensed with Gilson Medical Instruments pipettes. Volumes from 1 ml to 25 ml were measured with sterile disposable pipettes (Corning) and a Gilson battery-powered pippetting aid. Autoclaved distilled water was used to prepare aqueous solutions unless stated otherwise, a Jenway 1000 hotplate/stirrer was used to aid dissolving and mixing. Vortexing was carried out using an FSA Laboratory Supplies WhirliMixer. Centrifugation for samples up to 2 ml was performed at 4-20°C in an Eppendorf 4515 microcentrifuge, larger samples were centrifuged in a Sigma 4K15, compatible with 15 ml and 50 ml centrifuge tubes, 20 ml 'Universal' tubes and with carriers for standard reaction plates. Laboratory-ware or liquids requiring sterilisation were autoclaved in a Priorclave Tactrol 2. A Julabo TW8 water bath was used for experiments requiring incubations from 37°C to 90°C, a Grant SBB14 boiling water bath was used for temperatures up to 100°C.

Certified Nuclease-free reagents and plastic ware was used for experiments involving RNA, including Ambion RNase-free microcentrifuge tubes, RAININ nuclease-free filtered pipette tips and Ambion nuclease-free H_2O. Pipettes and benches were wiped with Ambion RNaseZap reagent before all RNA experiments.

2.2 General Techniques

2.2.1 Nucleic Acid Extraction

Genomic DNA was extracted using the Nucleon® Genomic DNA Extraction Kit (SL 8508). 250 mg of tissue was weighed and homogenized in 2.5 ml of Reagent A with a Polytron 2100 rotor homogeniser at 30,000rpm. The homogenate was centrifuged at 1300g for 10 minutes at room temperature. The supernatant was aspirated, and the pellet was re-suspended in 1.5 ml of Reagent B. 150µl of sodium perchlorate 70% (v/v) was added, and the suspension was inverted 7 times. 500µl of chloroform was added, and the suspension was inverted 7 times. 150µl of Nucleon resin was added, and the suspension was placed on a rotary mixer for 5 minutes, and centrifuged at 350g for 1 minute at room temperature. The upper phase was transferred to a clean microcentrifuge tube, and 2 volumes of cold EtOH 100% was added, and inverted to precipitate the DNA. The precipitate/EtOH mix was then centrifuged at 13,200rpm for 5 minutes at room temperature, and the supernatant discarded. 1 ml of cold EtOH 70% (v/v) was added, and inverted several times to wash the pellet, and then centrifuged at 13,200rpm for 5 minutes at room temperature. The supernatant was discarded and the pellet allowed to air dry for 10 minutes at room temperature. 100µl of distilled water was added, and the DNA was allowed to re-suspend overnight. The DNA was then vortexed until the pellet broke down.

Qiagen column and filter-based miRNeasy kit (217004) was used for RNA extraction. Whole tissues or cells were homogenised in Qiazol (700µl/50 mg Tissue or $1x10^7$ cells). Cultured cells were rinsed with PBS and homogenised by scraping with an RNase free pipette tip, and pipetted up and down to allow Qiazol digestion of the cells. Tissues were homogenised with a Polytron 2100 rotor homogeniser at 30,000rpm. The homogenized tissue and cells lysates were divided into 700µl aliquots, and the excess may be stored at -80°C for up to 6 months. The homogenate was placed at room temperature for 5 minutes, and following that, 140µl of chloroform was added and shaken vigorously for 15 seconds. The homogenate was placed at room temperature for 5 minutes, then centrifuged for 15 minutes at 12,000g at 4°C. The upper phase was transferred to a clean 1.5 ml RNase free tube, and 1.5 volumes of EtOH 100% (Sigma 200 proof) was added and mixed thoroughly by pipetting up and down. 700µl of the

sample was applied to an RNeasy mini spin column placed in a 2 ml collection tube, and centrifuged at 8000g for 15 seconds at room temperature. The flow through was discarded. 700µl of Buffer RWT (supplied with the kit, and adjusted to volume with EtOH 100% (Sigma 200 proof)) was applied to wash the column, and was centrifuged at 8000g for 15 seconds at room temperature. The flow through was discarded. 500µl of Buffer RPE (supplied with the kit, and adjusted to volume with 100% EtOH (Sigma 200 proof)) was applied to wash the column, and was centrifuged at 8000g for 15 seconds at room temperature. The flow through was discarded. 500µl of Buffer RPE (supplied with the kit, and adjusted to volume with EtOH 100% (Sigma 200 proof)) was applied to wash the column, and was centrifuged at 8000g for 2 minutes at room temperature. The flow through was discarded. The RNeasy mini spin column was placed in a fresh 2 ml collection tube, and centrifuged at 13,200rpm for 1 minute to eliminate the possibility of carryover of Buffer RPE. The RNeasy mini spin column was placed in a fresh 1.5 ml collection tube, 40µl of RNase-free water was applied directly to the column and centrifuged at 8000g for 1 minute at room temperature. For tissue lysates, the 40µl of elute was re-applied to the column and centrifuged at 8000g for 1 minute at room temperature. For tissue lysates with an expected higher yield of RNA, a further 40µl of RNase-free water was applied directly to the column and centrifuged at 8000g for 1 minute at room temperature.

The TURBO DNA-free protocol (AM1907) was carried out on RNA derived from tissues, to remove contaminating DNA from RNA preparations, and to subsequently remove DNase from the samples. TURBO DNase has a high affinity for DNA and is effective at removing trace amounts of this contaminant. Routine DNase treatment of samples containing <200µl, 4µl of TURBO DNase buffer and 1µl TURBO DNase was added to 44µl of RNA in an RNase-free microcentrifuge tube, and incubated at 37°C for 30 minutes. 5µl of DNase Inactivation reagent was added, and the mixture was flicked for 2 minutes, and then centrifuged at 10,000g for 1.5 minutes at room temperature. The supernatant containing the TURBO DNase-free RNA was transferred to a clean RNase-free microcentrifuge tube.

The RNase-Free DNase set (Qiagen 79254) on column DNase digestion was carried out on RNA derived from cells. This protocol was undertaken during the RNA extraction protocol as an insert to it. At the stage of adding 700µl buffer RWT,

the protocol diverted to the digestion ptotocol, and continued as follows. 350µl buffer RWT was applied to wash the column, and was centrifuged at 8000g for 15 seconds at room temperature. 10 µl DNase I stock solution was added to 70µl Buffer RDD, mixed gently by inverting and applied to the RNeasy mini spin column. The RNeasy mini spin column was incubated for 15 minutes at room temperature. 350µl buffer RWT was applied to wash the column, and was centrifuged at 8000g for 15 seconds at room temperature. The miRNeasy kit RNA extraction protocol was then re-joined at the point of the first application of 500µl of Buffer RPE.

2.2.2 Measuring Nucleic Acid Concentration

DNA and RNA concentrations were measured using a Nanodrop ND-1000, a spectrophotometer that is sensitive from 2-37000 ng/µl double-stranded DNA. Absorbance at 260nm were used for quantification of nucleic acids, optical density of 1 corresponding to 50ng/µl DNA and 40ng/µl RNA. Absorbance ratios (260 nm/280 nm) of approximately 1.8 for DNA and 2.0 for RNA indicated that the nucleic acid preparations were sufficiently free from protein contamination for downstream experiments. Averages of duplicate or triplicate readings were taken for samples requiring very precise quantification.

2.2.3 Polymerase Chain Reaction

All thermal cycling for standard PCRs was performed on an MJ Research PTC Gradient Cycler in 96-well plates (ABgene). PCR primers were designed using the online design tool Primer3 (Rozen et al. 2000) and purchased from MWG Biotech.

The Taq DNA polymerases used in the above PCR systems have fast processivity, but lack a proofreading capability, they are suitable for a majority of PCR applications but incorporate incorrect nucleotides approximately every 10,000 nucleotides. For applications where absolute fidelity of DNA replication was required, for example for cloning promoter or cDNA sequences, 'Kod Hot Start' DNA polymerase (Novagen) was used. Kod DNA polymerase is derived from *Thermococcus kodakaraensis* thermophilic bacteria and possesses 3'-5' exonuclease activity that excises mis-incorporated bases during PCR. Kod PCRs

were performed according to the manufacturers instructions, reaction mixtures and temperature cycling parameters were as follows:

Reaction mix		**Heat Cycling**		
	Vol. (µl)			
10x PCR buffer	2.5	94°C	2 min	
dNTPs (1mM)	2.5	94°C	15 sec	x35
$MgSO_4$ (25mM)	1.0	58-62°C	30 sec	
Fwd primer (5pmol/µl)	1.5	68°C	2.5 min	
Rvs primer (5pmol/µl)	1.5	68°C	10 min	
DNA	1.0-5.0			
Kod (1U/µl)	0.5			
H_2O	Up to 25ul			

2.2.4 Agarose Gel Electrophoresis

Unless otherwise stated 1% (w/v) agarose (Eurogentec) gels were used throughout, dissolved and electrophoresed in 1 X Tris-Borate EDTA (TBE) buffer (Fisher Bioreagents). Gels were electrophoresed at 6 V per cm of gel. BIO-RAD Power Pac 300 and BIO-RAD electrophoresis tanks were used, 1 ng / 100ml ethidium bromide (Sigma) was added to molten agarose before pouring gels, unless stated otherwise. Gels were visualised by UV transillumination on a BIO-RAD Fluor-S MultiImager. Promega 100bp or 1kb DNA ladders were used for sizing products. Samples were loaded with 6 X loading dye (50% glycerol, 0.05% bromophenol blue).

2.3 Tissue Culture

Primary Cardiomyocyte and Fibroblast cells were handled under sterile conditions using class II biological safety cabinets (Holten Safe 2010). Cabinets were cleaned before and after use with distilled water and 70% (v/v) ethanol. Waste plastics and fluid were decontaminated by steeping for 24hr in 10% (v/v) bleach, plastics were then incinerated and fluids were poured into domestic waste drains. Cells were maintained in 75 cm^2 tissue culture flasks with vented caps (Corning) in inCusafe 37°C, 5% carbon dioxide (CO_2) incubators. Tissue culture experiments involving primary cells were performed in a dedicated biological safety cabinet and maintained in separate incubators.

2.3.1 Cell Passage and Cryostorage

Cells were passaged regularly to prevent overcrowding in culture flasks, experiments were performed with cells of lowest possible passage number and experiments were completed in as few passages as possible. Unless stated otherwise, passaging was performed by removing culture media and rinsing cells gently twice with 7ml sterile PBS (Lonza) before detaching them from the flask with 2-10 minutes incubation at 37°C with 2ml 1X TE (0.05% trypsin (w/v); 0.2% (w/v) ethylenediamine tetraacetic acid (EDTA)). Cells were washed with 5 ml foetal calf-serum (FCS)-containing medium, which inactivates the trypsin, aspirated into a 20ml 'Universal' container, and centrifuged at 1500 rpm for 5 minutes. Media/TE was poured off and the cell pellets were re-suspended in cell media, fresh 75 cm^2 flasks with 13ml media were seeded with 1/3 of the cells from the previous passage.

For cyrostorage, cells from 3 x 75 cm^2 flasks were re-suspended in 6ml media/10% (v/v) dimethylsulphoxide (DMSO) and divide into aliquots into 4 x 2 ml cryovials. The cryovials were placed in an isopropanol freezing container (Nalgene) in a -80°C freezer overnight, ensuring freezing no faster than 1°C per minute. The next day cells were transferred for long-term storage in liquid nitrogen. When recovering cells from liquid nitrogen they were thawed to room temperature and pipetted into 13ml media in a fresh 75 cm^2 flask, the media

was changed the next day, cells were not used for experiments until at least two passages and a week out of liquid nitrogen.

2.3.2 Cell Counting

In order to accurately seed cell culture flasks and plates with a known number of cells, cells were counted with a haemocytometer (Hausser Scientific). Approximately 10µl of a cell suspension was pipetted under a cover slip onto the grid, the number of cells in each 1 mm square was recorded by counting the cells in each 0.25 mm squares, cell crossing the bottom or right-hand edge of any square were not counted. The average number of cells in each 1 mm square was derived, was multiplied by 10^4 to give the number of cells per ml in the suspension. Dilutions of the cell suspension were made in media to seed the correct number of cells per flask or well.

2.4 DNA Sequencing

Unless otherwise stated, DNA sequencing was performed by purifying PCR products to remove un-incorporated dNTPs, primers and salts, followed by dideoxy sequencing reactions, and a second purification step before capillary electrophoresis to separate sequencing products by size. Each step is outlined below.

2.4.1 PCR Clean-up

PCR products were retained in PCR reaction plates and purified for sequencing using the Agencourt AMPure kit. This relies on binding of DNA products over 100bp in length to paramagnetic beads in the kit solution (i.e. they are attracted to magnets but do not exhibit magnetism themselves). 36µl of AMPure was added to each 20µl PCR reaction, the plates were briefly vortexed and centrifuged to 1000 rpm for 1 second to collect the liquid to the bottom of the wells. They were left to stand for 5 minutes and then placed onto a SPRI Plate (solid phase reversible immobilisation plate) magnetic plate holder (Agencourt) for 10 minutes. The SPRI Plate has an individual ring magnet for each well in a 96-well plate, AMPure beads are held onto the sides of the wells of the 96-well

plate. Keeping the PCR plate on the SPRIPlate, the PCR reaction constituents were removed by inverting the plates and shaking forcefully upside-down. The beads were then washed with 200µl of freshly prepared 70% (v/v) ethanol for 30 seconds before shaking forcefully upside-down and centrifuging upside-down to 600rpm for 1 second to remove as much ethanol as possible. PCR Plates were removed from the SPRI Plate and left to air-dry for 20 minutes before the addition of 40µl H_2O per well. The PCR plates were vortexed to re-suspend the AMPure beads, then returned to SPRI Plates plates, 8µl was carefully pipetted out per sequencing reaction. If a PCR product was to be sequenced more than 3 times, multiple 20µl PCRs were performed.

2.4.2 Dideoxy Sequencing

Applied Biosystems BigDye Terminator n3.1 Cycle Sequencing kits were used all for sequencing reactions in this project, reactions were performed in 96-well plates. Unless stated otherwise all sequencing reactions included 3.5µl 5X sequencing buffer; 0.5µl Ready Reaction; 8µl template (purified PCR product); 3.2µl primer (1pmol/µl); 4.8µl H_2O. The temperature cycling program was:

1) 96°C 45 sec

2) 50°C 25 sec

3) 60°C 4 min

Repeat steps 1)-2) x25

2.4.3 Sequencing Reaction Purification

Sequencing reactions were purified to remove reaction constituents and unincorporated nucleotides and primers prior to electrophoresis using Agencourt CleanSEQ reagent. 10µl of CleanSEQ reagent was added to each sequencing reaction, followed by 62µl of freshly prepared 85% (v/v) ethanol. Plates were briefly vortexed and centrifuged to 1000 rpm for 1 second to collect the liquid to the bottom of the wells, then placed on an SPRIPlate for 3 minutes. Wells were emptied by forcefully shaking the plates upside-down, the CleanSEQ beads were

washed twice with 100 µl 85% (v/v) ethanol for 30 seconds each, emptying the wells between washes. Wells were then emptied as much as possible by centrifugation of inverted plates to 600 rpm for one second. Plates were removed from the SPRIPlates and air dried for 20 minutes, 40 µl of H_2O was added to each well and CleanSEQ beads were resuspended by vortexing. Plates were briefly centrifuged to 1000 rpm for 1 second and returned to SPRIPlates. 20 µl of sequencing products were loaded into optically clear barcoded 96 well plates. H_2O was added to unused wells to prevent drying of capillaries and plates were covered with Applied Biosystems Septa Seals, which prevented the evaporation of products but also allowed the capillaries to enter wells.

2.4.4 Capillary Electrophoresis

Sequencing capillary electrophoresis was performed on a 48-capillary Applied Biosystems 3730 Genetic Analyser with 36 cm capillaries. Electrophoresis was preceded by filling the capillaries with fresh POP-7 polymer (Applied Biosystems) and warming the capillaries to 60°C. Sequencing products were separated by size by electrophoresis at 8500 volts for 50 minutes.

2.4.5 Sequencing Analysis

Sequencing was analysed using Applied Biosystems SeqScape software version 2.1 Experimental sequences were aligned with known sequences derived from bioinformatic databases such as UCSC or ENSEMBL genome browsers or product information such as plasmid sequences.

2.5 DNA Cloning

Eukaryotic expression vectors were employed in this project in the promoter region studies, for the generation of recombinant DNA products of expression cassettes for future studies from blunt ended PCR products generated using KOD polymerase.

The StrataClone blunt PCR cloning technology uses the combined activities of topoisomerase I, from *Vaccinia* virus and Cre recombinase, from bacteriophage P1. *In vivo*, DNA topoisomerase I assists in DNA replication by relaxing and

rejoining DNA strands, then cleaving the phosphodiester backbone of a DNA strand after the sequence 5´-CCCTT, which forms a covalent DNA–enzyme intermediate which conserves bond energy to be used for re-ligating the cleaved DNA back to the original strand. The Cre recombinase enzyme catalyzes recombination between two *loxP* recognition sequences. The StrataClone blunt PCR cloning vector mix contains two blunt-ended DNA arms, of which one is charged with topoisomerase I, and the other contains a *loxP* recognition sequence on the other end. Blunt-ended PCR products produced by proofreading KOD polymerase are then ligated into the vector arms. The linear molecule (vector arm_{ori}–PCR product–vector $arm_{amp/kan}$) is transformed into a competent cell line which expresses Cre recombinase, which allows recombination between the vector *loxP* sites, creating a circular DNA molecule (pSC-B-amp/kan) which replicates in cells growing on media containing ampicillin or kanamycin. The pSC-B-amp/kan vector product includes a *lacZ* α-complementation cassette which allows for blue-white colony screening.

2.5.1 Transformation of Competent Bacteria

StrataClone SoloPack Competent Cells provided with the StrataClone Blunt PCR Cloning Kit (#240207) were used as hosts for eukaryotic expression vectors throughout this project. The PCR product was first ligated into the vector. The cloning mixture of 3 µl of StrataClone Blunt Cloning Buffer, 2 µl of PCR product (diluted 1:10) and 1 µl StrataClone Blunt Vector Mix amp/kan was combined, mixed by gentle pipetting, and incubated at room temperature for 5 minutes, then placed on ice. For transformation, one tube of competent cells per reaction was thawed on ice. 1 µl of the cloning mixture was added to the thawed competent cells, and mixed gently, and incubated on ice for 20 minutes, then 'heat shocked' at 42°C for 45 seconds before returning to ice for a further 2 mintues. 250 µl of pre-warmed SOC medium (Sigma) was added to the cells and they were placed in a shaking incubator (New Brunswick Scientific Inova 44) at 37°C, 180 oscillations per minute, for one hour. Unless otherwise stated all plasmids used in this project encoded ampicillin resistance for selection of transformed cells. 90 mm culture plates (Sterilin) of Luria agar (Sigma) containing 100 µg/ml ampicillin (Sigma) were spread with 40 µl of 2% (w/v) X-gal to allow for blue/white colony screening, and allowed to dry for 1 hour. 50 µl of

the transformation mixture were spread onto each of the Luria –amp/X-gal plates. Culture plates were inverted and placed in a 37°C incubator (Heraeus) overnight. Plates were checked for bacterial colonies the next morning, and white colonies were selected to be streaked on a Luria agar plate containing 100 µg/ml ampicillin, to allow for DNA expansion. The DNA from the colonies was then screened for positive clones through PCR. Primers specific to the vector were designed and used to amplify the insert region. These PCR products can then be sequenced as described in (2.4)

2.5.2 Glycerol Stocks

Successfully transformed bacteria were preserved for long-term storage by preparing glycerol stocks. 500ul of overnight broth cultures was mixed with 500ul sterile autoclaved glycerol, to give 50% (v/v) concentrations and frozen at -80°C. Bacteria were recovered from glycerol stocks by streaking for single colonies on selective agar.

2.5.3 Plasmid DNA Purification

Plasmid DNA was extracted from bacteria using the filter column based Qiagen Plasmid Midi kit. Bacterial cultures were streaked and grown overnight at 37°C on ampicillin Luria agar plates. Single colonies were picked and used to innoculate a 'starter' culture grown throughout the next day in 5 ml Luria broth (Sigma), containing 100 µg/ml ampicillin, in a shaking incubator at 37°C. 50 µl of this culture was used to inoculate 25 ml 100 µg/ml ampicillin Luria broth to produce an overnight culture from which the plasmid was extracted (25 ml was sufficient for most plasmids, however when low yields were obtained, the extraction was repeated with 100 ml culture). Bacteria were harvested by centrifugation at 6,000 g for 15 minutes at 4°C in a Beckman Coulter Avanti J-26XP. Culture media was poured off and the bacteria were re-suspended in 4 ml buffer P1 (50mM 2-amino-2-hydroxymethyl-1,3-propanediol, pH8; 10 mM EDTA, 100 µg/ml RNase A). 4 ml buffer P2 (200 mM NaOH; 1% sodium dodecyl sulphate (SDS)) was added and the solutions were kept on ice for five minutes. 4 ml chilled buffer P3 (3 M potassium acetate at pH5.5) was added to neutralise the lysate. The precipitated lysates were centrifuged at 20,000g at 4°C for 30

minutes, the supernatant was retained and centrifuged again at the same speed for a further 15 minutes. Columns were pre-wetted with 4 ml buffer QBT (750 mM NaCl; 50 mM 3-morpholinopropanesulfonic acid pH7 (MOPS); 15% (v/v) isopropanol; 0.15% (v/v) Triton-X 100). The supernatant was applied and the columns were allowed to empty by gravity flow, the columns were washed twice with 10 ml buffer QC (1 M NaCl; 50 mM MOPS pH7; 15% (v/v) isopropanol), and the plasmid DNA was eluted with 5 ml buffer QF (1.25 M NaCl; 50 mM Tris pH8.5; 15% (v/v) isopropanol) into polypropylene centrifuge tubes. Plasmid DNA was precipitated with 3.5 ml isopropanol and centrifuged at 15,000g for 30 minutes at 4°C. The supernatant was carefully poured off, and the pellets were resuspended in 2 ml 70% (v/v) ethanol and divided into aliquots into two 1.5 ml microfuge tubes. They were centrifuged at 16,200g for 10 minutes at 4°C. The ethanol was carefully pipetted off and the pellets were thoroughly air-dried (10-20 minutes) before re-suspending the DNA in 20 µl H_2O per tube and pooling the contents of the two tubes. Total plasmid yields were typically 50-90% of the maximum yield quoted for the maxi columns (500 µg).

2.5.4 Agarose Gel DNA Extraction

Unless stated otherwise agarose gel extraction of PCR products was performed with the Qiagen QIAquick Gel Extraction kit following the manufacturer's instructions, using a bench microcentrifuge at 10,000g. Bands in agarose gels were visualised on a UV transiluminator (UVP) and carefully excised with a scalpel blade. The bands were weighed and 300 µl of buffer QG was added per 100 µg of agarose before heating the agarose/buffer QG mixture to 50°C for 10 minutes. After centrifugation to adsorb the DNA to the membrane, the membrane was washed with centrifugations with 500 µl of buffer QG followed by 750 µl buffer PE (which contains 70% (v/v) ethanol). All traces of ethanol were removed by a final centrifugation for 1 minute. DNA was eluted in nuclease-free water.

2.6 Quantitative Real-Time PCR

An Applied Biosystems 7900HT Sequence Detection System (Taqman) was used for all quantitative real-time PCRs in this project. The system encompasses a

heating block for thermal cycling and detectors to measure fluorescence in each well of a 96-well or 384-well optical plate. Fluorescence is measured after every amplification cycle to quantify the accumulation of PCR product; during the exponential phase of PCR cycling the rate of product accumulation is proportional to template concentration, relative template abundance can therefore be quantified by monitoring increasing fluorescence in each well during temperature cycling. This is explained in more detail below along with the specific protocols for cDNA template preparation of and reaction set up.

2.6.1 Preparation of cDNA

cDNA preparations for quantitative real-time PCR (qRT-PCR) were made by reverse transcription from RNA templates. Applied Biosystems 'TaqMan Reverse Transcription Reagents' were used for cDNA synthesis using random hexamer or oligo dT primers. 1 µg of RNA template was used unless RNA concentrations were too low; the same amount of RNA template was always used in all reactions in the same experiment, dictated by the lowest RNA concentration. Reverse transcription reactions were performed in 96-well plates to allow multichannel pipettes to be used for PCR reaction set up, the reaction constituents and temperature programs used for each kit were:

Applied Biosystems TaqMan Reverse Transcription Reagents:

	Vol.
RNA	Up to 1µg
H_2O	Adjust to 7.7µl

Then add the following to each tube from a master mix:

	Vol.(µl)
10X Reaction Buffer	2.0
$MgCl_2$ (25mM)	4.4

dNTPs (2.5mM ea.)	4.0
Primers (50μM)	1.0
RNase Inhibitor (20U/μl)	0.4
MultiScribe RT (50U/μl)	0.5

Heat to 25°C for 10 minutes, 48°C for 30 minutes then 95°C for 5 minutes.

2.6.2 Real-Time PCR

Applied Biosystems Gene Expression Assays and Custom Gene Expression Assays were used for all qRT-PCRs in this project. The assays consisted of a 20 X reaction mix containing template-specific forward and reverse primers (18 mM each) and a probe that anneals between the two primers (5 mM). The probe DNA is fluorescently tagged at its 3' end, but fluorescence from intact probes is prevented by a quencher molecule that is bound to its 5' end. During PCR amplification, the 5'-3' nucleolytic activity of the DNA polymerase cleaves the quencher from the probe, resulting in fluorescence levels proportional to the amount of PCR product present. All Gene Expression Assays used in this project were designed to anneal across two exons in cDNA, guaranteeing that non-specific amplification did not occur from residual genomic DNA.

Every effort was made to ensure that the amount of template cDNA was the same in each reaction of an experiment, however, given the sensitivity of qRT-PCR, expression of the gene of interest was always measured relative to the GapDH housekeeping control gene. The gene of interest and GapDH were amplified in duplex PCR reactions, probes for the gene of interest were tagged to 'FAM' labelled fluorescent dyes, while GapDH probes were labelled with 'VIC' dye, they fluoresce at different wavelengths, allowing them to be measured in the same reaction without interference. Reactions were performed in 5 μl volumes in 384-well plates. The reaction constituents and temperature cycling parameters were:

Reaction Mixtures: 5µl:

	Vol.(µl)
2X Genotyping Master Mix	2.5
20X Gene Expression Assay	0.25
20X GapDH Expression Assay	0.25
cDNA	2.0

Temperature cycling:

50°C 2 min

95°C 10 min

95°C 15 sec ← x35

60°C 1 min

All samples were amplified in triplicate, at least three treatment replicates were included per experiment. Fluorescence of FAM and VIC dyes was measured for all reactions during temperature cycling, data was analysed using a combination of Applied Biosystems SDS (Sequence Detection Software) and Microsoft Excel software. SDS plotted amplification curves as cycle number vs. fluorescence for both dyes in every well. FAM and VIC fluorescence were analysed as separate data sets, a fluorescence threshold was identified for each data set where amplification curves were in their exponential phase. The 'cycle threshold value' (Ct value) for each amplification curve was interpolated by finding the precise fractional cycle number (to 5 decimal places) at which the curve crossed the fluorescence threshold. Ct values for FAM and VIC data were exported from SDS as text files and converted to Excel documents for data analysis. Relative levels of gene expression were calculated by the 'ΔΔCt method' (Livak KJ & Schmittgen TD. 2001). This method calculates gene expression normalised to the endogenous control relative to a calibrator from

within the experiment (i.e. a sample or sample group designated to have relative gene expression level of 1.0), it is advantageous because it does not require the inclusion of a standard curve from a serial dilution of template in each experiment. The ΔΔCt method is logically derived from the equation that dictates the rate of product accumulation during PCR:

For Gene Expression Assays designed by Applied Biosystems the efficiency is close to 1, therefore the amount of target can be calculated as:

Relative quantification (RQ) = $2^{-\Delta\Delta Ct}$

In order to use the ΔΔCt it was imperative to experimentally confirm that the amplification efficiencies of the target and control gene PCRs were the same (i.e. that $E_X = E_R$). Therefore the amplification efficiencies of each Gene Expression Assay were measured in duplex PCRs with the GapDH assay using a serial dilution of template. This process was performed for all Gene Expression Assays and Custom Gene Expression Assays for each different cDNA template (e.g. for cDNA from kidneys, carotid arteries and for each cultured cell line). A dilution series of cDNA template was prepared from neat to 1/1,000, typically including 1/5, 1/10, 1/50, 1/100, 1/500 and 1/1000 dilutions. Graphs were plotted of log (dilution) versus Ct for the target template and GapDH, the gradient of each line was compared, according to the Applied Biosystems guidelines they had to be within ±0.1 to be used to measure gene expression in this tissue. Each Gene Expression Assay for RNA from each tissue in this project passed this test.

2.6.3 Functional experiments of hyperterophy in the Primary cells

2.6.3.1 Neonatal cardiomyocyte & fibroblast isolation

Isolation of primary cardiomyocytes and fibroblasts took place from neonatal whole hearts. After dissection, the hearts were placed in 1x ADS buffer (per litre).

1x ADS Buffer

NaCl	6.8g	(S9888)

HEPES	4.76g	(H4034)
NaH_2PO_4	0.12g	(S3139)
Glucose	1.0g	(G7528)
KCl	0.4g	(P3911)
$MgSO_4$	0.1g	(M2643)

Made up to 1 litre with MilliQ water, pH to 7.35 with NaOH, sterilised and stored at 4°C.

Each heart was checked to remove excess connective tissue and surrounding fat, and gently squeezed to remove excess blood, and blood clots removed. The cleaned hearts were transferred to a clean dish containing 1x ADS buffer (enough to just cover the hearts). The hearts were chopped until homogenised using 'spring bow' scissors (tissue pieces should be small enough to pass through the tip of Pasteur pipette) and transferred to a Duran bottle along with the 1x ADS buffer. Small pieces of the tissue in the plate were washed off with fresh ADS and transferred to a Duran bottle. The tissue was digested in a number of stages, using a shaking water bath to incubate. The enzyme mix used to digest the tissue was made as follows:

Enzyme mix

Collagenase Type 2	0.03g	LS0004176
Pancreatin (porcine)	0.03g	P3292-25G

The constituent parts were weighed into two separate 50 ml Falcon tubes and 20 ml 1xADS buffer was added to each. They were then vortexed to dissolve the powder, and filter sterilised using syringe filters (0.2µm; 1 per ~15 ml). The filtered enzyme was placed in a sterile 100 ml Duran bottle and both falcons were 'washed' with a total volume of 10 ml of 1x ADS, and filter sterilized.

There are 6 stages of digestion which are listed below with their appropriate conditions.

Digest	Volume of the enzyme mix (ml)	Time (min)	Speed (strokes/min)
1	10	5	180
2	10	20	160
3	8	25	150
4	8	25	150
5	6	15	160
6	6	10	150

The Duran bottle was removed from the water bath and placed in the hood. The chopped tissue was allowed to settle, and the supernatant was removed and discarded. For each subsequent stage, the supernatant was removed and placed in a sterile falcon tube containing 2ml foetal calf serum (FCS), and centrifuged at 1000rpm for 5 minutes. The supernatant was discarded, and the pellet re-suspended in 4 ml FCS. The cell and supernatant mix was placed in the incubator with the lid of the falcon loosened to allow CO_2 to reach the cells. This was repeated until step 5. After step 6 in the digestion protocol, the supernatant was added to the re-suspended cells, and centrifuged at 1000rpm for 6 minutes. The supernatant was removed carefully and the pellet re-suspended in plating media (4 ml media per 10 hearts).

Pre-plating (to remove adherent non-myocytes)

The re-suspended supernatant was then plated in a 60 mm primaria dish, and incubated for 1 hour at 37^{o}C, 5% CO_2 to allow the cardiac fibroblasts to adhere to the plate surface. The cardiomyocytes remain in suspension. The floating cardiomyocytes were then washed to separate them from the fibroblasts. The media was used to wash the surface of the plate using a Pasteur pipette, and transferred to a clean 50 ml falcon. Fresh plating media was then applied, and

used to wash, and repeated as necessary, checking after each wash to ensure the cardiomyocytes had been removed. The plating media was replaced after 24 hours with maintenance media, which is serum free to reduce the potential contamination with fibroblasts.

Plating media

	ml	cat no
DMEM	340	42430025 (Invitrogen)
M199	85	2340020 (Invitrogen)
Horse serum	50	SCHFRA2052Hi (Autogen Bioclear)
Foetal calf serum	25	7.01 (Autogen Bioclear)
Pen Strep	5	15140122 (Invitrogen)
(10,000U/ml Penicillin)		
(10,000ug/ml Streptomycin)		

Maintenance media

	ml
DMEM	400
M199	100
Pen Strep (*100)	5
(10,000U/ml Penicillin)	
(10,000ug/ml Streptomycin)	

Serum Free media

	ml
DMEM	485
Pen Strep	5
(10,000U/ml Penicillin)	
(10,000ug/ml Streptomycin)	
L-Glutamate (200 mM)	5
Sodium pyruvate (100 mM)	5

All media was stored at 4 ^{o}C

1% (w/v) Gelatine Solution

5g in 500ml milliQ water, autoclave and store at 4^{o}C.

Gelatine (porcine skin) Type A, Sigma cat no. G1890 (100g)

Gelatine coating the dishes

1ml of 1% (w/v) gelatine was added to each of the 24 well, swirled to coat the bottom of the well, and the excess gelatine removed and returned to the bottle. The plates were air dried in the hood for at least 2 hours.

2.6.3.2 Hypertrophy assay of cardiomyocytes with ANG II stimulation

A 24 well plate was coated in 1% (w/v) gelatine and allowed to dry. The wells were seeded at $1x10^5$ density with cardiomyocytes, in plating media and incubated at 37°C overnight. The media was changed to serum free media after 24 hours. The cardiomyocytes were stimulated with Angiotensin II at a range of concentrations from 50nM up to 200nM and incubated at 37°C for 24 hour. The cells were washed twice with PBS, and 700ul of Qiazol was applied to each well, and the cells were scraped into solution. RNA was then extracted (2.2.1), and Gene expression of the stimulated cardiomyocytes was measured using Taqman qRT-PCR.

2.6.3.3 Phalloidin staining (to visualise f-actin)

The cardiomyocytes were washed twice with PBS (Lonza), and excess PBS was aspirated. 100µl of 4% (w/v) PFA was applied to the cells for 20 minutes at room temperature to fix the cells. The cardiomyocytes were washed twice with PBS (Lonza), and excess PBS was aspirated. The cells were then permeabilzed with 0.1% (v/v) TritonX-100 for 20 minutes at room temperature, and washed twice with PBS (Lonza), and excess PBS was aspirated. 100µl phalloidin (5µg/ml in 1% (v/v) BSA) solution per well was added, and incubated for 1hour at room temperature, protected from light. The cardiomyocytes were washed twice with PBS (Lonza), and excess PBS was aspirated. The cells were measured using the microscope.

2.6.3.4 Scratch assay

Fibroblasts were passaged and allowed to expand. When suitable numbers were acquired, the cells were lifted using 10% (v/v) trypsin-EDTA and were seeded at $4x10^5$ cell density in a 12 well plate, in triplicate and incubated at 37°C, 5% CO_2 for 24 hours. The cells were washed twice with PBS (Lonza) and replaced with serum free media to quiesce the cells and allow them to reach a synchronous stage of cell division. The cells were incubated 37°C, 5% CO_2 for 48 hours and then washed twice with PBS (Lonza), and the media replaced contained varying

concentrations of serum (0%, 1%, 5%, 10% & 20% (all v/v)). A single scratch was made, using a p200 tip. Reference marks were made on the base of the plate to ensure measurements at the time points were being made at the same location. The wound was measured at x10 magnification at 0 hours, 16 hours and 24 hours.

2.6.3.5 MTT Cell Viability Assay

Fibroblasts were passaged and allowed to expand. When suitable numbers were acquired, the cells were lifted using 10% (v/v) trypsin-EDTA and were seeded at $1.5x10^4$ cell density in a 96 well plate, in triplicate and incubated at 37°C, 5% CO_2 for 24 hours. The cells were washed twice with PBS (Lonza) and replaced with serum free media to quiesce the cells and allow them to reach a synchronous stage of cell division. The cells were incubated 37°C, 5% CO_2 for 48 hours and then washed twice with PBS (Lonza), and the media replaced contained varying concentrations of serum (0%, 1%, 5%, 10% & 20% (all v/v)). The cells were incubated at 37°C, 5% CO_2 for 24 hours. 15µl of dye was added to each well, and the plate was incubated at 37°C, 5% CO_2 for 4 hours. 100µl of stop solution was added to each well, and the plate incubated at 37°C, 5% CO_2 for 1 hour. Absorbance was recorded at 570nm using the Wallmac.

2.6.4 Statistical Analysis

The significance threshold for all analysis was set at 0.05. For statistical comparisons between two groups, 2 sample t-tests were applied. For statistical comparisons in data sets with more than two groups, analysis of variance was calculated, followed by the Dunnett's post-test, comparing all samples groups against a designated control group.

The Gene level analysis of the Exon array (Chapter 3) uses the False Discovery Rate (FDR) control, which is a statistical method used to correct for multiple comparisons in multiple hypothesis testing. The use of FDR controls the number of incorrectly rejected null hypotheses (or Type I errors).

2.6.5 Partek analysis

Partek Genomics Suite allows data to be imported from a variety of array chip platforms, from many different formats, including metaprobeset files, and plain text file formats from one colour and two-colour microarrays. It can allow analysis of gene expression, identification and annotation of genes and biomarkers of interest, and provides an informative construct of the output, to allow visualisation of the results. Partek genomics suite also automatically provides links to NetAffx, UCSC genome browser, integrated genome browser, and other internet databases, which aids further analysis of the array outcomes.

Affymetrix Exon Array

The CEL files were uploaded to Partek, and the data was normalised using the RMA default algorithm (quantile normalisation and Median polish for probe set summarization). The data was then transformed using PCA. ANOVA was used to identify significant differentially expressed genes. An ANOVA model, including pairwise contrasts and Genechip effects, was constructed using step up false discovery rate (FDR). The data was filtered to allow for the minimum congenic interval at markers D14Rat54 (5,116,492bp) to D14Got41 (34,375,424bp).

Illumina genome-wide expression assay

The Illumina RatRef-12 Expression BeadChip for genome-wide expression analysis contains in the region of 22,000 probes, selected primarily from the NCBI RefSeq database. The Direct Hybridization Assay offers the highest level of multiplexing for whole-genome expression profiling available. With up-to-date expression content and high-throughput processing, this array allows for the efficient production of high-quality data for large gene expression studies.

The data generated was quantile normalised and the final report was generated from Genestudios, and this data was uploaded to Partek. The data was then transformed using PCA. ANOVA was used to identify significant differentially expressed genes. An ANOVA model, including pairwise contrasts and Beadchip effects, was constructed using step up false discovery rate (FDR).

3. **Affymetrix Exon Array analysis in the heart of the stroke-prone spontaneously hypertensive rat, Wistar Kyoto and chromosome 14 congenic strains.**

3.1 Introduction

A genome wide array, utilizing the chromosome 14a strains was inspired by the previous work within the department, as the genotyping and phenotyping data gathered had already indicated that these strains were of interest, as such a severe phenotype of LVMI had been identified in the WKY.SPGla14a, with no effect on the blood pressure. The exon array was initiated as part of a collaboration with Klio Maratou & Tim Aitman (Euratools), and thought to be a useful method of generating more information from the single array experiment, as the design allows analysis on exons and their splicing, and also on gene transcripts.

The exon array utilizes up to 4 probes per exon, and around 40 probes per gene to enable a number of complementary levels of analysis – exons, Gene expression and alternative splicing. The use of multiple probes per gene allows for 'exon-level' analysis, which allows for identification of different isoforms (alternatively spliced forms) of the gene. This in turn allows the exon-level analysis to be applied on a whole genome scale, which enables the detection of specific alterations in exon usage that may play a central role in disease mechanism and etiology, and allows us to filter alternative splicing information. The second level of analysis is 'gene-level' expression, in which the multiple probes on different exons are summarized into an expression value of all transcripts from the same gene. This allows for a comprehensive coverage of the genome. The array itself has the highest resolution expression analysis, as it interrogates over 850,000 exon clusters within the known and predicted transcribed regions of the entire genome.

Splicing is the mechanism by which RNA is modified after transcription, where introns are removed from newly synthesized RNA, and the exons are joined together (Jurica MS & Moore MJ. 2003). This is required for mRNA to produce the correct protein through translation. The splicing event is controlled and performed by RNA molecules, and is catalyzed by the spliceosome. The spliceosome is a large RNA-protein complex containing 5 small nuclear ribonucleproteins (snRNP's)

Alternative splicing is a naturally occurring mechanism, and is the means by which there is increasing diversity in structure and function of proteins, and functionally distinct mRNA's, and allows for greater macromolecular and complexity of cells of both prokaryotic and eukaryotic organisms (Blencowe BJ. 2006). Viruses utilize alternative splicing as a mechanism to increase their diversity, whilst having a relatively small genome, whilst genome wide analyses indicates that 40-60% of all multi-exon human genes undergo alternate splicing (Modrek B & Lee C. 2002). Female specific alternative splicing of Drosophila melanogaster doublesex (dsx) pre-mRNA is an excellent example of how alternative splicing can be positively controlled (Lynch KW & Maniatis T. 1996). The pre-mRNA dsx gene contains 6 exons. In intron 3 of the dsx, there is a nonconsensus 3' splice site which is not recognised by the splicing machinery in males, meaning that exons 1-3 are directly joined to exons 5-6. This in turn leads to an mRNA which encodes a transcriptional regulatory protein which is required for male sexual differentiation. In females, the weak 3' splice site is recognised which leads to exons 1-3 joining onto exon 4. The RNA is then polyadenylated which leads to an mRNA which encodes a transcriptional regulatory protein which is required for female sexual differentiation (Coschigano KT & Wensink PC. 1993). The accuracy of alternative splicing is important, as splicing errors are thought to contribute to about 10% of human genetic diseases (Garcia-Blanco MA *et al*. 2004). Abnormally spliced mRNAs are found in a high level of cancerous cells, such as *BRCA1*. Many of *BRCA1*'s splice variants arise from mutations in consensus intronic splice donor and acceptor sites (Tesoriero AA *et al*. 2005). Cystic Fibrosis (CF) has been linked to mutations in either cis-acting elements or trans-acting factors which lead to abnormal splicing. 13-20% of the known 1200 CF disease-causing mutations are thought to affect splicing, and alternative splicing in the CF gene may also influence disease severity (Chu CS *et al*. 1993).

The data generated should provide us with a depth of knowledge of the congenic region of the chromosome 14 strains, and provide information on disease causing mechanisms in these strains. As alternative splicing has such a potential impact on the initiation of so many diseases, the exon level analysis was included as this had not been investigated previously in the SHRSP, WKY WKY.SPGla14a and SP.WKYGla14a.

3.2 Methods

The Affymetrix exon array was carried out in full by Dr Klio Maratou and Professor Tim Aitman of Imperial College London as part of a collaboration under the auspices of Euratools.

3.3 Results

3.3.1 Single Nucleotide Polymorphism analysis of SHRSP and WKY

Single Nucleotide Polymorphisms (SNPs) were analysed through the STAR consortium, whose main aim was to generate a haplotype map of the rat genome, and to present this in such a way to facilitate QTL gene identification (Saar K *et al*. 2008). The genotyping was achieved by utilising Affymetrix and Illumina platforms to align the SNP genotyping assays of SHRSP and WKY strains from the Glasgow breeding programme, alongside 167 of the most commonly used inbred rat lines.

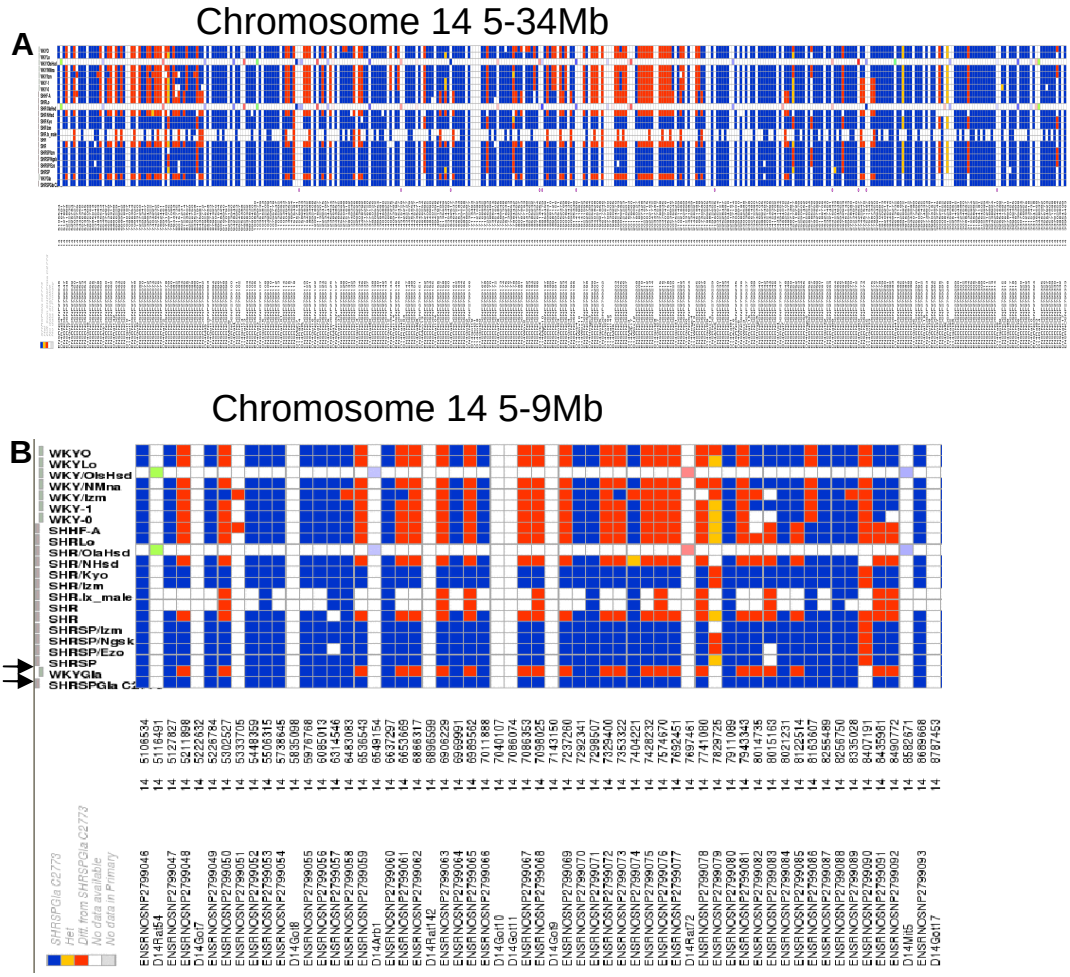

Figure 3.1 Schematic diagram of Single Nucleotide Polymorphism haplotype RGD analysis of SHRSPGla and WKYGla rat DNA

A) Shows a broad overview of chromosome 14 (5-34Mb), and B) is showing a more detailed view of the 5-9Mb region. SNP's are annotated in red and show changes relative to SHRSPGla. The SHRSPGla and WKYGla strains are located at the bottom of the diagram as indicated by the arrows to the left of the diagram. The alignment shows the differences and similarities between the Glasgow (Gla) strains and those from other breeding programmes, and also if SNP's are present.

Figure 3.1A shows that the 5-9Mb region on chromosome 14 has a high density of SNPs which is interesting as the QTL for Left Ventricular Mass Index (LVMI) is in this region (Figure 1.5). Congenic breeding to allow the introgression of a 29Mbp section of the SHRSP onto the WKY background, and a 102Mbp section of the WKY onto the SHRSP background has been established, and the strains have been confirmed by genotyping.

3.3.2 Exon array of 5 week Chromosome 14 animals

The exon array was carried out and filtered on the minimal congenic interval (29Mbp). Chromosome 14a congenic strain animals were analysed, along with the parental SHRSP and WKY strains, to investigate the potential for SNP's and alternative splicing in the QTL for LVMI (Figure 3.2). The data was filtered using a venn diagram, and the resulting area of intersect for the four strains indicates exons which are common (Figure 3.2). Fifty nine exons were differentially expressed across all 4 strains, of which 26 have a gene assignment. This led to 14 annotated genes to be investigated further (Table 3.1). The resulting exon data for each strain was filtered to identify expression changes related to exons (Table 3.2). As there are up to 4 probes per gene in the exon array, many of the genes assignments have duplicates, which could mean it is an overall change in the transcript causing the change in the exon array. Because of this, *Clock* has been isolated for further investigation as it has only one probeset showing a difference in the exon array and has also been identified by the alternative splicing analysis. The *Clock* gene is of particular interest, as it is located on chromosome 14, and is a circadian rhythm associated gene (Young M *et al*. 2001).

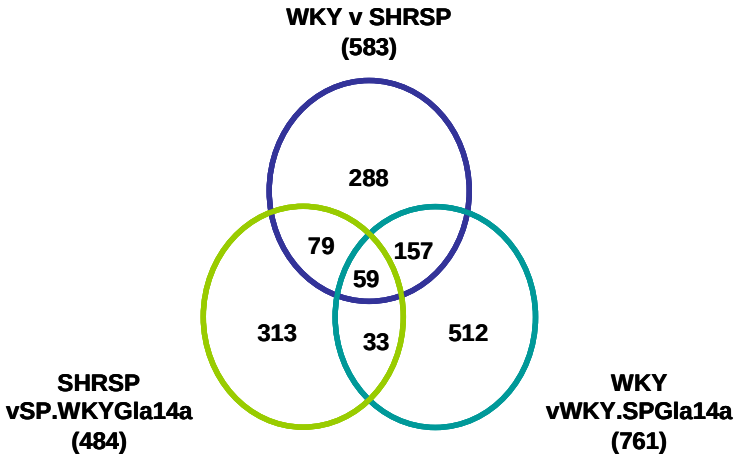

Figure 3.2 Venn diagram illustrating exon analysis of the SHRSP, WKY and chromosome 14 congenic strains

Venn diagrams illustrating exon array results in the heart in 5 week SHRSP, WKY, SP.WKYGla14a and WKY.SPGla14a rats. The number of probesets significantly differently expressed in each pairwise comparison are shown.

Table 3.1 Tables showing the output files from exon array
Table shows the output from the exon array anlysis, indicating the 26 exons which have gene assignments. These 26 gene assignments equate to 14 individual genes.

Probeset ID	Accession number	Gene assignment	Chromosome locus
5959530	XR_008179	RGD1565568_predicted	14: 5,888,451-5,945,589
6437639	XR_008179	RGD1565568_predicted	14: 5,888,451-5,945,589
6723207	XR_008179	RGD1565568_predicted	14: 5,888,451-5,945,589
6015233	XM_573551	RGD1565568_predicted	14: 5,888,451-5,945,589
6581067	XM_223745	LOC305633	14: 13,013,956-13,107,467
6649219	XM_223745	LOC305633	14: 13,013,956-13,107,467
6618452	XM_001073390	Ripx	14: 21,011,631-21,086,603
6580114	NM_021856	Clock	14: 34,218,466-34,258,054
5858860	NM_012946	Sparcl1	14: 6,766,346-6,797,580
6484105	NM_012946	Sparcl1	14: 6,766,346-6,797,580
6203753	NM_001108357	Mobkl1a_predicted	14: 20,911,418-20,944,224
6579583	NM_001108357	Mobkl1a_predicted	14: 20,911,418-20,944,224
6580066	NM_001108355	Cnot6l_predicted	14: 14,924,620-15,011,984
6544056	NM_001107206	Aff1_predicted	14: 7,015,191-7,114,671
6433275	NM_001107205	RGD1564709_predicted	14: 5,950,942-5,998,413
5659947	NM_001017496	LOC498335: Cxcl13	14: 15,126,337-15,131,368
5761726	NM_001017496	LOC498335: Cxcl13	14: 15,126,337-15,131,368
5935782	NM_001017496	LOC498335: Cxcl13	14: 15,126,337-15,131,368
6042163	NM_001017496	LOC498335: Cxcl13	14: 15,126,337-15,131,368
6685998	NM_001017496	LOC498335: Cxcl13	14: 15,126,337-15,131,368
6695863	NM_001014133	LOC360910: Abcg3l2	14: 5,573,149-5,613,575
5682078	NM_001004209	Dhrs8	14: 6,859,573-6,891,510
5850797	NM_001004209	Dhrs8	14: 6,859,573-6,891,510
5785795	NM_001004076	Abcg3	14: 6,235,275-6,289,605
6040515	NM_001004076	Abcg3	14: 6,235,275-6,289,605
6214440	ENSRNOT00000003472	Cipar1	14: 18,046,002-18,078,330

The signal intensity of the microarray probes is a relative measure of expression of the transcript. SHRSP and WKY congenic strains display a higher level of signal intensity than the WKY and SHRSP congenic strains at exon 8 (Figure 3.3B). This would suggest that exons may be spliced out of the WKY strain and SHRSP congenic strain in the *Clock* gene at exon 8.

Table 3.2 Alternative splicing analysis of the Affymetrix exon array output data
The alternative splicing outcome is detailed, which indicates 6 genes showing evidence of alternative splicing. *Clock* gene is common to both sets of analysis (highlighted in red).

Transcript ID	Accession number	Gene_assignment	Chromosome locus
7123570	NM_001017496	LOC498335: Cxcl13	14: 15,126,337-15,131,368
7116203	NM_001004209	Dhrs8	14: 6,859,573-6,891,510
7122910	NM_001107206	Aff1_predicted	14: 7,015,191-7,114,671
7117187	NM_001107212	Adamts3_predicted	14: 19,756,887-19,963,451
7122822	---		
7117864	NM_021856	Clock	14: 34,218,466-34,258,054
7117158	NM_001105999	Ankrd17	14: 19,248,809-19,387,059

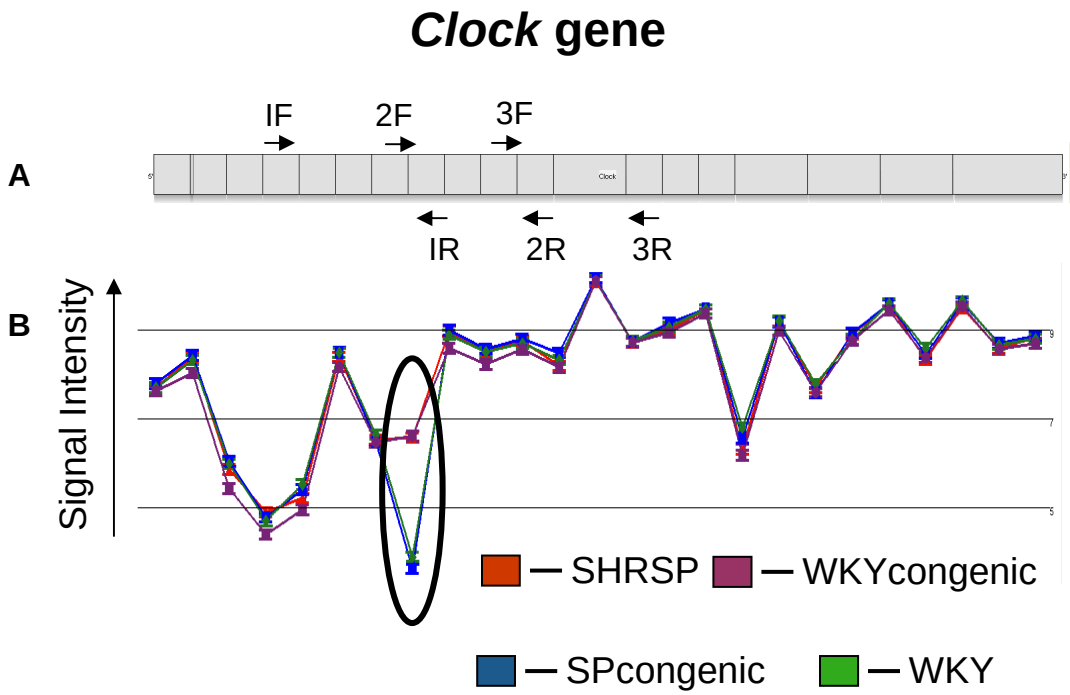

Figure 3.3 A schematic view of the *Clock* exon array analysis.
A) Positioning of the PCR primers relative to exons on the ORF of *Clock* gene. The primers can be used in a variety of F & R combinations. B) Comparison of the signal intensity from the exon array of the parental and congenic strains.

3.4 End point PCR and DNA sequencing to investigate alternative splicing in the *Clock* gene

Primers were designed for end-point polymerase chain reaction (PCR) to cover the predicted alternatively spliced exon 8 region in the *Clock* open reading frame (ORF). Primer positions are illustrated, and show the region between exons 4-14 was included in the design to ensure full coverage of the expected splice site (Figure 3.3A). PCR products were amplified using the SHRSP and WKY parental strains and the chromosome14a congenic strains on heart cDNA. The primers were used in their numerical pairs (primer pair 1F &1R, 2F & 2R and 3F & 3R), and also in combination to identify PCR products covering the splice site was produced (using primers 1F & 2R and 1F &3R).

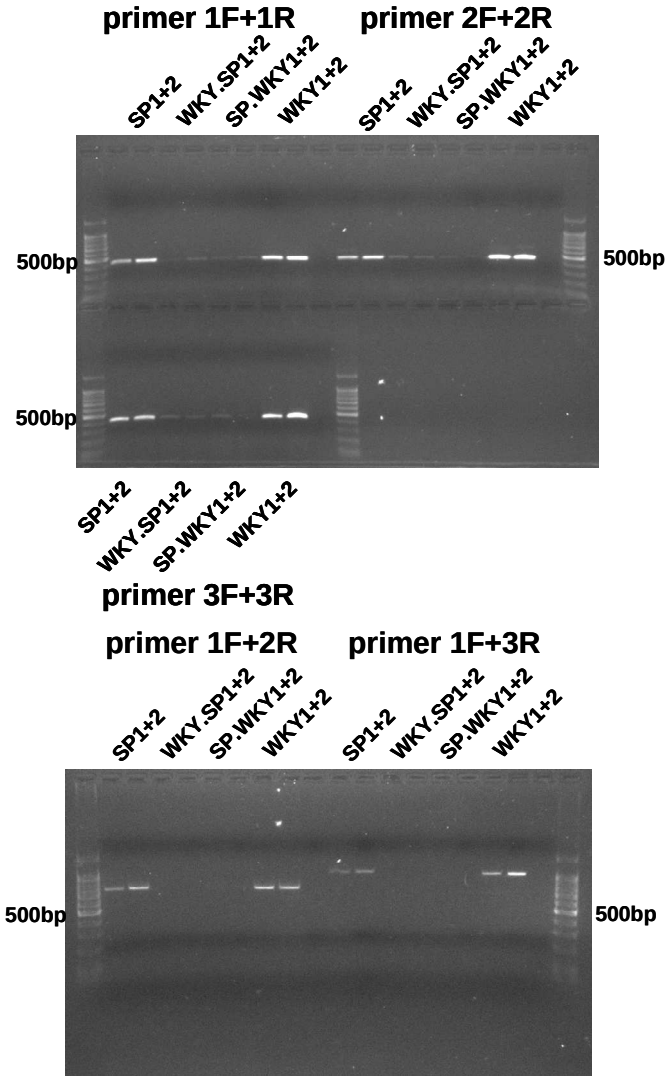

Figure 3.4 *Clock* Primer PCR products
Amplified PCR products from *Clock* ORF in biological replicates of SP, WKY.SPGla14a, SP.WKYGla14a, and WKY cDNA with the primer pairs as illustrated, electrophoresed on a 1% agarose gel.

The bands obtained are of the expected size for all the primer pairs, and clearly show no alternative splicing is occurring in the ORF of the *Clock* gene (Figure 3.4). The congenic strains show a lower intensity of PCR product. A full list of expected sizes of PCR products is available as a supplementary table in the appendix. To further investigate potential alternative splicing in the ORF of the *Clock* gene, the SHRSP, WKY, SP.WKYGla14a and WKY.SPGla14a PCR products were sequenced, and the resulting template was read using the ABI 3700. Data were analysed using Seqscape v2.1 to align the sequence derived from the sequencing reaction with the draft genome sequence of the Brown Norway strain (Figure3.5A).

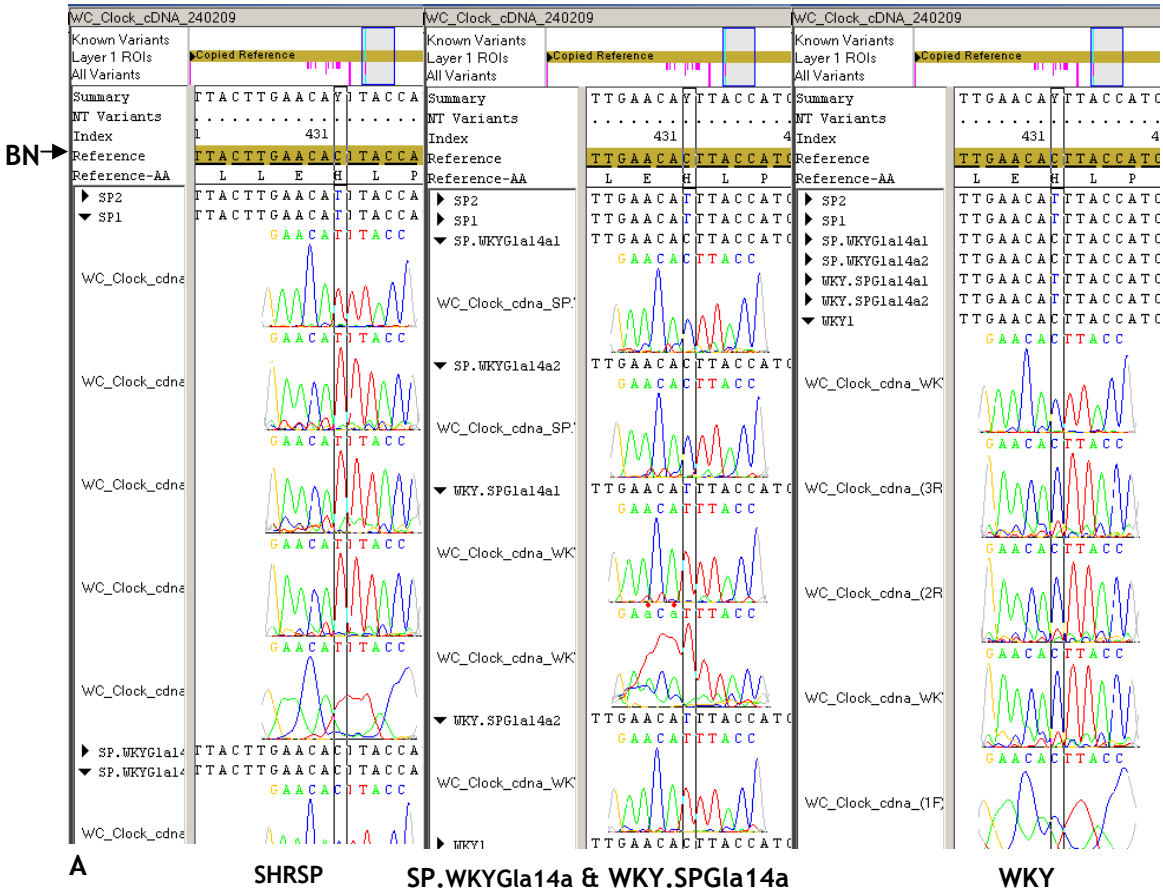

B

Position from ATG	Brown Norway	SHRSP	SP.WKY.gla14a	WKY.SP.gla14a	WKY	Change in aa
432	C	T	C	T	C	No
816	G	G	A	G	A	No

Figure 3.5 Sequence analysis of *Clock* PCR products
A) Sequence alignment of *Clock* PCR products of each of the 4 strains analysed. The SNP identified at +432bp upstream of the initiator ATG codon is shown. BN indicates the Brown Norway reference sequence to which the generated sequence has been aligned. B) The positioning of the SNPs identified in the ORF of the *Clock* gene, and the differences when comparing the sequence derived from the PCR products with that of the Brown Norway. It also indicates if any amino acid changes have occurred as a result of the SNP.

Figure 3.6 SNP positioning within the ORF of the *Clock* gene.
The sequence shows the SNP's as identified previously (Figure 3.5). The letters in the rows labelled WKY have a 2 colour system of blue and black showing where the exons are located. The yellow highlighting indicates the amino acid codon. The original base is highlighted in green, with the change in lower case letters.

Two SNPs were identified within the coding region of the *Clock* gene, which do not cause a change in amino acid (Figure 3.6). This may explain the difference in signal intensity in the exon array analysis, as base pair mutations may prevent the binding of the exon specific probes. On further investigation of the *Clock* gene via ensembl, it was noted that the exon array had misguided the identification of exon 8 as being alternatively spliced, and exon 9 was actually the target. The PCR primers were extended in their design to cover a region of the ORF, and this indicated the SNP in exon 5. To confirm the exon probes' location in relation to the SNPs, an alignment was made of the probes to the *Clock* gene sequence. The probe ID's were identified from the NetAffx website, and were confirmed using ensembl, ensuring the correct probe was covering the exon (Figure 3.7). The probe sequence was then aligned using Integrated genome browser (Nicol JW *et al*. 2009) (Figure 3.8). The positioning of the probes for 6580114 over the SNP (+816) suggests that the lower signal intensity detected in exon 9 is due to the probe not binding as efficiently to this region, consistent with the PCR analysis. The analysis of the Affymetrix exon array data then focussed on the minimum congenic interval of the chromosome 14a strains (29Mbp) and the gene level analysis was then carried out (genome wide scan) to identify positional candidates in the SHRSP, SP.WKYGla14a, WKY.SPGla14a and WKY strains.

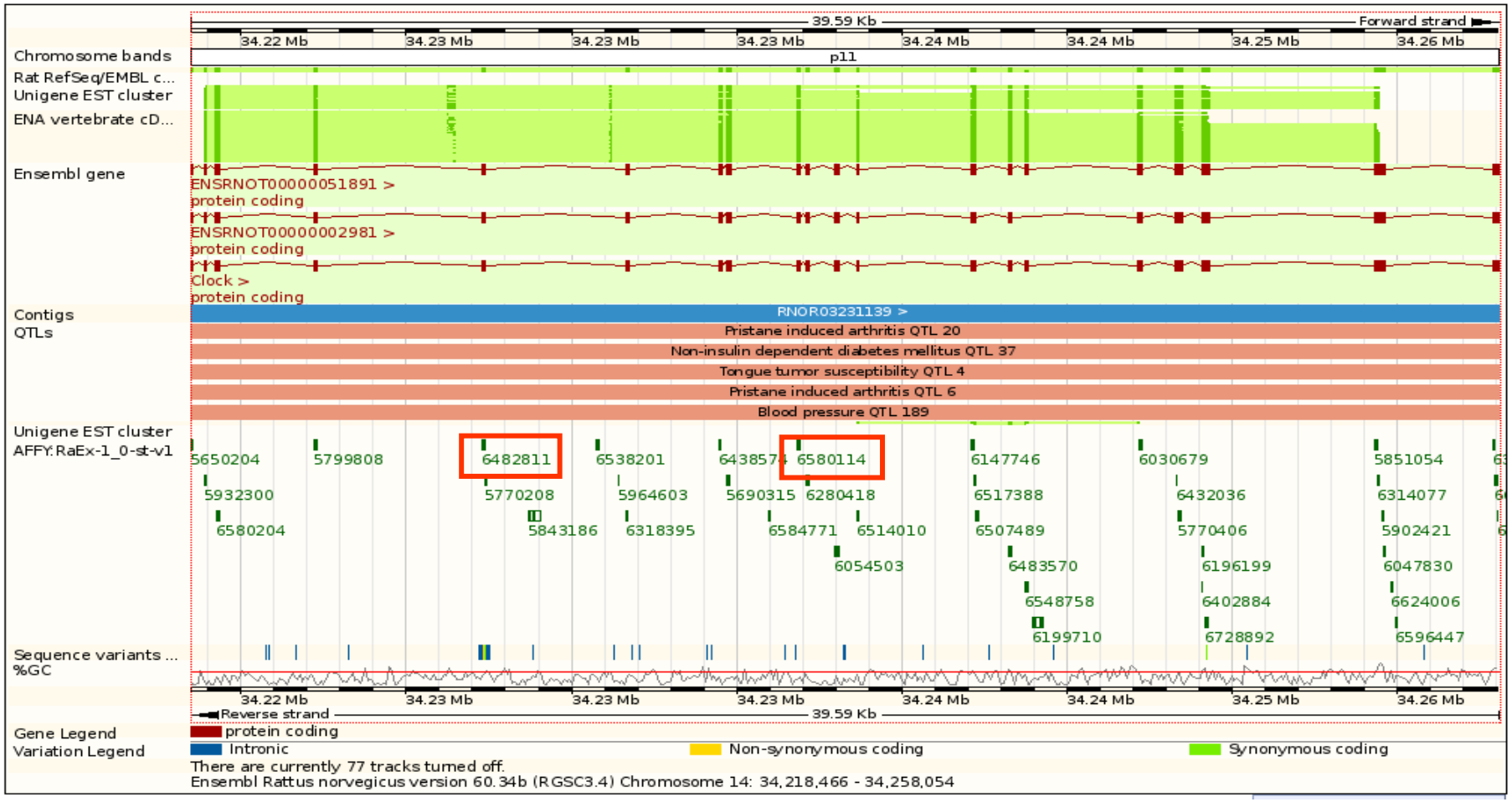

Figure 3.7 Ensembl schematic of *Clock* gene, showing the exons.

The screenshot from Ensembl shows the exon arrangement of *Clock* ORF. The numbers outlined in red refer to the probe ID's for the exon array obtained from the NetAffx website. The probes are in the location of the regions containing the SNPs.

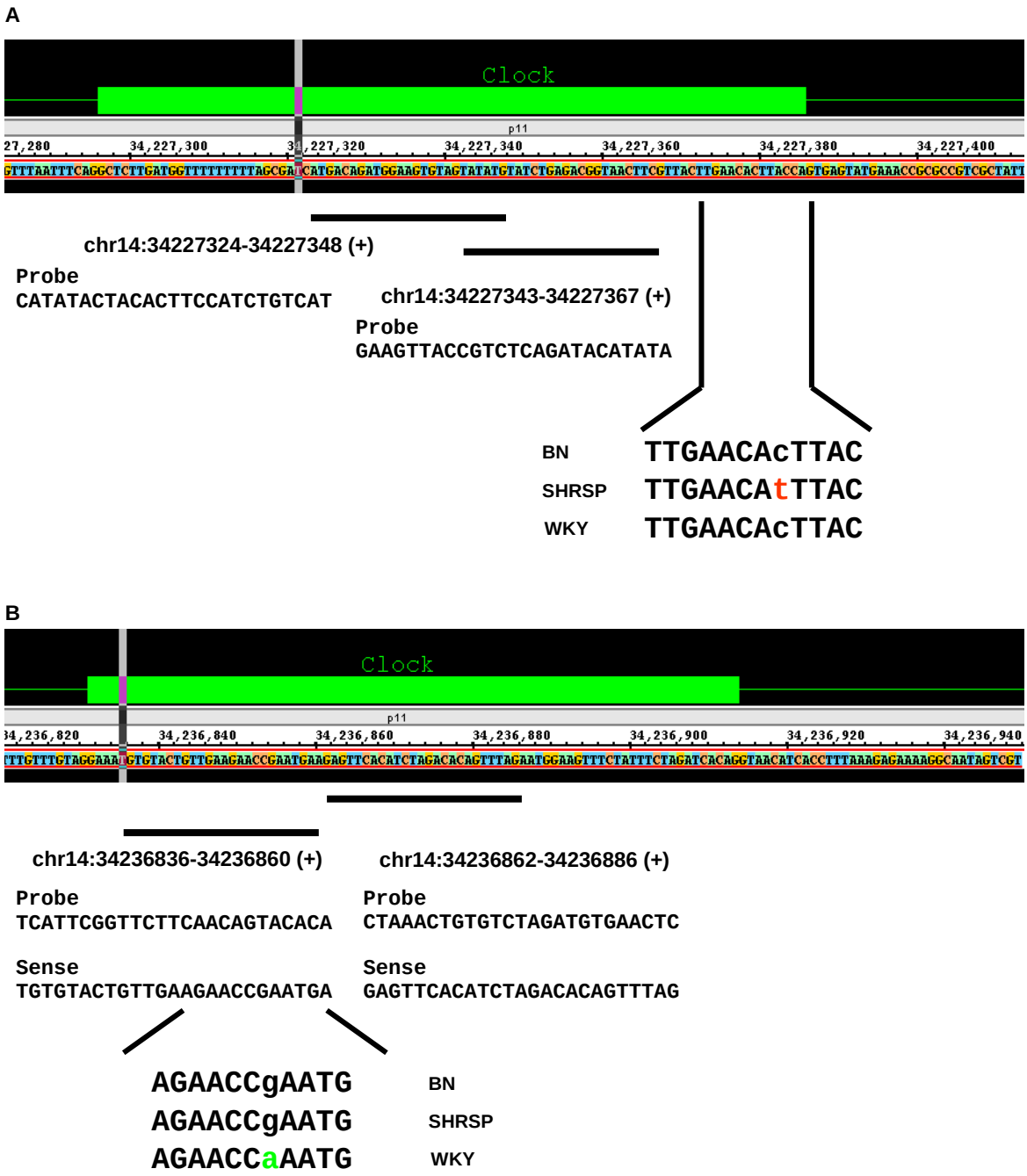

Figure 3.8 Location of *Clock* exon probes used in the array.
A)The exon probes for 6482811 were identified and aligned with the *Clock* ORF using IGB. The 25-mer probes are shown (thick lines under the sequence), along with their position on chromosome 14. The SNP (+432 C/T) lies outside the area of the probes. B)The exon probes for 6580114 were identified and aligned. The probes position is shown on the alignment, along with their chromosome location. The probe sequence is translated to the reverse compliment (labelled sense), and the position of the SNP (+816 G/A) is shown, relative to it's position on the probe.

3.5 Gene level analysis

The transcript level analysis of the exon array was carried out, and the data were analysed by filtering to the minimum congenic interval (29Mbp) and to the genome wide scan. 5 week old SHRSP, WKY and Chromosome 14a congenic strain animals were analysed, along with the parental SHRSP and WKY strains at the 5 week time point, to investigate the potential for differential gene expression. The resulting data for each strain were filtered in a venn diagram, and the resulting area of intersect for the four strains indicates genes which are common (Figure 3.9). The genes indicated by the overlay are Chemokine ligand 13 (*Cxcl13*) - SPvWKY fold change =-2.9 and ATP Binding Cassette, sub family G (*Abcg3)* - SPvWKY fold change =-1.4

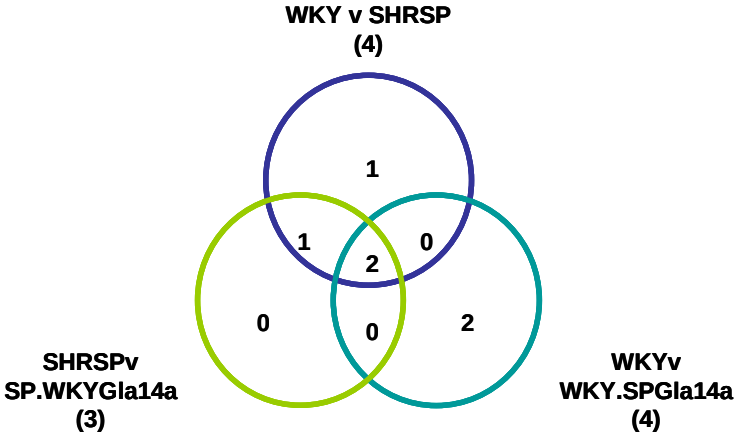

Figure 3.9 Venn Diagram of minimum congenic interval analysis of the Exon microarray
Venn diagrams illustrating microarray results of heart gene expression in 5 week SHRSP, WKY, SP.WKYGla14a and WKY.SPGla14a rats. The number of probesets from the minimum congenic interval (29Mbp) which are showing significance in differential expression in each pairwise comparison are shown.

The genome wide scan of the exon array has provided only a small number of gene targets. The comparison is made between WKY v SHRSP, and SP.WKYGla14a v SHRSP. From this analysis, the following have been identified: *Ckap21*, a chromosome 3 gene, and *Cxcl13*. On the basis of the data from the minimum congenic interval (Figure 3.9) and the genome wide scan, *Cxcl13* and *Abcg3* were investigated further. All other genes identified by pairwise comparisons of the minimum congenic interval are listed (Table 3.3)

Table 3.3 Genes identified in minimum congenic interval analysis
Table shows the results of the exon array, displaying the genes which are identified as being differentially expressed in each pairwise comparison, within the minimum congenic interval.

Comparison	Probe ID	Gene Annotation	Chromosome locus
SPvSP.WKYGla14a	7116203	Hsd17b11	14: 6,859,573-6,891,510
SPvSP.WKYGla14a	7124689	LOC498350	14: 33,403,956-33,446,249
SPvWKY	7117751	RGD1359460	14: 33,107,963-33,123,992
(SPvWKY)v (SPvSP.WKYGla14a	7117187	Adamts3	14: 19,756,887-19,963,451

The genes identified are of interest as they are located within the minimum congenic interval, however, they appear to have no apparent functional link to LVMI. Their functions are as follows: Hsd17b11, a substrate which has been implicated in supporting gestation and modulating γ-aminobutyric acid receptor activity, and is located in the QTL for body weight (Chai Z *et al* 2003); LOC498350 is similar to testicular haploid expressed gene product isoform 2, and is found in the blood pressure QTL; RGD1359460 encodes for the MMR_HSR1 domain containing protein; and Adamts3 is a disintegrin and metalloproteinase with thrombospondin motifs. The protein encoded by this gene is a major procollagen II N-propeptidase, and a deficiency of this protein may be responsible for dermatosparaxis in animals, which is a genetic defect of connective tissues, causing skin fragility (Le Goff *et al* 2006).

3.5.1 Validation of *Cxcl13* & *Abcg3* using qRT-PCR

The gene level analysis indicated *Cxcl13* and *Abcg3* as potential positional candidate genes, and the results were validated by qRT-PCR. *Cxcl13* mRNA expression, relative to SHRSP in hearts from 5 week old rats showed approximately 2.5 fold higher expression in SP.WKYgla14a relative to SHRSP, and approximately 2 fold higher expression in WKY relative to WKY.SP.gla14a (Figure 3.10A). In hearts of 16 week old rats, *Cxcl13* mRNA expression, relative to SHRSP, showed approximately 3 fold higher expression in SP.WKYgla14a relative to SHRSP, and approximately 7 fold higher expression in WKY relative to WKY.SP.gla14a (Figure 3.10C). Expression of *Abcg3* mRNA relative to SHRSP in hearts from both 5 + 16 week old rats showed no change in expression SP.WKYgla14a relative to SHRSP, and no change in WKY relative to WKY.SP.gla14a (Figure 3.10B + 3.10D). Comparisons were analysed using the student's pairwise t-test. Experimental data for *Abcg3* did not validate the findings from the microarray (Figure 3.9).

The qRT-PCR results confirm the findings from the minimum congenic interval analysis of expression of *Cxcl13* at the 5 and 16 week of age time point (Figure 3.10). The increased size of the error bars is due to technical variation within the samples. Further investigation of the *Cxcl13* gene was carried out through sequencing, both of the coding region and the regulatory regions.

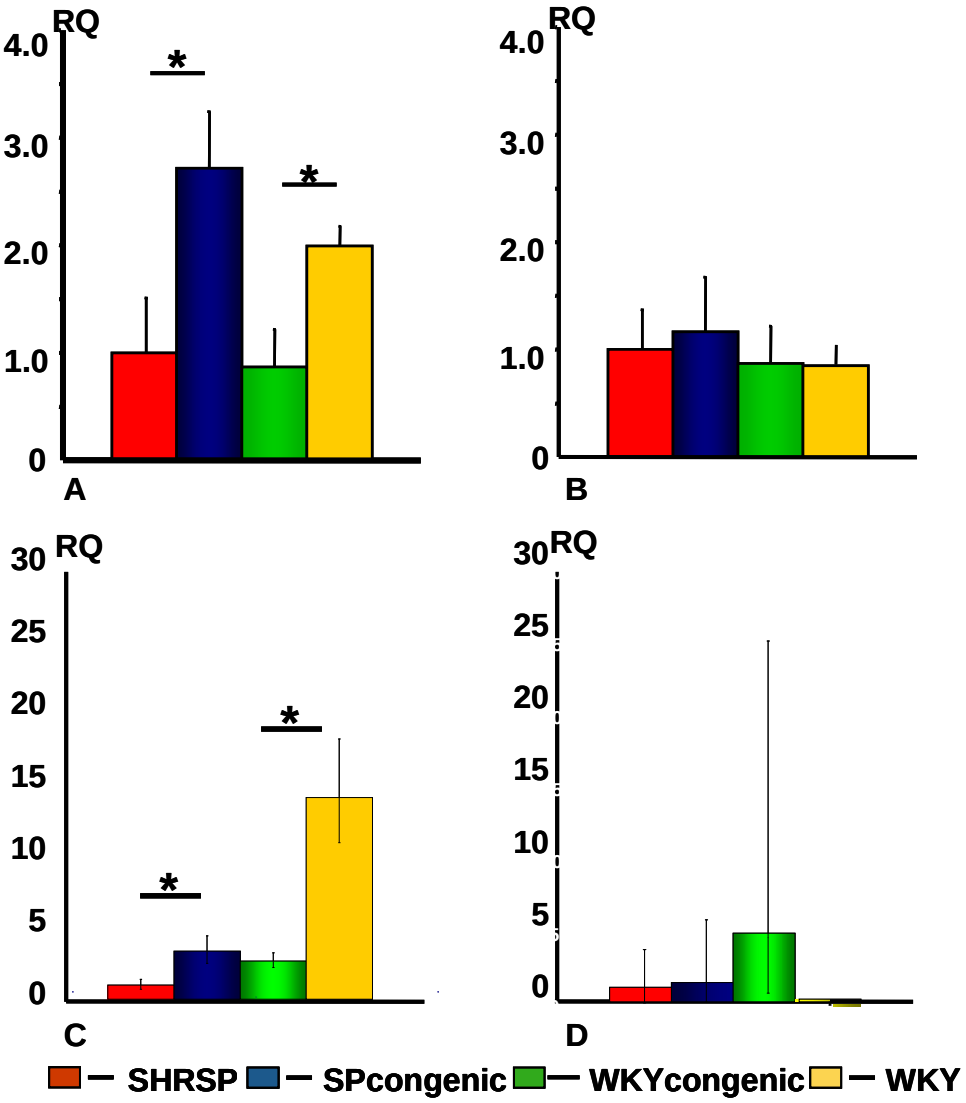

Figure 3.10 qRT-PCR of *Cxcl13* and *Abcg3* in 5 week and 16 week SHRSP, SP.WKYGla14a, WKY.SPGla14a and WKY strains

Expression is shown as an RQ value of SHRSP. A) *Cxcl13* has a significantly increased level of expression in SP.WKYGla14a relative to SHRSP and in WKY relative to WKY.SPGla14a at 5 weeks C) and also 16 weeks. B) No significant increase in expression of *Abcg3* in SP.WKYGla14a relative to SHRSP and in WKY relative to WKY.SPGla14a at 5 weeks D) and 16 weeks. n-4 *$p<0.05$

3.5.2 Sequencing of the coding and regulatory regions of *Cxcl13*

Primers for end-point PCR were designed to investigate the full open reading frame (ORF), 2500bp of the 5' promoter region for *Cxcl13* and the 3' untranslated region (UTR) OF *Cxcl13*. The PCR was carried out using the parental strains and the spontaneously hypertensive rat (SHR) on liver cDNA with the ORF primers, and on genomic DNA with the promoter and 3' UTR primers. To validate the amplification products generated, the SHR, SHRSP and WKY PCR products were sequenced and read using the ABI 3700. This data was then analysed using Seqscape v2.1 to align the sequence derived from the sequencing reaction with the Brown Norway strain. The sequence generated was additionally analysed by Transfac analysis, which is a unique knowledge base containing data on transcription factors, their experimentally-proven binding sites, and regulated genes. It can be used to search DNA sequences for potential transcription factor binding sites. A zPicture alignment will also be carried out to confirm the findings from the Transfac analysis. zPicture is a dynamic alignment and visualization tool that is based on blastz alignment program, and can be automatically submitted to rVista 2.0 to identify conserved transcription factor binding sites. The percentage homology derived from the zPicture indicates how conserved the 2 species are in the region analysed. As the rat and mouse species diverged more than a million years ago, if an area shows more than 50% homology, then it is defined as being well conserved.

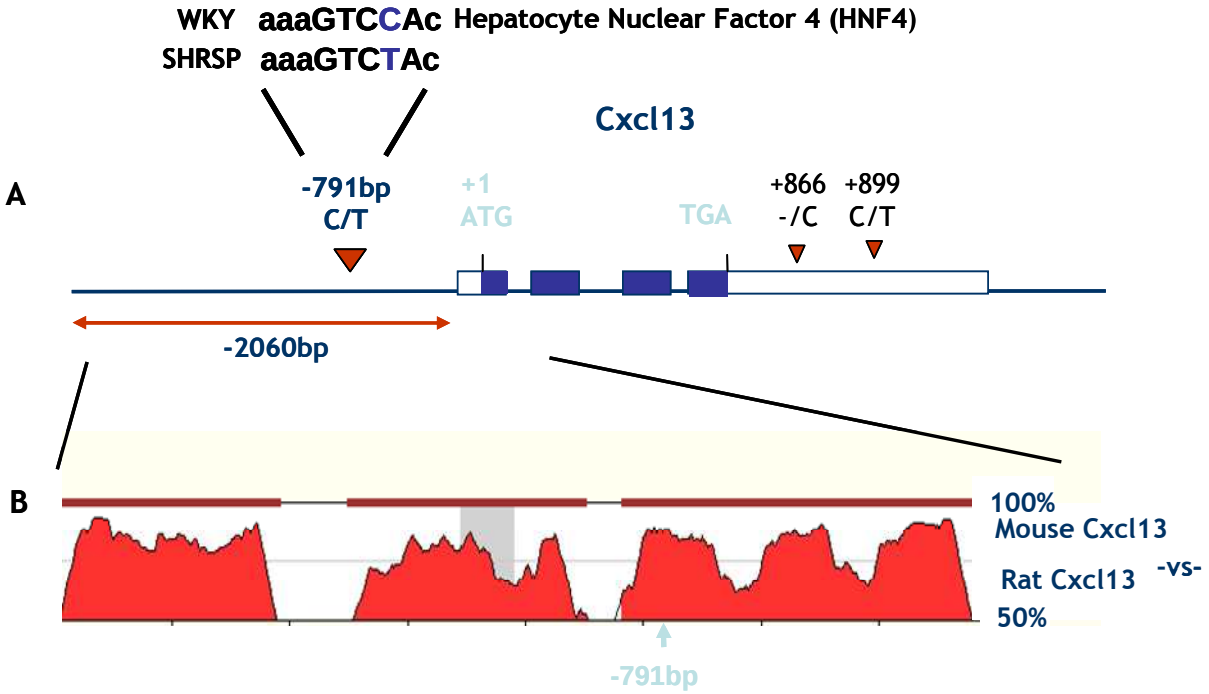

Figure 3.11 Sequence analysis of *Cxcl13* promoter region, ORF and 3'UTR. A) Sequencing results of the amplified PCR products of the *Cxcl13* promoter region, ORF and 3'UTR, and the positioning of the SNPs. Transcription factor analysis (Transfac) is shown of the upstream promoter region. B) A zPicture alignment shows percentage homology between the rat and mouse *Cxcl13* upstream promoter regions.

Table 3.4 Position of the SNPs within the *Cxcl13* sequence
The positioning of the SNP's found is shown in a table, which illustrate that no changes have resulted.

Position from start codon	Brown Norway	SHRSP	WKY	SHR
-791	T	T	C	C
+866	C	C	-	-
+899	C	T	C	C

3.5.3 Validation of receptors of *Cxcl13* using qRT-PCR

Chemokine receptors are cytokine receptors found on the surface of certain cells which interact, and their expression in different cell types and their binding response to specific cytokines are highly variable (Murdoch C & Finn A. 2000). The sequencing results showed no evidence of SNP's within the ORF, and the qRT-PCR data has shown there is a significant increase expression of *Cxcl13* in the strains analysed. To investigate whether *Cxcl13* was signalling through a potential functional effect we assessed the levels of the postulated *Cxcl13* receptors. Expression of the receptors for *Cxcl13*, *Cxcr5* (Chromosome 8), *Cxcr3* (Chromosome X) and *Ccrl1* (Chromosome 8) has been quantified by Taqman qRT-PCR relative to GapdH in hearts from 5 week old rats, in the SHRSP and WKY strain. *Cxcr5* is not expressed in the heart in either of the parental strains. *Cxcr3* shows low levels of expression in both SHRSP and WKY, which is not statistically different when comparing the strains with each other via the students pairwise t-test. *Ccrl1* shows higher levels of expression than that of *Cxcr3*, but this is not a significant change (Figure 3.12).

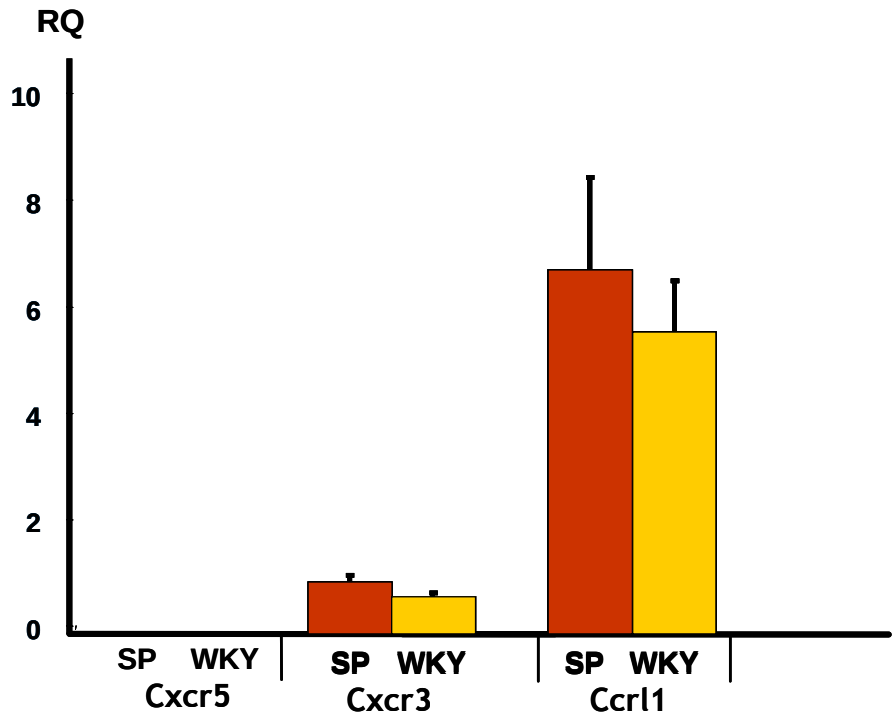

Figure 3.12 qRT-PCR of *Cxcr5*, *Cxcr3* and *Ccrl1* in 5 week parental strains
Expression is shown as an RQ value of *Cxcr3* SHRSP. Expression of *Cxcr3* does not change in WKY when compared to SHRSP. Expression of *Ccrl1* does not change in WKY when compared to SHRSP. n-4.

3.6 Discussion

The experiments related to this chapter analysed gene level expression from the exon array, at both exon level and transcript level. Subsequent analysis strategies including sequencing, Transfac analysis of the ORF and regulatory regions, and gene expression in SHRSP, SP.WKYGla14a, WKY.SPGla14a and WKY strains were applied to investigate this further. *Cxcl13* and *Abcg3* were both implicated in the gene level analysis of the exon array, and on subsequent Taqman qRT-PCR analysis, it was shown that *Cxcl13* displays a significantly higher level of expression in SP.WKYGla14a relative to SHRSP and in WKY relative to WKY.SPGla14a (Figure 3.10). No significant change in expression of *Abcg3* in SP.WKYGla14a relative to SHRSP and in WKY relative to WKY.SPGla14a, suggesting that *Abcg3* is not differentially expressed, and therefore does not represent a positional candidate gene for LVMI and was not prioritised for further analysis. *Cxcl13* was further investigated by the analysis of the ORF and regulatory regions to determine the presence of SNP's. There is evidence of a SNP in the 5' upstream region (-791 bases of the start codon, change of C/T (WKY/SP) of *Cxcl13* which is in the Hepatocyte Nuclear Factor 4 region (HNF4) (Figure 3.11). This base pair change leads to a loss of this region in *Cxcl13* in the SHRSP. The zPicture analysis confirms the homology between Rat and Mouse in the region of the transcription factor, and this would suggest that this change has been conserved since the 2 species diverged. There is evidence of 2 SNP's downstream of the ORF. HNF4, along with the Hepatocyte nuclear factor 1 (HNF1) binding site, appears to have a crucial role in cell type-specific transcription of the HNF1 gene (Miura N & Tanaka K. 1993). HNF4 is also associated with a susceptibility to non-insulin dependent Diabetes Mellitus (Barroso I et al. 2008). HNF1 is a key transcription factor involved in the expression of many liver-specific genes. Analysis of the 3' downstream promoter region indicated that 2 SNP's are present (Figure 3.11).

Cxcl13 is a small cytokine which belongs to the CXC chemokine family, and is also known as B lymphocyte chemoattractant (BLC). Chemokines are a superfamily of pro-inflammatory markers which are up-regulated in the myocardium of patients with chronic heart failure. It is expressed highly in the liver, spleen and lymph nodes and is also involved in immune response and

lymph node development, and is found in the extracellular space. It is a chromosome 14 gene, located in the QTL regions of mammary carcinoma susceptibility, serum renin concentration, body weight QTL, pristane induced arthritis and non-insulin dependent diabetes mellitus. It has been reported that complications associated with rheumatoid arthritis (RA), which include atherosclerosis, increased risk of MI, stroke, pericarditis, endocarditis, left ventricular failure, valvulitis and fibrosis are increased by 50% with the onset of RA, compared with healthy individuals (Aviña-Zubieta JA *et al*. 2008). Patients who suffer from non-insulin dependent diabetes mellitus also have an increased risk of cardiovascular complications, and this accounts for up to 50% of the deaths associated with this disorder (Chiasson JL *et al*. 2003).

The chemokine family is of interest as some members have been shown to have an effect in cardiac remodelling after MI, such as *Cxcr4*, which is the receptor for *Cxcl12* (*SDF-1*). *Cxcr4* has been treated selectively with AMD3100, which is a *Cxcr4* receptor anatagonist, and the results are a reduction in infarct size and improved ventricular function (Proulx C *et al*. 2007). There is also an association between changes in cytokine production and cardiovascular morbidity in renal and non-renal failure subjects. A SNP found in the Interleukin 6 gene, associated with an increase in plasma levels in patients undergoing dialysis and is linked to coronary artery disease and high blood pressure in healthy men (Humphries SE *et al*. 2001). *Cx3cr1*, a chemokine receptor which is a component of the inflammatory system, has been identified and its genotype shows an association with an increased susceptibility to cardiovascular disease (Moatti D *et al*. 2001).

Apolipoprotein E-deficient mice have been reported to have T-Cell and B-cell aggregates in segments of aortic adventitia, adjacent to atherosclerotic lesions. The aggregates are precursors to aortic tertiary lymphoid organs, which have a similar organization to lymph nodes. This provides evidence that aorta tertiary lymphoid organs organize the antigen-dependent T-cell and B-cell (auto)immune response to atherosclerosis. Also, smooth muscle cells underlying intimal plaques are activated and express the *Cxcl13* and *Ccl21* (Grabner R *et al*. 2009).

Cxcl13 has also been implicated in the quilty effect (QE), which is a feature of cardiac allograft, and is suspected of being associated with acute rejection. The

main feature of the cardiac allograft is a localised lymphocytic infiltration in the endocardium, which may also affect the myocardium. This alloantigen stimulation leads to an excess of *Cxcl13* production, which along with its receptor, *Cxcr5*, are found in the molecular pathway for both the QE and acute rejection (Di Carlo E *et al*. 2007). *Cxcl13* expression in the kidney is increased in aged animals, but barely detectable in young kidneys (Schiffe L *et al*. 2009), so further investigation in other tissues from the strains, and at older time points would clarify this. *Cxcl13* is selectively chemotactic for B cells, and interacts with its chemokine receptor *Cxcr5* to control the organization of B cells in the follicles of lymphoid tissues. Receptors are found selectively on surface of target cells, and *Cxcr5* is normally found on follicular dendritic cells. *Cxcl13* receptor analysis gene expression in heart RNA was carried out using Taqman qRT-PCR analysis in SHRSP, SP.WKYGla14a, WKY.SPGla14a and WKY strains. *Cxcr5* mRNA analysis of the heart would suggest that it is below the level of detection (Figure 3.12). The suggestion is that *Cxcl13* is not binding to *Cxcr5* in the heart tissue, which is not regarded as the typical function of this molecule, and would indicate that *Cxcl13* is signalling through one of the novel receptors. The results show expression of *Cxcr3* or *Ccrl1* when comparing WKY to SHRSP. The receptors have been implicated in a number of diseases including renovascular hypertension, non-insulin dependent diabetes mellitus, coronary restenosis and pristane induced arthritis.

Ventricular wall stress stimulates brain natriuretic peptide synthesis and release from cardiomyocytes, and this stress can also produce an increase in the levels of cytokines, such as tumor necrosis factor-alpha (TNF-α) or interleukin-6 (IL-6), which amplifies the signal due to it's pleiotropic effect (Nian M *et al*. 2004). A possible relationship has been established between increased blood pressure and LVH with inflammatory activation in patients with essential hypertension. This has been identified by a study of the altered profiles cytokines and receptors in patients with essential hypertension. A significant increase in the levels of plasma has been identified in hypertensive patients with LVH, when compared with non-LVH group, which is thought to be as a direct result of an increase in blood pressure, leading to an increase in mechanical stress (Roselló-Lletí E *et al*. 2009).

The exon array experiment was designed to investigate the possibility of alternative splicing in the chromosome 14 genes of the SHRSP, SP.WKYGla14a, WKY.SPGla14 and WKY strains. The *Clock* gene was implicated by Partek analysis of the array, and exon array signal intensity (Figure 3.3 & 3.4B). The subsequent analysis with PCR amplifications did not validate this finding. However, SNPs were found in the ORF (no change in amino acid), and the exon probe alignment to this region of the *Clock* gene showed that the probes were located over the SNP (position + 816 in the ORF) in exon 9. This explains the change in signal intensity (Figure 3.3B). The second SNP (position + 432 in the ORF) in exon 5 was discovered as a by-product of the PCR's to investigate the change in signal intensity in exon 9. On further analysis of the exon probes, it was found that they were not located in the area of the SNP. *Clock* is a circadian rhythm gene which is located within the QTLs for blood pressure, pristane induced arthritis, non-insulin dependent diabetes mellitus and for tongue tumour susceptibility. Normal BP measurements vary on a daily basis, and normotensive subjects will experience a decrease during sleep. Circadian rhythm genes are of great interest in the study of LVH as they have previously been linked to a non-dip in the ambulatory BP in hypertensive patients. Night time BP is used as an excellent prognostic tool for cardiovascular mortality, and is also connected to target organ damage (Verdecchia P. 2000). A model based on coupling clustering and binary classification of genes which allows discrimination between the different levels of response, has been developed. Through the use of canonical pathways, this has indicated circadian rhythm genes using ingenuity pathway analysis (Hopcroft LEM *et al*. 2010). This further supports the *Clock* gene and its role in BP control, and should be investigated further.

The exon array indicated the potential that SNPs possess, as several have been located within the strains analysed, and may provide a link to the effects they have on disease progression. However, the exon array provided a relatively few number of gene targets, which did not allow much potential for downstream investigation. On the basis of this, it was decided that an Illumina array should follow, as this would allow full investigation into the congenic regions of the Chromosome 14a rats, and the effect it has on the severe phenotype.

4. **Illumina microarray analysis of the heart: Gene expression profiling in chromosome 14a congenic strains in neonatal, 5 week old and 16 week old animals**

4.1 Introduction

In the previous chapter the Affymetrix exon array provided so few targets to follow up, and with the identification of significant phenotypic changes at early time points, it was decided that an Illumina microarray, which provides genome wide analysis, would be carried out with the incorporation of the earlier, neonatal time point. The earlier time point will be of interest as it should provide information on causative genes in hypertrophy, prior to the onset of disease. The phenotypic data, along with evidence from the literature lends itself to looking at gene expression at the neonatal time point, as differences are already established in the LVMI, Systolic BP, RWT and MPI data from the 5 week old rats. This would allow identification of genes which initiate left ventricular hypertrophy (LVH), and also allow identification of how those genes are involved in the progression of disease. As a result of the inclusion of this time point, it is essential to have an understanding on the development of the pre-natal heart, and how it changes post-natal. The heart is the first functional organ in the body, and allows for gas exchange systems to develop in the placenta. The pre-natal heart mainly uses anaerobic glycolysis as its source of energy, and post-natal, this will switch to aerobic metabolism of non-esterified fatty acids as its source of energy (Kinnula VL & Hassinen I. 1977; Clark CM. 1971). For this transition to take place, maturation of the mitochondria must occur, and the levels of fatty acids and lactate circulating must increase (Lopaschuk GD *et al*. 1992). Fewer mitochondria are a characteristic of immature myocytes, as is lower activities of the enzymes of the tricarboxylic acid cycle and electron transport chain. Total creatine and phosphocreatine, along with creatine kinase (CK) activity are also increased during the period of cardiac cell maturation. CK catalyses creatine to convert to phosphocreatine, and consumes adenosine triphosphate (ATP). Phosphocreatine is used as a buffering system to allow the rapid buffering and regeneration of ATP in cells with high levels of energy consumption. CK is also used as a biomarker for MI. SHR and WKY rats have been studied at 1 day old, 11 days and 12 weeks and it was shown that there are significant changes in systolic, diastolic, and mean pressures in SHR neonates. Heart rate and heart weight/body weight ratios also show an increase, and confirm that heamodynamic and physiological parameters of both early and advanced stages of hypertension, which are significant in adult

rats, are already altered at birth (Gray SD. 1984). Hypertrophy in the heart is a structural consequence of one or more factors, which include an increase in the number of myocytes, an increase in the size of myocytes, and the amount of connective tissue elements or vasculature. Cardiac hypertrophy is a complex biological process which involves remodelling of the architecture of the heart, which may be in response to an increase in the work load. The stimuli for this process appear to be both mechanical and humoral in nature. It has also been shown that early onset of LV volume overload, with hypertrophy, leads to a delay in the switch from anaerobic to aerobic metabolism in the neonatal heart (Kantor PF *et al*. 1999). As the neonatal SHR rats are exposed to elevated blood pressures, development of cardiac hypertrophy may only be temporally and quantitatively accelerated. Studies have shown that haemodynamic changes account for only a small proportion of the left ventricular mass (LVM) and genetic effects may be of greater influence. It has been proven that gene expression is heritable and genetic control of transcription can have an effect on both physiological traits and disease phenotype (Hubner N *et al*. 2005). Gene transcription in the heart is also heritable, and is thought that this may have a role in the control of LVM regulation (Petretto E *et al*. 2006).

The neonatal time point will be investigated through a genome-wide gene expression profiling. The Illumina RatRef microarray uses in the region of 22,500 probes for analysis of expression profiling. The direct hybridization assay utilises gene specific probes, which are designed using a multi-step algorithm to optimize several parameters including a lack of similarity to other genes, absence of highly repeated sequence in the genome, sequence complexity, self-complementarity for hairpin structure prediction, melting temperature for hybridization uniformity and distance from 3' end of the transcript. The bead system uses oligonucleotides, immobilized in microwells and randomly distributed across the array substrate. A 60-mer address sequence on each bead is used for a hybridization based procedure to map the array, and operates with a single probe per gene, which is in contrast to the Affymetrix exon array, utilising up to 4 probes per gene.

Previous measurements from our laboratory in neonatal rat hearts taken at sacrifice demonstrate differences in heart weight/body weight ratio in SHRSP and also in the chromosome 14 congenic strains. Although the results are not significant, there is a trend towards heavier hearts in SP.WKYGla14a compared to SHRSP, and WKY weighing more than WKY.SPGla14a (Figure 4.1A). Body weight does not change across the 4 strains (Figure 4.1B), when the heart weight/body ratio is considered, the same trends are observed (Figure 4.1C). Only WKY heart weight/body weight ratio is significantly increased, when compared to SHRSP.

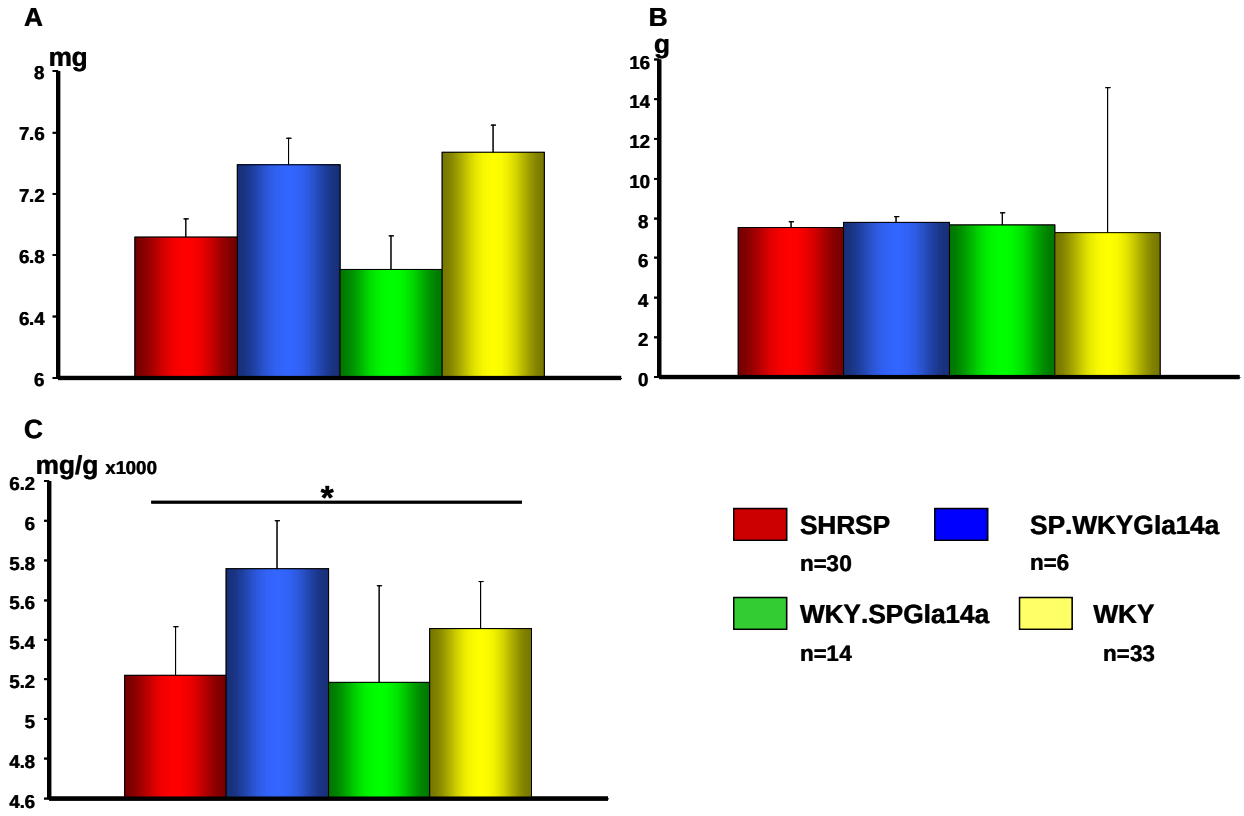

Figure 4.1 Weights of neonatal rats in the SHRSP, SP.WKYGla14a, WKY.SPGla14a and WKY
A) Heart weight of neonates (measured in g). B) Body weights of neonates (measured in g). C) Ratio of heart weight to body weight in neonates. *$p<0.05$

As this suggests the weight of the heart is not changing between the strains, functional experiments in the neonatal heart will investigate the cellular effects of hypertrophy, specifically on isolated fibroblasts and cardiomyocytes, as it is important to understand the different cell types, and their response to stimulation and trauma. Growth and development of the ventricle during the early stages of foetal and neonatal, depends largely on 3 phases of changes which occur in the cardiomyocyte population (Clubb FJ & Bishop SP. 1984). As cardiomyocytes stop proliferating at around 3-5 days after birth, it is essential to isolate cells prior to this. ANG II promotes cardiomyocyte hypertrophy, and drives up blood pressure by initiating systemic vasoconstriction, so stimulation of our isolated cardiomyocytes with increasing concentrations of ANG II, and gene expression analysis of RNA extracted from the cells will inform as to how the different strains respond to this treatment. Phalloidin staining which is designed to stain cells and allow for accurate sizing will be used to investigate the effects of ANG II stimulation on cardiomyocytes. As cardiomyocytes are a major cause of remodelling in the heart, sizing of these cells in the SHRSP and WKY strains will identify if this is a possible cause for the severe phenotype of WKY.SPGla14a, and define if there is a link to hypertrophy. The scratch assay is designed to study cell migration, and to some extent, it mimics how cells migrate, and react to tissue trauma, *in vivo*. Fibrosis is the formation or development of excess fibrous connective tissue, normally as a reparative or reactive process, so the scratch assay should give an indication to how the different strains are responding, and their potential fibrotic build up. To confirm any differences in cell migration is due to cell migration and not to the cells growing, the cell proliferation assay (MTT assay) will be performed on cells treated in the same way as those in the scratch assay. These techniques should provide a valuable insight into the functional aspects of hypertrophy in the SHRSP, SP.WKYGla14a, WKY.SPGla14a and WKY strains.

4.2 Methods

4.2.1 TotalPrep RNA Amplification

RNA amplification for array analysis was prepared using the Illumina® TotalPrep RNA Amplification Kit (AMIL1791). Before proceeding, RNA was analysed for purity to ensure the RNA was free of contaminating proteins, DNA, phenol ethanol and salts involved in the RNA isolation procedure. Ratio of A_{260} to A_{280} should fall in the range of 1.7-2.1. Integrity was analysed using the Agilent® 2100 bioanalyzer, and ensured the RNA sample is full length, and short samples may produce small cDNA's which may potentially lack a portion of the coding region. The RNA Integrity Number (RIN) is calculated by analysing information from both the RNA bands and RNA peaks (potential degradation) and provides a more complete overview of the condition of the RNA. Typically, a RIN value of 8.0+ was deemed acceptable for further work on the sample. Examples of the agilent graphs are in the appendix (Figure A.1A). Throughout this procedure, it is important to use RNase free tubes, RNase free Rainin tips, pipettes which have been cleaned thoroughly with RNase Zap and Nuclease free water. Incubations were performed using an MJ Research PTC Gradient Cycler. RNA samples were diluted to 45.45ng/µl, and the concentration confirmed by nanodropping each sample in triplicate. Reverse transcription mastermix is comprised of the following reagents to synthesize first strand cDNA:

Reverse Transcription	vol in µl
T7 Oligo(dT) Primer	1
10X First strand buffer	2
dNTP Mix	4
RNase Inhibitor	1
Arrayscript	1
Diluted RNA	11

The mix was pipetted up and down 2-3 times, flicked 3-4 times, and centrifuged briefly to collect at the bottom of the tube. The reaction is incubated for 2 hours at 42°C, with the lid temperature set to 16°C or the lid temperature disabled. The reaction was placed on ice before proceeding with the Second strand cDNA synthesis. Second strand cDNA synthesis master mix was prepared on ice as follows:

Second Strand Synthesis	vol in µl
Nuclease free water	63
10X Second strand buffer	10
dNTP Mix	4
DNA polymerase	2
RNase H	1

The second strand master mix was added to the reverse transcription reaction, pipetted up and down 2-3 times, flicked 3-4 times, and centrifuged briefly to collect at the bottom of the tube. The mix is incubated for 2 hours at 16°C. The reaction was placed on ice before proceeding with the cDNA purification. 250µl cDNA binding buffer was added to each sample and pipetted up and down 2-3 times, flicked 3-4 times, and centrifuged briefly to collect at the bottom of the tube. The cDNA sample/cDNA binding buffer was applied to the centre of a cDNA filter cartridge (seated in a wash tube, supplied with the kit), and centrifuged for 1 minute at 10,000g. The flow through was discarded and the cDNA filter cartridge replaced in the wash tube. 500µl wash buffer (supplied with the kit, and adjusted to volume with 100% EtOH (Sigma 200 proof)) was applied to the cDNA filter cartridge and centrifuged for 1 minute at 10,000g. The flow through was discarded and the cDNA filter cartridge was placed in an elution tube. 20µl of nuclease free water (preheated to 55°C) was applied to the cDNA filter cartridge, and incubated for 2 minutes at room temperature, then centrifuged for 1 minute at 10,000g. The eluate was transferred to 0.5ml

RNase free PCR tube. *In Vitro* transcription (IVT) synthesis of cRNA master mix was prepared on ice as follows:

In Vitro transcription	vol in µl
T7 10X reaction buffer	2.5
T7 enzyme mix	2.5
Biotin-NTP mix	2.5

Biotin-NTP is used at it biotinylates the nucleic acids, and also binds with high affinity to streptavidin, which in a Cy3 labelled form, is used downstream as a means of detecting the signal from the hybridization of the cRNA to the BeadChip. The IVT master mix was added to each cDNA sample, pippetted up and down 2-3 times, flicked 3-4 times, and centrifuged briefly to collect at the bottom of the tube. The reaction was incubated for 14 hours at 37°C, then for up to 48 hours at 4°C. The reaction was quenched by the addition of 75µl of nuclease free water, and placed on ice before proceeding immediately to the cRNA purification step. 350µl of cRNA binding buffer and 250µl of 100% EtOH (Sigma 200 proof) was added to each sample, and pipetted up and down 2-3 times. The cRNA/100% EtOH mix was applied to a cRNA filter cartridge, and centrifuged for 1 minute at 10,000g. The flow through was discarded and the cRNA filter cartridge replaced in the collection tube. 650µl of wash buffer was applied to the cRNA filter cartridge and centrifuged for 1 minute at 10,000g. The flow through was discarded and the cRNA filter cartridge replaced in the collection tube. The cRNA filter cartridge was centrifuged for an additional 1 minute at 10,000g to remove any traces of the wash buffer, and was placed in a clean collection tube. 200ul of nuclease free water (preheated to 55°C) was applied to the cRNA filter cartridge, and incubated for 10 minutes at 55°C, then centrifuged for 1.5 minute at 10,000g. The samples were assessed by nanodropping and Agilent® 2100 bioanalyzer, and had to pass stringent checks before proceeding to hybridization to the BeadChip. An example of the shape of bell shaped curve expected is in the appendix (Figure A.1B). The samples were diluted to 150ng/µl, and the concentration confirmed by nanodropping each sample in triplicate.

4.2.2 Hybridization to the BeadChip

The hybridization buffer and humidity control buffer (HCB) were heated at 58°C for 10 minutes to dissolve any salts, and cooled to room temperature before use. The BeadChip Hyb chamber apparatus was set up, and 200µl was added to each well, and the apparatus lid was applied and left at room temperature. The BeadChips were removed from the packaging and placed on the Hyb chamber insert. 5µl of the diluted cRNA was added to 10µl HYB buffer, and heated for 5 minutes at 65°C, vortexed, pulse centrifuged and allowed to cool to room temperature. The sample mixes were then applied to the inlet ports on the BeadChip, the BeadChip was loaded into the Hyb chamber, and incubated for 16 hours at 58°C, with rocking. A 1X High-Temp wash buffer was prepared, and placed in the hybex waterbath insert within the hybex heating base, which was set to 55°C overnight. The BeadChips were removed from the Hyb chamber, and submerged face up in a pyrex beaker containing wash E1BC buffer, and the coverseal removed carefully, then placed in a slide rack in a wash chamber containing wash E1BC buffer. The slide rack was placed in the hybex waterbath, and the BeadChips were incubated for 10 minutes at 55°C. The slide rack was removed, and placed in the wash chamber containing wash E1BC buffer used previously, and plunged in and out of the buffer 5 to 10 times, then placed on an orbital shaker for 5 minutes at room temperature. The rack was removed and placed in a staining chamber containing 250ml 100% EtOH (Sigma 200 proof) and plunged in and out of the buffer 5 to 10 times, then placed on an orbital shaker for 10 minutes at room temperature. The rack was removed and placed in a staining chamber containing 250ml of fresh wash E1BC buffer and plunged in and out of the buffer 5 to 10 times, then placed on an orbital shaker for 2 minutes at room temperature. 4ml of Block E1 buffer was added to individual wash trays, and the BeadChip was placed in it, face up, using tweezers, then the wash tray was placed on an orbital shaker for 10 minutes at room temperature. Streptavidin-Cy3 was diluted to 1:1000 with Block E1 buffer, and placed in a clean individual wash tray. Streptavidin-Cy3 acts as secondary agent to the biotinylated cRNA hybridized to the BeadChip, and is used to detect the intensity of this signal. The BeadChip was transferred to the wash tray and then this was placed on an orbital shaker for 10 minutes at room temperature. The BeadChip was transferred to a slide rack placed in a clean staining dish containing 250ml fresh wash E1BC buffer, and plunged in and out of the buffer 5

times, then placed on an orbital shaker for 5 minutes at room temperature. The BeadChip was then dried by placing the slide rack on clean paper towels, and placing in plate holder, and centrifuging at 275 g for 4 minutes at room temperature. The dried BeadChips are then transferred to the Illumina BeadArray Reader to scan, and the output data is visualised using Beadstudio software.

4.3 Results

4.3.1 Illumina Microarray of neonatal, 5 week and 16 week hearts of SHRSP, WKY and chromosome 14a congenic strains.

The Illumina microarray and Partek analysis was carried out using RNA extracted from the same 5 & 16 week of age rats previously used in the Affymetrix exon array from the hearts of the chromosome 14a congenic strain animals, along with the parental SHRSP and WKY strains (Results Chapter 3). Neonatal hearts of the same strains were subjected to the same handling and RNA extraction conditions as the previous samples. The neonatal, 5 & 16 week of age time points investigate the potential for differential gene expression, with the progression of disease, and allow identification of genes which may be expressed prior to the onset of disease, thus having a causative effect. The data for each strain was filtered in a venn diagram and the resulting area of intersect for the four strains indicate genes which are common (Figure 4.2). The results of the neonatal microarray indicate 4 significantly differentially expressed positional genes. These are Osteopontin (*Spp1*), Hydroxysteroid (17-beta) dehydrogenase 13 (*Hsd17b13*), Zinc finger protein (*Zfp644*), which are all located within the congenic region of chromosome 14a strains, and Ras-related associated with diabetes (*Rrad*) which is located on chromosome 19. *Spp1's* expression in cardiomyocytes coincides with heart failure development from hypertrophy (Singh K *et al*. 1999). This is of particular interest as *Spp1* has also been implicated to an increase in LVMI, a precursor to LVH, which is a phenotypic characteristic of the SHRSP and WKY.SPGla14a congenic strain. Signal intensities of each probe implicated in the microarray has been analysed across the 3 time points used. The results show that *Spp1* expression is showing greater variability in the neonates (Figure 4.3). The increased signal intensity in SHRSP relative to SP.WKYGla14a, and increased signal intensity in WKY.SPGla14a relative to WKY is a similar profile to that of the LVMI measurements, which is interesting as it would suggest that there may be a link between the phenotypic data and the *Spp1* expression. The *Spp1* signal appears to have decreased at 5 weeks of age, with no difference in signal intensity. The other genes identified appear to have no apparent links to LVH, and while still of interest, will not be focussed on in this project.

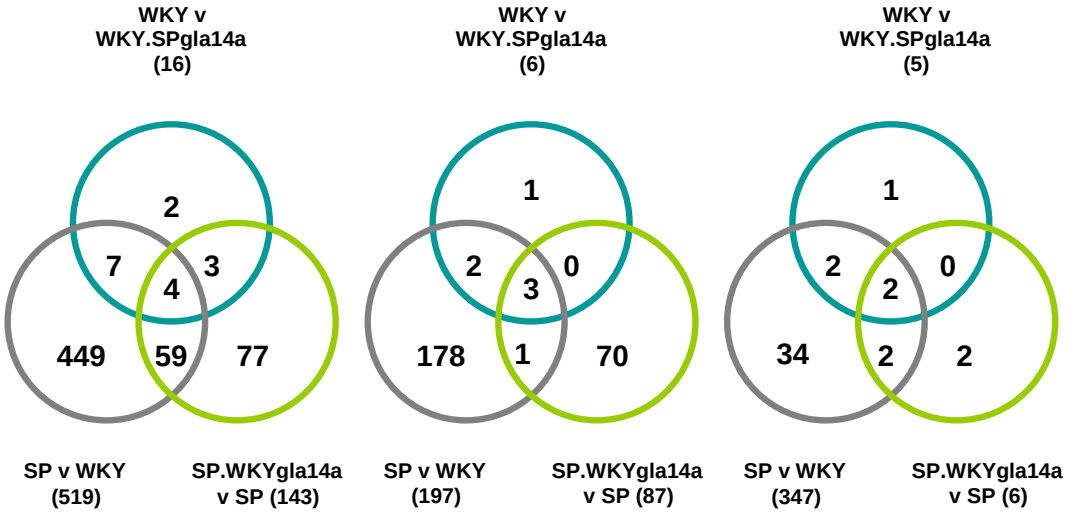

Figure 4.2 Microarray analysis of the A) neonatal, B) 5 week and C) 16 week SHRSP, WKY, SP.WKYGla14a and WKY.SPGla14a strains.
Venn diagrams illustrating microarray results of gene expression profiles in the heart of rats. The number of probes significantly differently expressed for each time point in each pair wise comparison are shown in the areas of intersect on the venn diagrams.

Table 4.1 Genes which have been implicated in the microarray, across the time points
Genes are shown which have been implicated by the microarray at each time point, and their chromosome position has been identified.

Time point	Gene	Chromosome locus
Neonatal	Osteopontin	14: 6,422,741-6,426,400
	Hydroxysteroid (17-beta) dehydrogenase 13	14: 6,901,197-6,917,228
	Zinc finger protein	14: 3,645,610-3,720,694
	Ras-related associated with diabetes	19: 272,791-275,957
5 week	chemokine (C-X-C motif) ligand 13	14: 15,126,337-15,131,368
	Hydroxysteroid (17-beta) dehydrogenase 13	14: 6,901,197-6,917,228
	LOC498327	
16 week	Arhgap24	14: 8,026,136-8,346,326
	LOC498329	

Principal component analysis (PCA) is a mathematical procedure which can transform a number of closely related variables into a number of uncorrelated variables called principal components, which are still related to the original variables. This transformation is handled so that the first principal component has as high a variance as possible (to account for as much of the variability in the data as possible). Each component which follows has the highest variance possible with the condition that it must be orthogonal to the previous components (Jolliffe IT. 2002). This is then taken into account when we build the ANOVA model. The experimental samples were randomised across 4 array chips, and introduce another aspect to the variables which can be accounted for with the PCA analysis. The PCA mapping shows that there is a minor chip bias (Figure 4.3A), which is confirmed by PCA mapping of the sample groups, as this shows grouping of the each strain at each time point, which is to be expected (Figure 4.3B). The PCA plot allows for an assessment to be made of the experimental and technical aspects of the array.

The signal intensities of the microarray probes of the neonatal targets (*Spp1, Hsd17b13, Rrad & Zfp644*) were plotted to identify differences between the strains, and to confirm which targets should be prioritised for further analysis. The intensity profile of *Spp1's* mirrors the profile of the LVMI data previously generated, and the signal intensity profiles of the other neonatal targets (*Hsd17b13, Rrad & Zfp644)* are shown (Figure 4.4 B, C & D). The initial analysis will be validation of the microarray by gene expression studies.

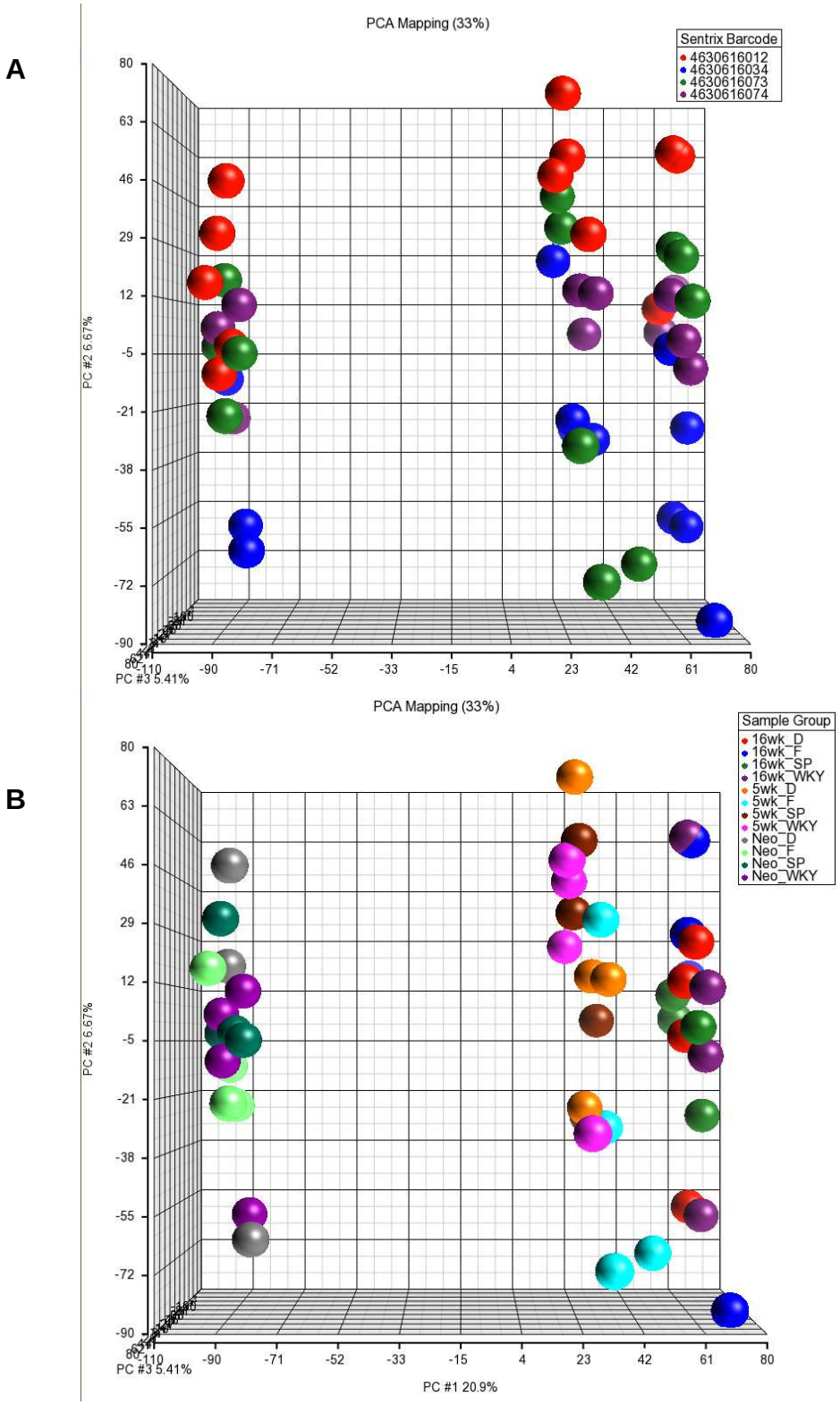

Figure 4. 3 Principal component analysis mapping of the Illumina microarray data
A) Overlaying the PCA plot with the sentrix barcode indicates a bias has occurred in the microarray experiment. This means a sample may show a bias, depending on the chip it is hybridized to. B) Overlaying the PCA plot with the sample group data confirms the bias caused by chip location of each sample.

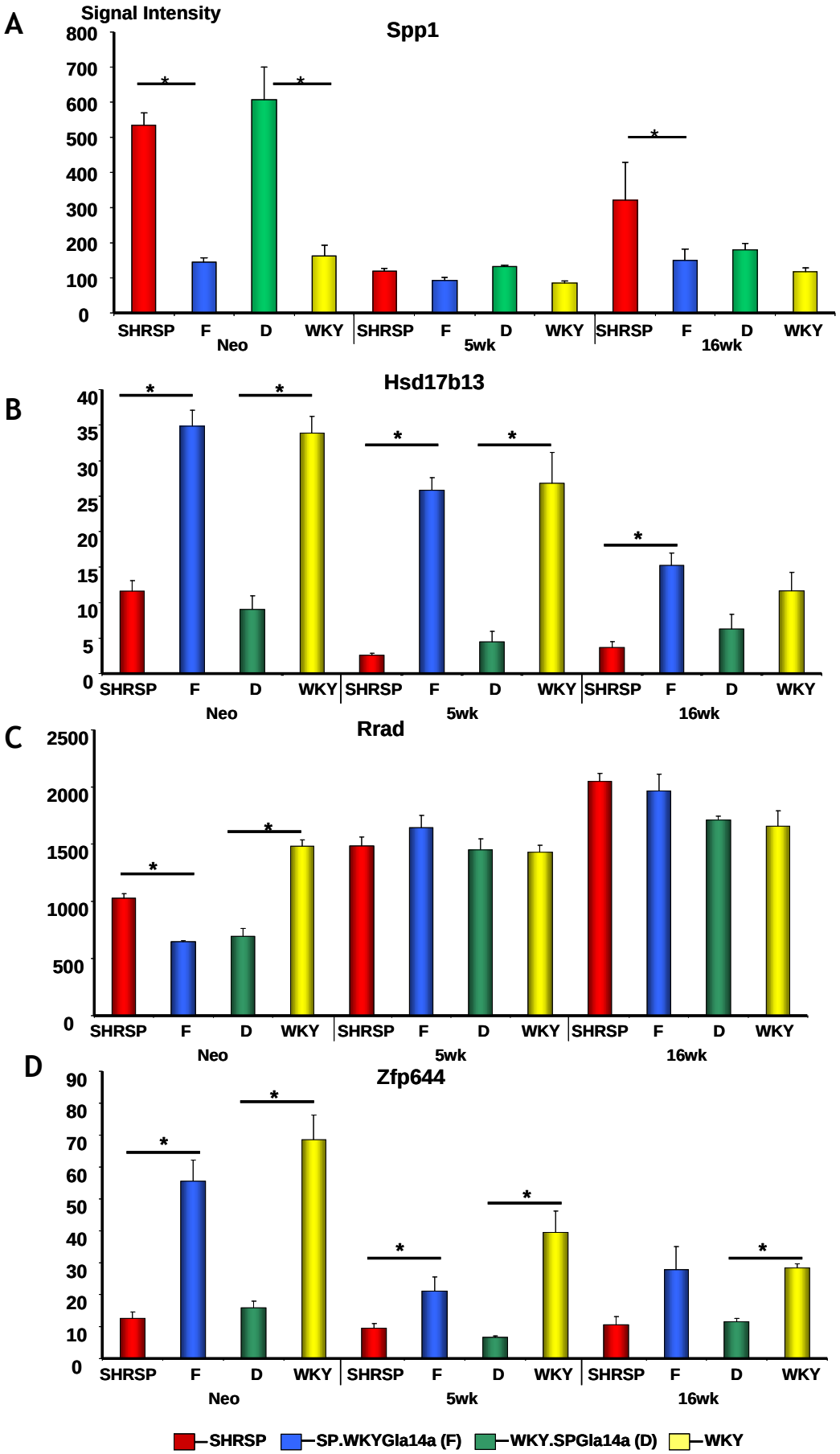

Figure 4.4 Microarray signal intensities of target genes in neonatal, 5 week and 16 week SHRSP, SP.WKYGla14a, (F) WKY.SPGla14a (D) and WKY strains.

The graphs show the microarray signal intensities of the genes identified in neonatal hearts. The intensities have been shown at the 5 week and 16 week time point. A) *Spp1*. B) *Hsd17b13*. C) *Rrad*. D) *Zfp644*. n-4 *p<0.05

4.3.2 Validation of microarray targets by qRT-PCR in neonatal hearts

Validation of the Illumina microarray gene targets focussed mainly on the neonatal time point. The 5 & 16 week of age gene expression was also performed to validate the signal intensity profiles (Figure 4.4). *Spp1* has been validated through the use of 2 probes (labelled Rn00681031_m1 & Rn00563571_m1) sitting on different exon boundaries, with both giving similar results. In the neonatal hearts, gene expression levels identified by the microarray validate the signal intensity (Figure 4.5A). *Arhgap24* was also included in the validation, as it has been implicated at the 16 week time point, and it is also located on chromosome 14, within the congenic region. It is also shown to have a difference in expression in the analysis of the 5 week WKY compared with WKY.SPGla14a. Due to technical problems which occurred with the samples, validation of the 5 week data is incomplete. *Spp1* was the only gene to be investigated at the 5 week of age time point and large error bars are present (Figure 4.5B). The 16 week data has also proved problematic to validate (Figure 4.5C). Large error bars are seen on both the 5 week and 16 week gene expression graphs (Figure 4.5B & C) which was due to technical and biological issues with the housekeeping gene (GapDH). *Zfp644* was not analysed during these experiments as a suitable Taqman probe was not available at the time. Comparisons were analysed using the student's pair wise t-test.

The qRT-PCR results confirm the findings of the neonatal signal intensity analysis of the microarray data of *Spp1* (Figure 4.4A). The gene expression profiles of the other target genes confirm the signal intensities in the neonatal hearts (Figure 4.4 B, C &D) and follow the origin of the Chromosome 14a strains, and this supports the hypothesis that one or more of these genes may contribute to the hypertrophic phenotype. Further investigation of the *Spp1* gene was prioritised as it was the top hit from the microarray. This will be carried out through sequencing, both of the coding region and the regulatory regions. This will illustrate any SNPs which may be contributing to the change in gene expression of *Spp1*, in the comparison between the chromosome 14a congenic strains and the parental strains.

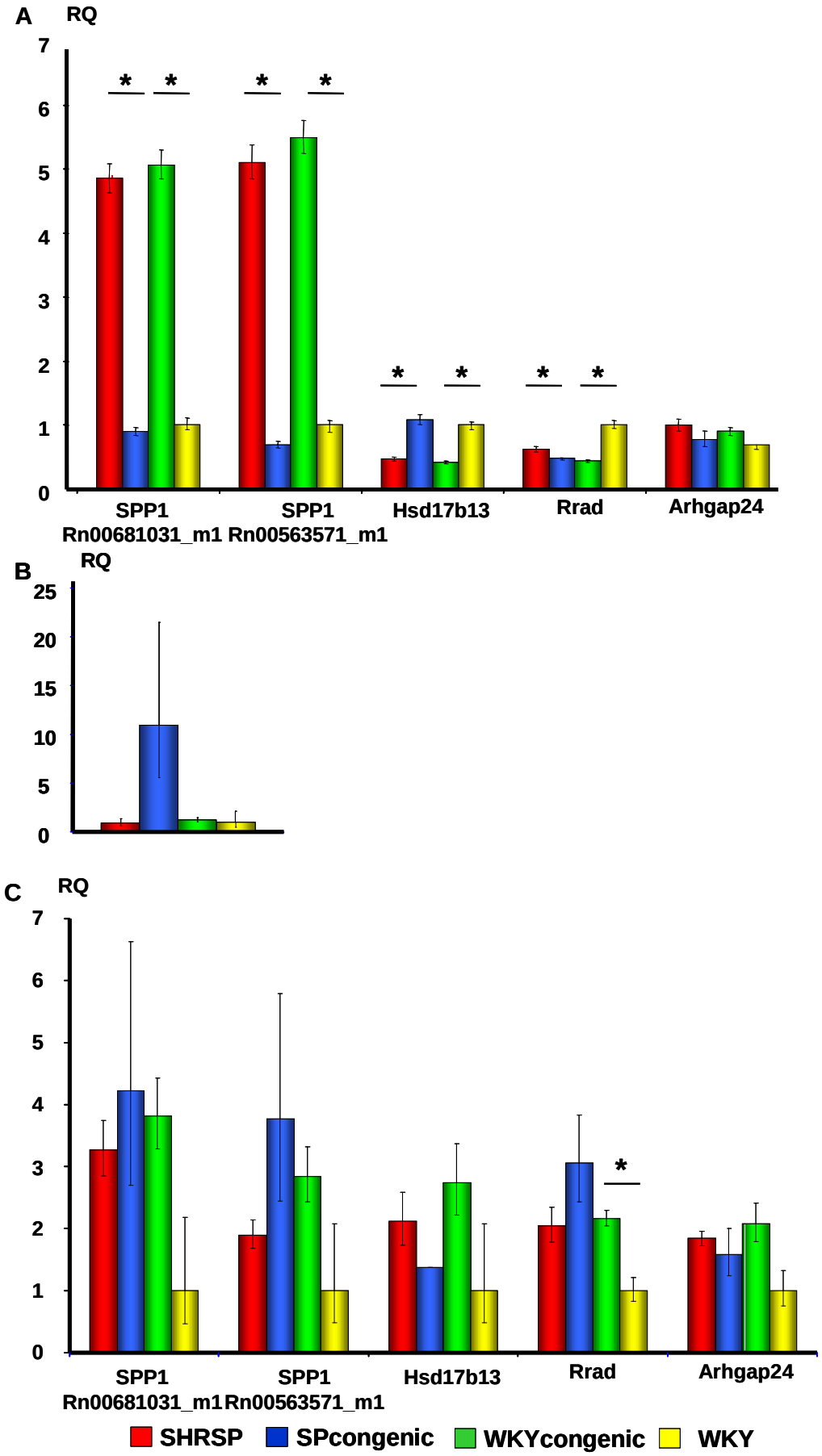

Figure 4.5 Validation of microarray with mRNA expression in SHRSP, SP.WKYGla14a, WKY.SPGla14a and WKY at the A) neonatal, B) 5 week and C) 16 week time points in the heart
Expression is shown as an RQ value of SHRSP. A) Neonatal expression of microarray probes B) 5 week Spp1 expression. C) 16 week expression of microarray probes. n-4 *p<0.05.

4.3.3 *Spp1* Primer design and sequencing

Primers were designed to cover the ORF of the *Spp1* gene, PCR was carried out, and the amplified products were sequenced and aligned to Brown Norway sequence using Seqscape v2.1. The 5' upstream region of *Spp1* is not well annotated, so to facilitate the primer design and subsequent sequencing, an alignment was carried out of 7 common mammals, and primers were designed to the conserved areas of sequence. The mus musculus strain was chosen as the focus for the design, as it shares the greatest homology with the rat. The primers were chosen carefully, locating areas of greatest homology (Figure 4.7). The section of sequence shown represents a small part of the alignment generated. A single reverse primer was designed which was rooted in the first exon of the ORF, to ensure the products amplified were in the upstream region of *Spp1*. The sequence generated was then used to design further primers to ensure full coverage of the upstream region of the *Spp1* gene. The PCR products were then cloned and transformed into a strataclone blunt ended vector, and positive inserts were chosen by blue/white colour selection. The DNA from the cloned products was checked by PCR and sequencing to confirm the correct insertion and orientation had been achieved. This alignment was useful in identifying conserved nucleotides (Figure 4.7). Despite the alignment, a number of primer designs had to be implemented to successfully amplify the *Spp1* upstream region in the SHRSP and WKY. The primer locations for the ORF and 5' upstream region are shown (Figure 4.6). SNPs found in the 5' promoter and ORF are shown (Table 4.2), and the SNP causing the amino acid change is illustrated in a screenshot of the Seqscape analysis (Figure 4.8).

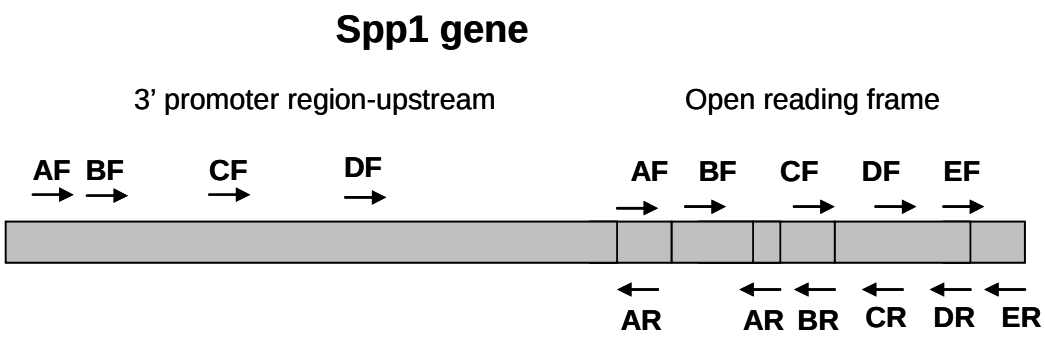

Figure 4.6 Schematic of *Spp1* open reading frame and proposed 5' promoter region

The primer positions are marked onto the schematic drawing to show their location. The reverse primer for the alignment of 7 different species upstream region of *Spp1*shows the reverse primer has been rooted in the first exon of the open reading frame.

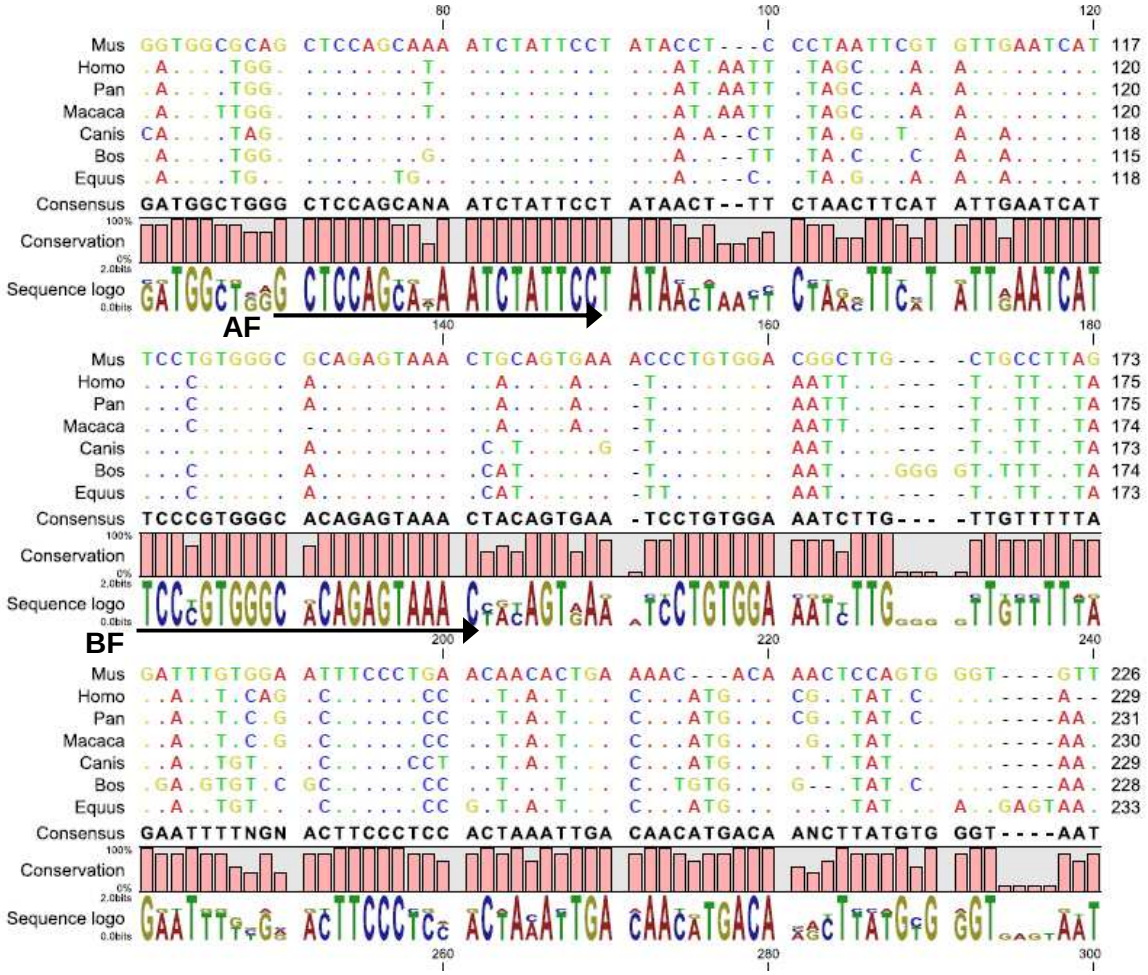

Figure 4.7 Alignment of the 7 eutherian mammals, to generate primers to sequence unknown *Spp1* promoter region in Rat.

2000 base pairs from 7 mammals of the 5' upstream region of *Spp1* were aligned using CLC software. Each base is represented by a different colour. The coloured dots are used to indicate a base which is conserved from the mouse to the other strains. A difference in base is annotated by the appropriate letter in place of a dot to indicate the base has not been conserved in that location between the mouse and other mammals. The conservation bar chart beneath the alignment represents the amount of homology between the mammals. The alignment shows the conserved regions between the 7 mammalian strains which were used for the primer design. The arrows labelled AF and BF are 2 of the primers designed to cover the region. The primer design followed standard rules, i.e. ~50% GC content, and avoiding a poly A tail.

Table 4.2 Positions of SNPs in the upstream region and ORF of *Spp1*

The positioning of the SNPs identified in the 5' upstream region and the ORF of the *Spp1* gene, and the differences when comparing the sequence derived from the PCR products with that of the Brown Norway. It also indicates if any amino acid changes have occurred as a result of the SNP.

Position from ATG	Brown Norway	SHRSP	WKY	Change in aa
1301	G	T	G	-
1915	G	A	G	-
+450	C	C	T	-
+559	A	C	A	Yes:Isoleucine ->Leucine

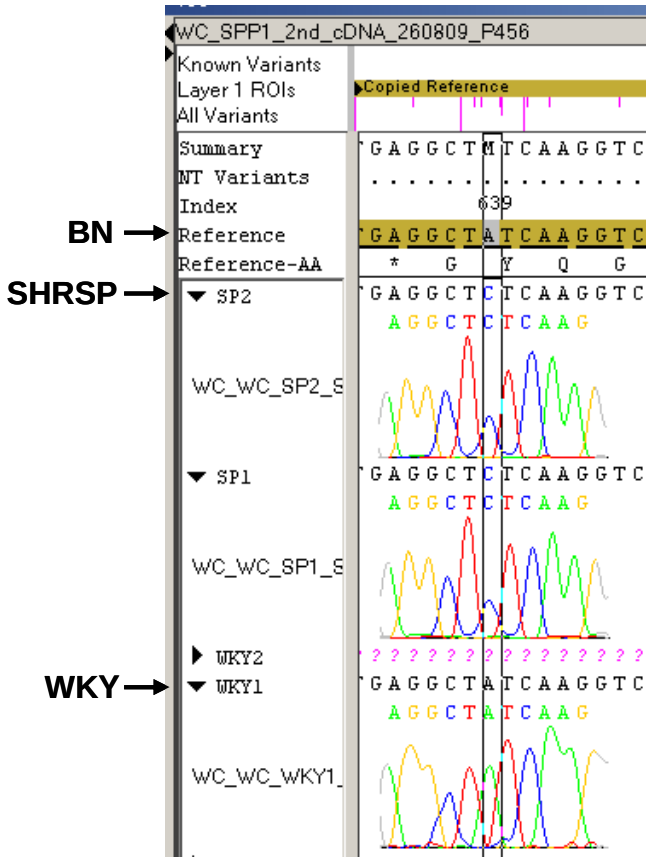

Figure 4.8 SNP found in *Spp1* open reading frame

A screenshot of the Seqscape v2.1 analysis of *Spp1* open reading frame, showing the +559 (from ATG) SNP (A→C), which causes a change in amino acid (WKY-I →SHRSP-L).

4.3.4 Functional experiments of hypertrophy

In this section, functional experiments have been applied to heart cardiomyocytes and fibroblasts isolated from neonatal hearts from the SHRSP, SP.WKYGla14a, WKY.SPGla14a and WKY strains. Expression of the *Spp1* gene is analysed in cardiomyocytes and fibroblasts of the parental strains. The qRT-PCR results confirm *Spp1* gene expression is significantly higher in SHRSP cardiomyocytes, when expressed relative to SHRSP fibroblasts (Figure 4.9). Expression of *Spp1* is assessed in neonatal cardiomyocytes in the SHRSP, WKY and chromosome 14a congenic strains, which have been stimulated with increasing concentrations of ANG II. ANG II promotes cardiomyocyte hypertrophy, and drives up blood pressure by initiating systemic vasoconstriction, so it is expected that an increase in *Spp1* expression in cardiomyocyte cells will be detected, with increasing ANG II concentrations. *Spp1* expression in SHRSP cardiomyocytes was unable to be determined, as expression levels of the housekeeping gene GapDH were extremely low for these samples, meaning a full analysis of this strain could not be completed. Expression of *Spp1* in the WKY and WKY.SPGla14a, with increasing concentrations of ANG II is not significantly different. *Spp1* expression in ANG II stimulated SP.WKYGla14a cardiomyocytes is found to be significantly higher with the 150nM and 200nM concentration, when compared to the WKY control (Figure 4.10E). Phalloidin staining was performed on SHRSP and WKY cardiomyocytes (an example of which is seen in Figure 4.10D) which have been stimulated with increasing concentrations of ANG II (0, 50nM, 100nM, 150nM and 200nM). This assay is designed to stain cells and allow for accurate sizing. Cardiomyocytes are a major cause of remodelling in the heart, so sizing of these cells in the SHRSP and WKY strains will identify if this is a possible cause for the extreme phenotype, and a link to hypertrophy. The results show that when stimulated with ANG II, SHRSP cardiomyocytes significantly increase in size (Figure 4.10A). WKY cardiomyocytes stimulated with ANG II show an increase in cell size from the addition of 100nM upwards (Figure 4.10B). When the cardiomyocytes sizes are compared between SHRSP and WKY, WKY cells are significantly larger than those of SHRSP at all concentrations of ANG II, including in the the non ANG II stimulated control (Figure 4.10C). This does not suggest that the increase in WKY cells is due to hypertrophy, but rather that this occurs naturally.

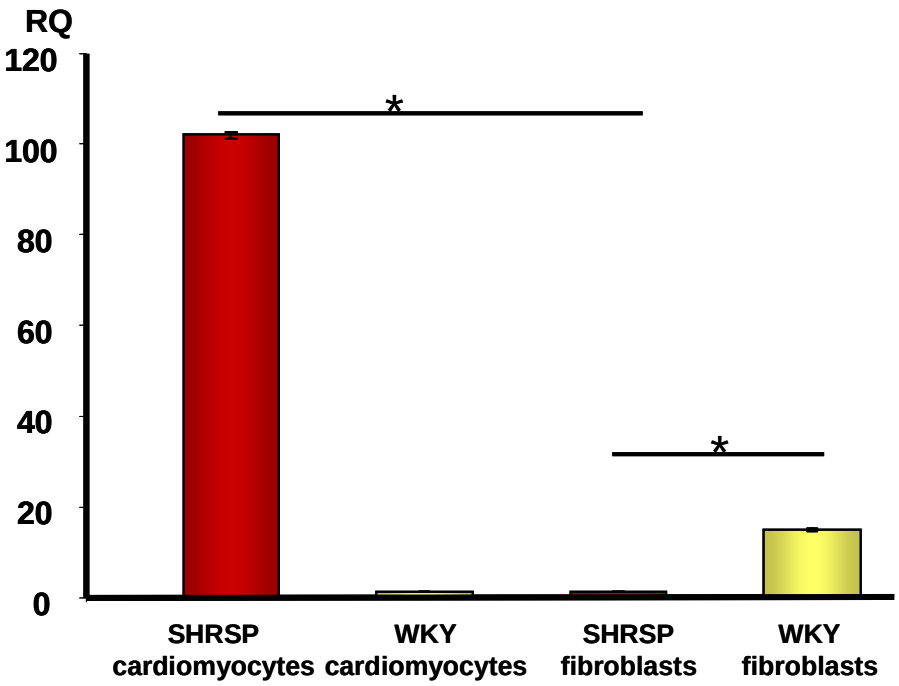

Figure 4.9 *Spp1* expression in the SHRSP and WKY cardiomyocytes and fibroblasts
qRT-PCR measured by Taqman in neonatal rat heart cells relative to GapdH and calibrated to expression in the SHRSP fibroblasts, n-3. * $p<0.05$

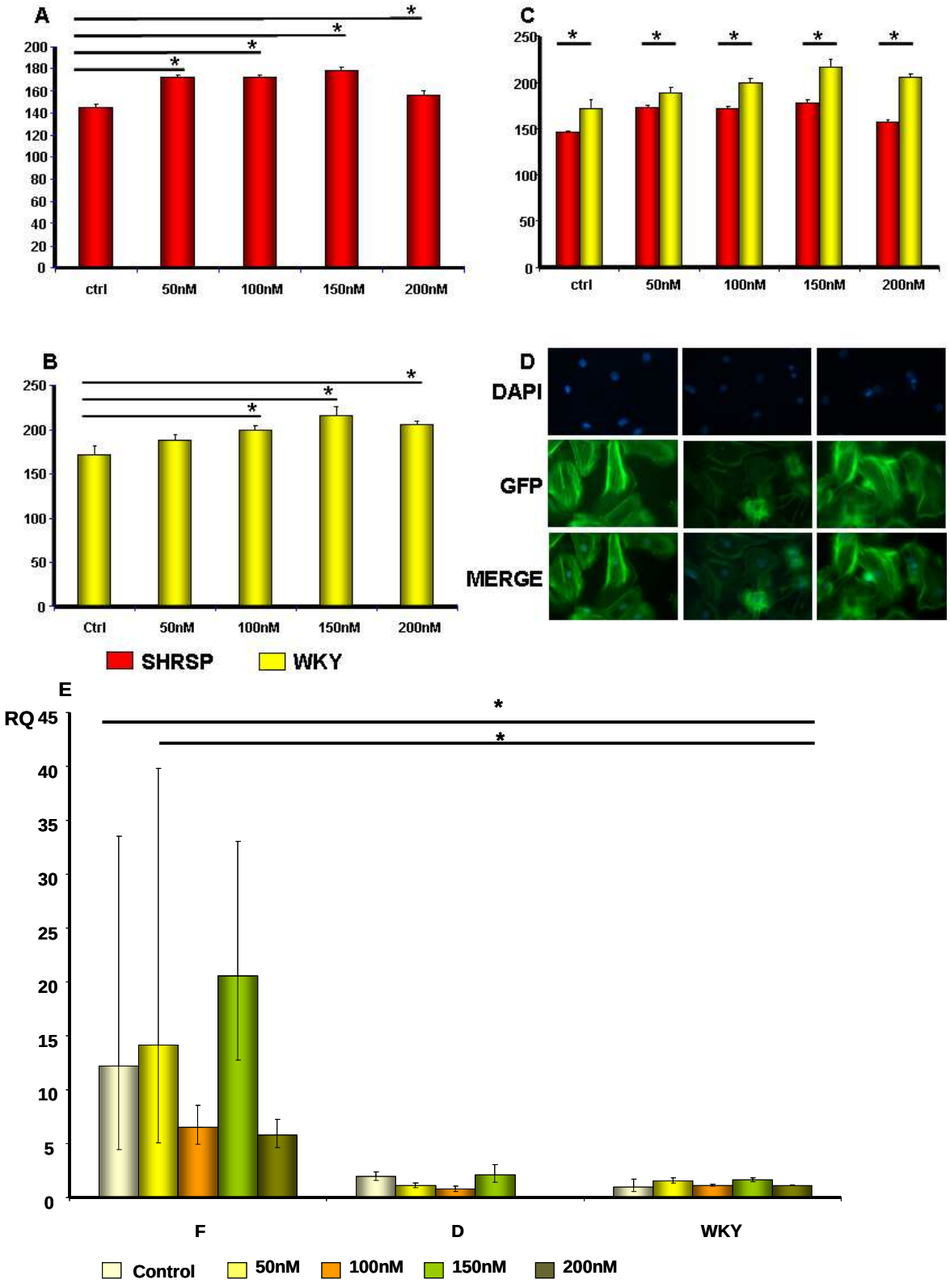

Figure 4.10 Cell sizing of SHRSP and WKY cardiomyocytes, and *Spp1* expression in ANG II stimulated SP.WKYGla14a, WKY.SPGla14a and WKY cardiomyocytes

A) ANG II stimulation of SHRSP cardiomyocytes, of all concentrations, significantly increases the size of the cell. B) ANG II stimulation of WKY cardiomyocytes, of 100nM, 150nm, and 200Nm concentration, significantly increases the size of the cell. C) Comparing the cell size of SHRSP and WKY, there is a significant increase in size of WKY. All sizes were measured in microns D) Some examples of Phalloidin staining in cardiomyocytes. E) *Spp1* expression in ANG II stimulated cardiomyocytes. A, B&C n-3 E n-1 * $p<0.05$.

The scratch assay is designed to study cell migration, and to some extent, it mimics how cells migrate, and react to tissue trauma, *in vivo*. As the WKY.SPGla14a strain has previously shown with the phenotypic results that it has high levels of fibrosis, this experiment compared it with the WKY strain, and the assay was carried out on the fibroblast cells. Comparing the percentage decrease in wound width, between the WKY and WKY.SPGla14a, at increasing concentrations of serum in the media, both strains show similar levels of recovery, with the peak migration with 10% serum. Both strains show an increase in percentage (Figure 4.11). However, if the actual distance migrated is taken into account the WKY.SPGla14a strain migrates further, at all concentrations, again with the peak migration at 10% serum (Table 4.3). To confirm that these effects are due to migration, and not to cell proliferation, an MTT assay is performed. Fibroblasts from WKY and WKY.SPGla14a were subjected to the same conditions of quiescence and serum added back to the media, as the scratch assay, and the levels of proliferation were measured. The rate of proliferation in WKY fibroblasts is not increasing with the increased levels of serum in the media. Although the WKY.SPGla14a fibroblasts are showing a pattern of increased proliferation with increased levels of serum in the media, it is only with the addition of 20% serum that a significantly different result is achieved (Figure 4.12).

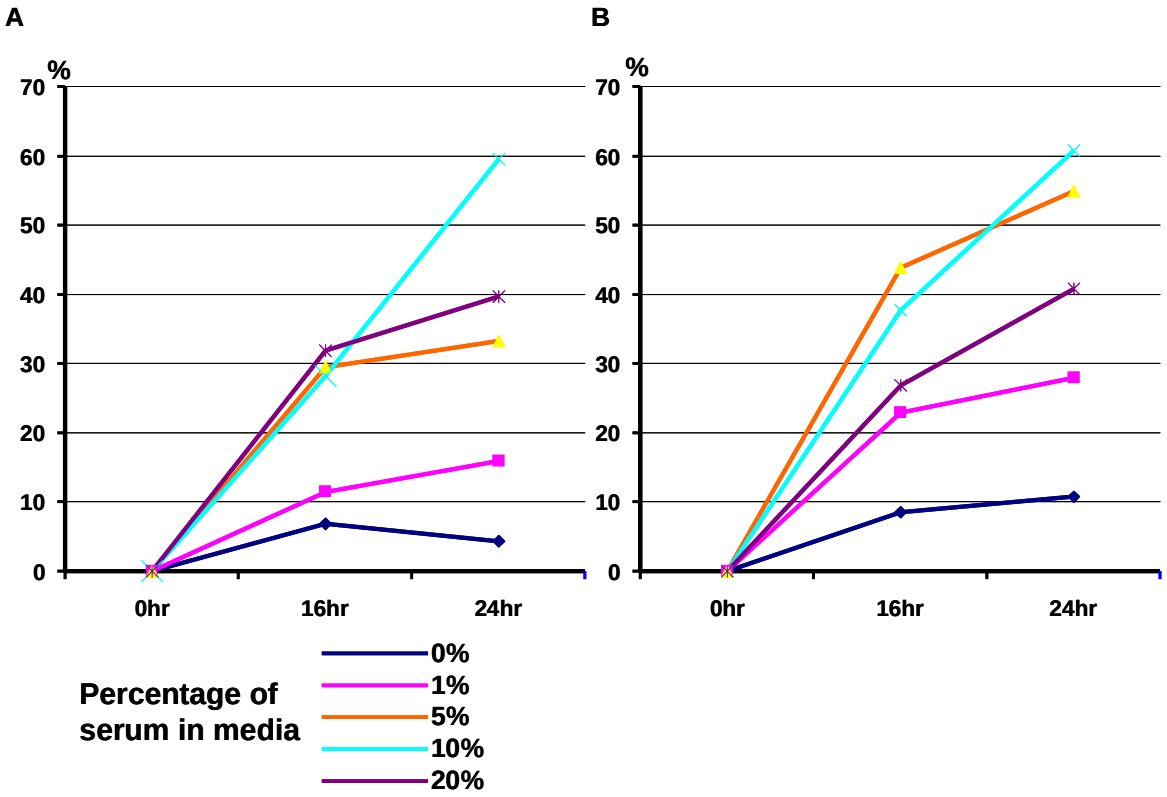

Figure 4.11 Scratch assay, showing percentage distance migrated following the scratch trauma, with increasing concentrations of serum in the media, on WKY and WKY.SPGla14a fibroblasts
A) WKY fibroblasts migration with increasing concentrations of serum in the media, over time. B) WKY.SPGla14a fibroblasts migration with increasing concentrations of serum in the media, over time.

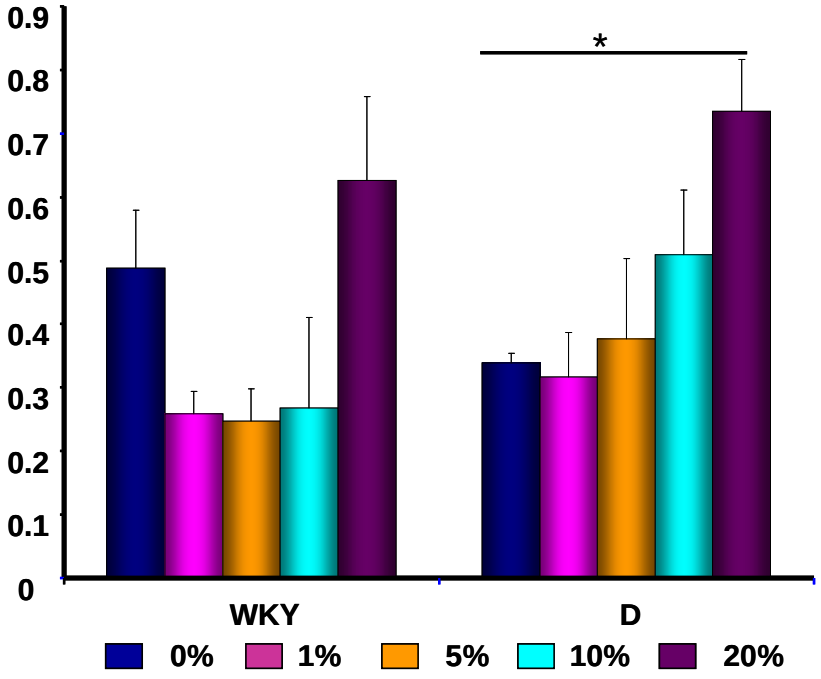

Figure 4.12 MTT assay of WKY and WKY.SPGla14a congenic (D) with increasing serum in the media
The graph shows rates of proliferation of the WKY fibroblasts are not increasing with the increased levels of serum in the media. WKY.SPGla14a fibroblasts show a pattern of increasing proliferation. n-1 * $p<0.05$

Table 4.3 Scratch assay, showing actual distance migrated, on WKY and WKY.SPGla14a fibroblasts
The measurements of actual distance moved following the scratch trauma are shown.

Strain	Time	diff in microns	1%	5%	10%	20%
WKY	0 hr	0	0	0	0	0
	16hr	29.68	55.99	126.47	62.64	150.76
	24hr	18.61	77.93	142.70	131.66	188.15
WKY.SPGla14a	0hr	0	0	0	0	0
	16hr	34.26	110.38	238.52	189.65	132.04
	24hr	42.84	134.86	299.05	305.44	201.43

4.4 Discussion

The experiments in this chapter were designed to validate and functionally follow up the results of the Illumina microarray. Particular emphasis was placed on the neonatal time point as it had been shown from previous phenotypic data generated within this laboratory, that hypertrophy is initiated before 5 weeks of age, prior to the onset of hypertension. Expression profiles compared across all 4 strains identified 4 positional candidate genes. Validation by gene expression confirmed *Spp1* as a positional candidate gene, and on this basis, was investigated through a series of experiments, including sequencing of the open reading frame and 3' upstream promoter region. *Spp1* was prioritised for further analysis due the signal intensity profile which mirrors the profile of LVMI data across the 4 strains. *Spp1* is an acidic phosphoprotein adhesion molecule, which is produced by mineralized tissue cells, epithelial cells, and activated immune system cells. It has cytokine-like, chemotactic and pro-adhesive properties, and is expressed by infiltrating macrophages during wound healing, and has also been implicated in wound repair in the heart (Murry CE *et al*. 1994). It has been identified in vasculature, where it contributes to vascular smooth muscle cell re-modelling functions in response to endothelial cell damage (Ashizawa N *et al*. 1996). *Spp1* synthesis is stimulated by calcitrol (1,25-dihydroxy-vitamin D_3), and is produced by a variety of tissue types including fibroblasts, osteoblasts, some bone marrow cells, hypertrophic chondrocytes, endothelial cells, and non-bone cells in the inner ear, brain, kidney, and placenta. Regulation of the *Spp1* gene depends on the cell type expressing it. In the bone, Runx2 and Osterix (Osx) are transcription factors needed for *Spp1* expression (Nakashima K *et al*. 2002). Runx2 and Osx bind promoters of osteoblast-specific genes such as *Col1a1*, *Bsp*, and *Spp1* and upregulate transcription (Ducy P *et al*. 1997). Hypocalcaemia and hypophosphataemia are events which stimulate the kidney proximal tubule cells to produce calcitrol, which lead to an increase in *Spp1* transcription, translation and secretion (Yucha C & Guthrie D. 2003). This is due to the presence of a specific vitamin D response element (VDRE) in the *Spp1* gene promoter. *Spp1* expression is also stimulated upon exposure of cells to pro-inflammatory cytokines, which are mediators of acute inflammation (tumour necrosis factor α [*TNFa*], infterleukin-1β [IL-1β]), ANG II, *TGFβ* and parathyroid hormone (PTH).

Hyperglycaemia and hypoxia are also known to increase *Spp1* expression (Sodhi CP *et al*. 2001).

Functional experiments of hypertrophy identified over-expression of *Spp1* in the SHRSP primary cardiomyocytes, which supports the potential for its role in this condition. Transgenic mice generated to specifically over-express *Spp1* in cardiomyocytes showed a high degree of lethality, with most dying 10-15 weeks after birth. *Spp1* expression is inhibited by Dox, an inhibitor of matrix metalloproteases which can also attenuate cardiac hypertrophy in mice (Errami M *et al*. 2008). It is only upon administration of Dox at 5 weeks of age, that survival of these mice increased to that of the control mice (Renault MA et al. 2010). This supports *Spp1*'s role not only as an inducer of myocarditis, but also maintains the severity of the process. *Spp1* has also previously been identified in rat cardiac fibroblasts, where it contributes to ANG II induced re-modelling. Interleukin-18 stimulates an increase in expression of *Spp1* in fibroblasts, which leads to diastolic dysfunction and cardiac fibrosis in mouse models (Yu Q *et al*. 2009). Knock out mice lacking the *Spp1* gene have characteristic features, of reduced fibrosis in response to cardiac injury, increased ventricular dilation and systolic dysfunction. This deficiency in fibroblast formation is linked to decease in remodelling via matrix metalloproteases (MMPs). Studies have shown that *Spp1* is cleaved by at least 2 classes of proteases: thrombin and MMPs (Scatena M *et al*. 2007). Furthermore, *Spp1* conditional transgenic mice have shown that a decrease in *Spp1* expression reduces fatality, but interstitial fibrosis is maintained (Renault MA *et al*. 2010). It has also been identified in cultured cardiomyocytes, where its expression is associated with LVH (Graf K *et al*. 1997). Cardiac re-modelling is a key element in LV dysfunction and can affect the clinical course of heart failure. The hallmarks of re-modelling are cardiomyocyte hypertrophy, extracellular matrix deposition (ECM) and fibrosis, and can also include a change in expression of many cardiac genes. Activated fibroblasts or myofibroblasts are the source of ECM proteins in scar formation, and may serve as a matrix for cell colonization during tissue regeneration (Lenga Y *et al*. 2008). *Spp1* plasma levels and *Spp1*-expressing CD4+ lymphocytes correlate with the severity of heart failure, which suggests that mechanisms in heart failure are associated with *Spp1* expression, and also plasma levels may be used as clinical marker (Francia P *et al*. 2010).

DNA sequencing was undertaken of the upstream regulatory region, however primer design within this region was problematic due to the number of repetitive elements present. As the Brown Norway sequence is also poorly annotated, an alignment was made around the promoter regions of mouse and human to detect areas of homology. From the subsequent PCR products, SNP's were identified in the upstream region of *Spp1*. Transcriptional repression is one of the mechanisms by which the precise control of gene expression is regulated, however, sequencing is still ongoing, following which Transfac analysis of this region will take place. To date, a single SNP in the ORF causing a change in amino acid (isoleucine to leucine) has been identified in the SHRSP strain (Table 4.2). This amino acid region was aligned with mouse and human, it was found that it was not conserved across the species, which suggests that this is unlikely to affect gene function. This is supported by the presence of a Leucine residue in the same position in the mouse (Figure 4.13). In addition, to confirm the presence of the SNP, sequencing will be undertaken of the Chromosome 14a congenic strains.

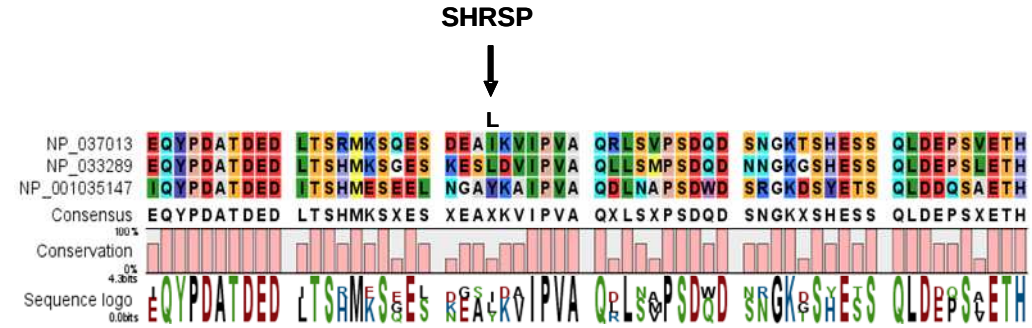

Figure 4.13 *Spp1* amino acid alignment in the rat, mouse and human.
The alignment shows the amino acid in rat WKY (I) is not conserved across the species. Also the change to Leucine (L) in the SHRSP is conserved in the mouse.

Primary cardiomyocyte and fibroblast cells from neonatal rats of the SHRSP, WKY and the congenic strains were isolated to allow for further analysis into the functional effects of hypertrophy. Expression levels of *Spp1* were investigated in the SHRSP and WKY parental strains in the cardiomyocytes and fibroblasts, and it was shown that *Spp1* expression is significantly higher in SHRSP cardiomyocytes, and WKY fibroblasts (Figure 4.5A). Increasing concentrations of ANG II stimulation of the cardiomyocytes showed that this had no effect in changing the levels of *Spp1* expression in the WKY and WKY.SPGla14a strains. A significant

change was detected in *Spp1* gene expression at 150nM and 200nM concentrations of ANG II stimulation in the SP.WKYGla14a, when compared with WKY control (Figure 4.5B). *Spp1* gene expression in the SHRSP has not been reported due to failure of GapdH amplification. Cell sizing of the cardiomyocytes indicates that WKY cells are significantly larger than SHRSP, and ANG II stimulation, although increasing the size does not change the difference seen between the strains (Figure 4.7). Stimulation of the SP.WKYGla14a and WKY.SPGla14a strains with ANG II, and subsequent analysis of *Spp1* expression should also take place to confirm the development of hypertrophy. As WKY.SPGla14a was identified as having an extreme phenotype of fibrosis, independent of BP, investigation of this strain, comparing with the WKY parental was focussed on for subsequent experiments. The scratch assay showed the WKY.SPGla14a fibroblasts migrated further following the scratch trauma, compared with WKY. This supports the hypothesis that the WKY.SPGla14a strain is involved in fibrosis. The MTT assay was performed to confirm the migration found in the scratch assay is due to the addition of serum, and not due to proliferation of the cells. WKY.SPGla14a fibroblast proliferation was found to be significantly higher with 20% serum in the media, but when this is compared with the scratch assay findings with the same concentration, it is found to have decreased cell migration (Table 4.3). This then suggests that the migration achieved in the scratch assay is due to the increased levels of serum added to the media, and not due to cell proliferation. This is to be expected as serum is known to be required for cell growth and survival. Significant myocardial inflammation develops in ANG II hypertension, which is responsive to aldosterone blockade (Rocha *et al*. 2002). ANG II is a critical factor in cardiac re-modelling which involves hypertrophy, fibroblast proliferation, and extracellular matrix production. *Spp1* inhibits ANG II induced inflammation and iNOS, a factor involved in cell injury after ischaemia reperfusion. It would be of interest to test this in vitro, so further investigations will include *Spp1* knock out using siRNA transfection techniques. The effects of this can be tested using Taqman qRT-PCR gene expression analysis, specifically with *Col1a1,* matrix metalloprotease 2 (*MMP2)* and matrix metalloprotease 9 (*MMP9*), which will identify if the stimulation is having an effect on collagen production in the cells. Other genes to be investigated by Taqman qRT-PCR gene expression analysis in the ANG II stimulated cardiomyocytes include *Col1a1*, *MMP2* and *MMP9*. Brain

natriuretic peptide (BNP) is released from the ventricles in response to stretching of the cardiomyocytes and is considered to be a superior marker of overload LV dysfunction (Birner CM *et al*. 2007). Atrial natriuretic peptide (ANP) is a powerful vasodilator released from the atria in response to high BP to reduce it. This would especially be of interest as ANG II suppresses ANP secretion via the AT1 receptor (Oh YB *et al*. 2010).

It should be noted that the other genes identified at the neonatal time point, and validated through Taqman qRT-PCR gene expression analysis will be investigated further. *Spp1* was prioritised for further investigation, and was the focus of this investigation as its signal intensity profile from the microarray mirrored the profile of LVMI and therefore represents an excellent positional candidate gene for LVMI in the SHRSP.

5. General discussion

The experiments performed in this project applied a wide range of functional genomic techniques in the investigation of hypertrophy in the SHRSP. The exon array and Illumina microarray techniques have provided valuable chromosome 14 gene candidates in this field. The hypertrophy candidate gene *Spp1* has been examined through expression profiling from the Illumina microarray, ORF and promoter sequence analysis, and functional studies utilising primary cells isolated from neonatal hearts. The functional studies were designed to examine the expression and response of *Spp1*, following ANG II stimulation in the cardiomyocytes, and how the cells reacted following tissue trauma in the fibroblasts. These techniques have provided an excellent springboard for future experiments relating to *Spp1*, and its role as a functional positional candidate of LVH. The scratch assay has provided valuable information on how the fibroblasts in the WKY.SPGla14a strain migrate after the scratch to re-establish cell-cell contact, and this contributes to fibrosis. It also provides us with information on how the ECM helps to form cell interactions. To fully understand the role of the fibroblasts, and how they are reacting to form the cell-cell contact, the media from the cells should be removed and analysed. Collagen assay performed on this media will indicate the levels of collagen being released in response to the trauma. This will also help us to understand collagen's role in fibrosis. The cells should be removed for gene expression analysis. Again, this will help our understanding of the genes involved, and their role in the functional pathway of *Spp1*. Further work in *Spp1* would include a knockdown transfection of primary fibroblasts using siRNA technology. RNA will be extracted from the transfected fibroblast cells and analysed for *Spp1* gene expression to confirm the transfection. To further confirm the pathways of hypertrophy, analysis of related genes, such as *Col1a1* and *MMP2* should also be analysed, as this will provide valuable information about how the cells are responding to the knock out of *Spp1*. BNP and ANP will also be measured, as this will helping the development of the functional pathways which *Spp1* is involved in. The role of BNP and ANP's involvement in *Spp1's* expression requires further work studies, as they are markers of hypertrophy, and will confirm at the neonatal time point, *Spp1's* role as a causative gene in LVH.

The knock out mice model of *Spp1* has previously identified its role in LVH, as mice lacking *Spp1* show reduced fibrosis in response to myocyte hypertrophy

induced cardiac injury. They have also shown an increase in ventricular dilation and systolic dysfunction, confirming *Spp1*'s role in cardiac remodelling (Trueblood NA *et al*. 2001). A trend in reduced apoptosis has been noted, which confirms a function of *Spp1* of being an antiapoptotic, which supports the theory that *Spp1* induces the protective mechanism of wound healing after myocardial injury (Chandrashekhar Y *et al*. 2004). The ideal next step from this data would be to generate a *Spp1* knock out in the WKY.SPGla14a congenic strain, and to analyse the effect on phenotype. Real-time PCR can be carried out on various genes including *Spp1*, *Col1a1* and *MMP2* will be carried out, and this should lead towards building a pathway and potential mechanism for the functional role of *Spp1*.

Promoter studies will be undertaken to evaluate the potential functional effects of the SNP's in the upstream region of *Spp1*. Similar experiments will be undertaken for the *Cxcl13* promoter, as it has a SNP in a potential transcription factor binding site. Transcriptional repressor proteins can associate with their target genes either directly through a DNA-binding domain or indirectly by interacting with other DNA-bound proteins. A repressor protein can inhibit transcription selectively, by masking a transcriptional activation domain, blocking interaction of an activator with other components of the transcription machinery, or by displacing an activator from the DNA. DNA response elements can exert allosteric effects on transcriptional regulators, such that regulators may activate transcription in the context of one gene, yet repress transcription in another.

Western blot analysis will be undertaken with protein extracted from SHRSP, WKY, SP.WKYGla14a and WKY.SPGla14a hearts, at neonatal, 5 week of age and 16 week of age time points. This will ascertain the potential functional change the SNP in the ORF of *Spp1*, due to the change in the amino acid.

Cxcl13 does display differential expression in chromosome 14a congenic strains. Although *Cxcl13* does not have any obvious links to hypertrophy, this does not discount the information gathered from the exon array. The SNP in the 5' promoter region of *Cxcl13* resulted in the loss of the HNF4 transcription factor loss the WKY strain. The 3'UTR SNP should also be investigated further. The 3' region is a common area for microRNA's, and a SNP in this region could be

suggestive of miR control of the expression of the gene. The area will be scanned, and any miRs in the region of the SNP will be investigated through normal expression techniques. Post-transcriptional work will also be carried out to see if the change found in the exon array may be related to *Cxcl13*'s protein. Western blot analysis will indicate if there are differing levels of *Cxcl13* protein in the heart tissue, when comparing the parental strains of SHRSP and WKY and the congenic strains of SP.WKYGla14a and WKY.SPGla14a.

The *Clock* gene has been fully investigated for potential alternate splicing suggested by the exon array and the signal intensity plots. The SNP's found have been verified through probe alignment to the sequence and confirmed that alternative splicing is not occurring in *Clock*. The probes for exon 5 did not align with the +432 SNP, which has previously been identified and is illustrated on the ensemble page for the *Clock* gene. The probes for exon 9 aligned with the +816 SNP and this confirms the change in signal intensity, as the probes would not have hybridized to this region. This SNP has not been identified previously, and should be investigated further.

Hsd17b13, *Rrad* and *Zfp644* were identified by the neonatal Ilumina microarray as being potential positional candidates for hypertrophy. As *Rrad* is positioned on chromosome 19, this would suggest that it is having a trans effect on the chromosome 14a congenic strains. *Hsd17b13* and *Zfp644* are located on chromosome 14. These microarray targets will be investigated further, as the neonatal gene expression analysis confirmed the findings of the array.

The results of the 5 week heart exon analysis filtered on the minimal congenic region (29Mbp) and the results of the Illumina genome-wide analysis from the same animals compared well. There were additional positional candidate genes on chromosome 14, however, the additional time points in the Illumina experiments proved vital in the identification of *Spp1* as the lead candidate at the neonatal timepoint. This is an excellent candidate gene for left ventricular hypertrophy and will provide the basis for further functional and translational expetiments.

Appendix

Table A.1 Primers name and oligonucleotide sequence

Primer name	Oligonucleotide sequence
Clock_1F	TTCGACAGGACTGGAAACCT
Clock_1R	TGCGCTGTATAGTTCCTTCG
Clock_2F	AGGAGCCATCCACCTATGAA
Clock_2R	CCAAATCCACTGCTGTCCTT
Clock_3F	GTCCTGGGAACATCAGGCTA
Clock_3R	TGTGTGCGAGGACTTTCTTG
Cxcl13_up_1F	CTCCCTTTTCCCCTCCTTTA
Cxcl13_up_1R	ATCCTTTGTGCAGCTGTTCC
Cxcl13_up_2F	GGCTAGAACTGCCAGACAGG
Cxcl13_up_2R	CCATTGAGCTGACATGAACG
Cxcl13_up_3F	CCTCGTTCATGTCAGCTCAA
Cxcl13_up_3R	CTCACCCTTGGTAGGTGCTC
Cxcl13_up_4F	CACCGAGGACTGAACACACA
Cxcl13_up_4R	CCTTGGCAGAATCAACATCA
Cxcl13_up_5F	AGAACTTGGTTGGCCTTTCA
Cxcl13_up_5R	GCTGCGATGTCAGTTTTCAA
Cxcl13_up_6F	TTTCACCCTCGAATCTCTGC
Cxcl13_up_6R	AATGTTTTCACCCGCTTTTG
Cxcl13_cDNA_1F	GGAGTCTGGAGCTGGAAACA
Cxcl13_cDNA_1R	CCCAGGGCGTATAACTTGAA
Cxcl13_cDNA_2F	CAAGTTATACGCCCTGGGAAT
Cxcl13_cDNA_2R	GGAGCTTGGGGAGTTGAAGT
Cxcl13_cDNA_3F	GCAGCCCTGCTTCTTCTACT
Cxcl13_cDNA_3R	TAGCTTTCTTGGCCTTGGTC
Cxcl13_3'UTR_1F	GCATGCCACAAGTTTTCCTT
Cxcl13_3'UTR_1R	AGACCTGCTCTGCATCACCT
Cxcl13_3'UTR_2F	GTCACCCCAAAAGACACCTG
Cxcl13_3'UTR_2R	GGGTCACAGTGCAAAGGAAT

Primer name	Oligonucleotide sequence
Spp1_up_AF	GCTCCAGCAZAATCTATTCC
Spp1_up_BF	TCCTGTGGGCRCAGAGTAAAC
Spp1_up_CF	CAAGACAATATTAAATATTT
Spp1_up_DF	CTAAGTGAYTTGCCCAAGGT
Spp1_up_AR	TGGCTGGCTTCCTCGAGAATG
Spp1_up_AR	TGGCTGGCTTCCTCGAGAATG
Spp1_AF	CATCCTTGGCTTTGCAGTCT
Spp1_AR	AAACGTCTGCTTGTGTGCTG
Spp1_BF	AAGCCTGACCCATCTCAGAA
Spp1_BR	GCAACTGGGATGACCTTGAT
Spp1_CF	GGAGTCCGATGAGGCTATCA
Spp1_CR	TGAAACTCGTGGCTCTGATG
Spp1_DF	CATCAGAGCCACGAGTTTCA
Spp1_DR	TCAGGGCCCAAAACACTATC
Spp1_EF	TGCTTGTTTCTCAGTTCAGTGG
Spp1_ER	TCACACCAACAAAAATAATCACAA

Table A.2 PCR product size
The sizes in bp show the expected product size of the PCR reaction from Chapter 3

Primer combination	Size in bp
Clock 1F + 1R	432
Clock 2F + 2R	437
Clock 3F + 3R	420
Cxcl13_cDNA_1F + 1R	234
Cxcl13_cDNA_2F + 2R	155
Cxcl13_up_1F + 1R	454
Cxcl13_up_2F + 2R	473
Cxcl13_up_3F + 3R	497
Cxcl13_up_4F + 4R	402
Cxcl13_up_5F + 5R	506
Cxcl13_up_6F + 6R	463
Cxcl13_3'UTR_1F + 1R	759
Cxcl13_3'UTR_2F + 2R	618

Table A.3 PCR product size
The sizes in bp show the expected product size of the PCR reaction from Chapter 4

Primer combination	Size in bp
Spp1_cDNA_AF + AR	459
Spp1_cDNA_BF + BR	446
Spp1_cDNA_BF + CR	713
Spp1_cDNA_CF + DR	556
Spp1_cDNA_DF + ER	531
Spp1_cDNA_BF + DR	966
Spp1_ups_AF + AR	2000
Spp1_ups_BF + AR	1958
Spp1_ups_CF + AR	1459
Spp1_ups_DF + AR	1054

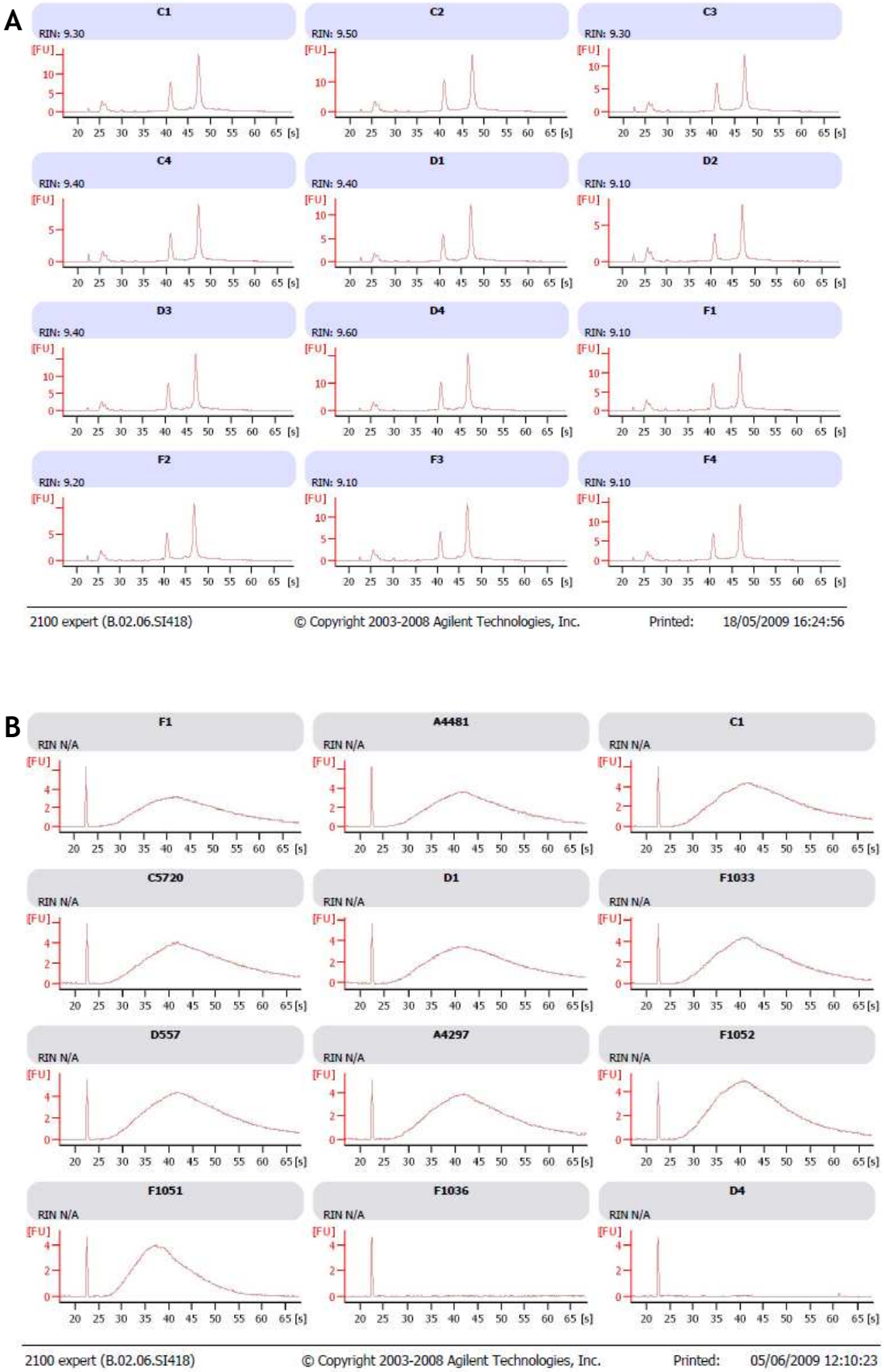

Figure A.1 Agilent analysis of RNA and cRNA used in the Illumina microarray

A) Agilent analysis of RNA achieving an acceptable RIN and peak profile, allowing the samples to be used in IVT enzyme step. B) Agilent analysis of cRNA achieving an acceptable bell shaped curved as stipulated by Illumina, allowing the samples to be hybridized to the gene expression chip.

Table A.4 Taqman gene expression assay probe ID's
The applied biosystems taqman probe ID's for the gene expression assays in Chapter 3 & 4

Gene	Taqman assay probe ID
Spp1	Rn00681031_m1
Spp1	Rn00563571_m1)
Arhgap24	Rn01443832_m1
Hsd17b13	Rn01450041_m1
Rrad	Rn00584263_m1
Cxcl13	Rn0140028_m1
Abcg3	Rn01450015_m1
Ccrl1	Rn01445226_m1
Cxcr3	Rn00584589_m1
Blr1 (Cxcr5)	Rn02132880_s1

FDR ReportPartek Inc.
www.partek.com December 23 2010
12:05:11 pm

FDR Report
Significance Level: 0.05; Total number of p-values: 197
Method: Step Up
Variable NameCutoff Value# of Significant p-values
p-value(date)0.012690450
p-value(strain)0.0045685318
p-value(Batch)0.0007614213
p-value(date * strain)0.0002538070
p-value(16wk * SHRSP vs. 16wk * WKY)0.0007614213
p-value(16wk * SHRSP vs. 16wk * SP.WKYGLA14a)0.0002538071
p-value(16wk * WKY vs. 16wk * WKY.SPGLA14a)0.001522846
p-value(16wk * SP.WKYGLA14a vs. 16wk * WKY.SPGLA14a)0.001269045
p-value(16wk * SHRSP vs. 16wk * WKY.SPGLA14a)0.0002538071
p-value(16wk * WKY vs. 16wk * SP.WKYGLA14a)0.0002538070
p-value(5wk * SHRSP vs. 5wk * WKY)0.001015234
p-value(5wk * SHRSP vs. 5wk * SP.WKYGLA14a)0.0007614213
p-value(5wk * WKY vs. 5wk * WKY.SPGLA14a)0.001015234
p-value(5wk * SP.WKYGLA14a vs. 5wk * WKY.SPGLA14a)0.0005076142
p-value(5wk * SHRSP vs. 5wk * WKY.SPGLA14a)0.0002538070
p-value(5wk * WKY vs. 5wk * SP.WKYGLA14a)0.0002538070

Figure A.2 FDR report of the Genel level analysis of the Affymetrix exon array
The FDR report shows the p-values for each of the pairwise comparisons in the analysis, filtered to the minimum congenic interval 29Mbp.

FDR ReportPartek Inc.
www.partek.com December 23 2010
12:02:23 pm

FDR Report
Significance Level: 0.05; Total number of p-values: 21792
Method: Step Up
Variable NameCutoff Value# of Significant p-values
p-value(Age)0.02192559556
p-value(Strain)0.002569751120
p-value(Sentrix Barcode)0.005433192368
p-value(Age * Strain)0.000651615284
p-value(Neo * WKY vs. Neo * SP)0.0011908519
p-value(Neo * F vs. Neo * SP)0.000328102143
p-value(Neo * F vs. Neo * D)0.000603432263
p-value(5wk * WKY vs. 5wk * SP)0.000452001197
p-value(5wk * F vs. 5wk * SP)0.00019961587
p-value(5wk * WKY vs. 5wk * D)1.37665e-0056
p-value(5wk * F vs. 5wk * D)0.000706681308
p-value(16wk * WKY vs. 16wk * SP)0.000796164347
p-value(16wk * F vs. 16wk * SP)1.37665e-0056
p-value(16wk * WKY vs. 16wk * D)1.14721e-0055
p-value(16wk * F vs. 16wk * D)0.000786986343
p-value(5wk * SP vs. Neo * SP)0.01067134651
p-value(5wk * F vs. Neo * F)0.01212145283
p-value(5wk * D vs. Neo * D)0.0111834874
p-value(5wk * WKY vs. Neo * WKY)0.01003124372
p-value(16wk * SP vs. 5wk * SP)0.002790011216
p-value(16wk * F vs. 5wk * F)0.003441631500
p-value(16wk * D vs. 5wk * D)0.00153956671
p-value(16wk * WKY vs. 5wk * WKY)0.003503581527
p-value(Neo * WKY vs. Neo * D)3.67107e-00516

Figure A.3 FDR report of the Genel level analysis of the Illumina array
The FDR report shows the p-values for each of the pairwise comparisons in the analysis of the genome-wide expression profiling array.

References

Ansel, K. M., Ngo, V .N., Hyman, P .L., Luther, A .A., Förster, R., Sedgwick, J. D., Browning, J. L., Lipp, M., & Cyster, J. G., 2000, "A chemokine-driven positive feedback loop organizes lymphoid follicles", *Nature,* vol. 406, pp. 309-314.

Antoniucci, D., Seccareccia, F., Menotti, A., Dovellini, E. V., Prati, P. L., Rovelli, F. & Fazzini, P. F., 1997, "Prevalence and correlates of echocardiographic determined left ventricular hypertrophy in 2318 asymptomatic middle-aged men: the ECCIS project. Epidemiolgia e Clinica della Cardiopatia Ischemica Silente.", *Giornale italiano di cardiologica,* vol. 4, pp. 363-369.

Ashraf, S. S., Sochacka, E., Cain, R., Guenther, R., Malkiewicz, A. & Agris, P. F., 1999, "Single atom modification (O->S) of tRNA confers ribosome binding RNA", vol. 5, pp. 188–194.

Ashizawa, N., Graf, K., Do, Y. S., Nunohiro, T., Giachella, C. M., Meehan, W. P., Tuan, T. & Hsueh, W. A., 1996, "Osteopontin is produced by rat cardiac fibroblasts and mediates A_{II}-induced DNA synthesis and collagen gel contraction", *Journal of Clinical investigation,* vol. 98, pp. 2218-2227.

Aviña-Zubieta, J. A., Choi, H. K., Sadatsafavi, M., Etminan, M., Esdaile, J. M. & Lacaille, D., 2008, "Risk of cardiovascular mortality in patients with rheumatoid arthritis: a meta-analysis of observational studies", *Arthritis & Rheumatism,* vol. 59, pp. 1690-1697.

Barroso, I., Gurnell, M., Crowley, V. E., Agostini, M., Schwabe, J. W., Soos, M. A., Maslen, G. L., Williams, T. D., Lewis, H., Schafer, A. J., Chatterjee, V. K., & O'Rahilly, S., 1999, "Dominant negative mutations in human PPARgamma associated with severe insulin resistance, diabetes mellitus and hypertension", *Nature*, vol. 402, no. 6764, pp. 880-883.

Barroso, I., Luan, J., Wheeler, E., Whittaker, P., Wasson, J., Zeggini, E., Weedon, M. N., Hunt, S., Venkatesh, R., Frayling, T. M., Delgado, M., Neuman, R. J., Zhao, J., Sherva, R., Glaser, B., Walker, M., Hitman, G., McCarthy, M. I., Hattersley, A. T., Permutt, M. A., Nicholas J. Wareham, N. J. & Panagiotis Deloukas, P., 2008, "Population-Specific Risk of Type 2 Diabetes Conferred by *HNF4A* P2 Promoter Variants: A lesson for Replication Studies", *Diabetes,* vol. 57, no. 11, pp. 3161-3165.

Berk, B. C., Fujiwara, K. & Lehoux, S., 2007, "ECM remodeling in hypertensive heart disease", *Journal of Clinical Investigation,* vol. 117, pp. 568–575.

Birner, C. M., Ulucan, C., Fredersdorf, S., Rihm, M., Lowel, H., Stritzke, J., Schunkert, H., Hengstenberg, C., Holmer, S., Riegger, G., Luchner, A., 2007, "Head-to-head comparison of BNP and IL-6 as markers of clinical and experimental heart failure: superiority of BNP", *Cytokine* vol. 40, pp. 89–97.

Blencowe, B. J., 2006, "Alternative Splicing: New insights from global analysis", *Cell,* vol. 126, pp. 37-47.

Botstein, D., Raymond L., White, R. L., Skolnick, M. & Davis, R. W., 1980, "Construction of a Genetic Linkage Map in Man Using Restriction Fragment Length Polymorphisms", *American Journal of Human Genetics*, vol. 32, pp. 314-331.

Carretero, O. A. & Oparil. S, 2000, "Essential Hypertension Part I: Definition and Etiology", *Circulation,* vol. 101, no. 3, pp. 329-325

Castoldi, G., Redaelli, S., van de Greef, W. M., di Gioia, C. R., Busca, G., Sperti, G. & Stella, A., 2005, "Angiotensin II modulates frizzled-2 receptor expression in rat vascular smooth muscle cells", *Clinical Science (London),* vol. 108, pp. 523–530.

Chai, Z., Brereton, P., Suzuki, T., Sasano, H., Obeyesekere, V., Escher, G., Saffery, R., Fuller, P., Enriquez, C. & Krozowski, Z., 2003, "17β-Hydroxysteroid Dehydrogenase Type XI Localizes to Human Steroidogenic Cells", *Endocrinology*, vol. 144, no. 5, pp 2084-2091.

Chandrashekhar, Y., Sen, S., Anway, R., Shuros, A. & Anand, I., 2004, "Long-term caspase inhibition ameliorates apoptosis, reduces myocardial troponin-I cleavage, protects left ventricular function, and attenuates remodeling in rats with myocardial infarction", *Journal of the American College of Cardiology,* vol. 43, no. 2, pp. 295-301.

Chiasson, J. L., Josse, R. G., Gomis, R., Hanefeld, M., Karasik, A. & Laakso, M., 2003, "Acarbose Treatment and the Risk of Cardiovascular Disease and Hypertension in Patients With Impaired Glucose Tolerance", *Journal of the American Medical Association,* vol. 290, no. 4, pp. 486-494.

Chu, C. S., Trapnell, B. C., Curristin, S., Cutting, G. R. & Crystal, R. G., 1993, "Genetic basis of variable exon 9 skipping in cystic fibrosis transmembrane conductance regulator mRNA", *Nature Genetics,* vol. 3, pp. 151–156.

Clark, C. M., 1971, "Carbohydrate metabolism in the isolated fetal rat heart", *The American journal of physiology,* vol. 220, no. 3, pp. 583-588.

Clark, J. S., Jeffs, B., Davidson, A. O., Lee, W. K., Anderson, N. H., Bihoreau, M. T., Brosnan, M. J., Devlin, A. M., Kelman, A. W., Lindpaintner, K. & Dominiczak, A. F., 1996, "Quantitative trait loci in genetically hypertensive rats. Possible sex specificity", *Hypertension*, vol. 28, no. 5, pp. 898-906.

Clemitson, J. R., Dixon, R. J., Haines, S., Bingham, A. J, Patel, B. R., Hall, L., Lo, M., Sassard, J., Charchar, F. J. & Samani, N. J., 2007, "Genetic dissection of a blood pressure quantitative trait locus on rat chromosome 1 and gene expression analysis identifies SPON1 as a novel candidate hypertension gene", *Circulation Research,* vol. 100, no. 7, pp. 992-999.

Clubb, F. J. & Bishop, S. P., 1984, "Formation of binucleated myocardial cells in the neonatal rat. An index for growth hypertrophy", *Laboratory investigation; a journal of technical methods and pathology,* vol. 50, no. 5, pp. 571-577.

Coschigano, K. T., & Wensink, P. C., 1993, "Sex-specific transcriptional regulation by the male and female doublesex proteins of *Drosphila*", *Genes and Development,* vol. 7, pp. 42-54.

Cowley, A. W. Jr., 2006, "The genetic dissection of essential hypertension", *Nature Reviews Genetic,* vol. 7, pp. 829-840.
Davidson, A. O., Schork, N., Jaques, B. C., Kelman, A. W., Sutcliffe, R. G., Reid, J. L., & Dominiczak, A. F., 1995, "Blood pressure in genetically hypertensive rats. Influence of the Y chromosome", *Hypertension*, vol. 26, no. 3, pp. 452-459.

Di Carlo, E., D'Antuono, T., Contento, S., Di Nicola, M., Ballone, E. & Sorrentino, C., 2007, "Quilty Effect Has the Features of Lymphoid Neogenesis and Shares CXCL13–CXCR5 Pathway with Recurrent Acute Cardiac Rejections", *American Journal of Transplantation,* vol. 7, pp. 201–210.

Dietrich, W. F., Miller, J., Steen, R., Merchant, M. A., Damron-Boles, D., Husain, Z., Dredge, R., Daly, M. J., Ingalls, K. A., J, T., O'ConnorEvans, C. A., DeAngelis, M. M., Levinsonkruglyak, D. M. L., Goodman, N., Copeland, N. G., Jenkins, N. A., Hawkins, T. L., Stein, L., Page, D. C. & Lander, E. S., 1996, "A comprehensive genetic map of the mouse genome", *Nature,* vol. 380, pp. 149-152.

Dmitrieva, R. I., Hinojos, C. A., Grove, M. L., Bell, R. J., Boerwinkle, E., Fornage, M., & Doris, P. A., 2009, "Genome-Wide Identification of Allelic Expression in Hypertensive Rats", *Circulation: Cardiovascular Genetics*, vol. 2, pp. 106-115.

Doggrell, S. A. & Brown, L., 1998, "Rat models of hypertension, cardiac hypertrophy and failure", *Cardiovascular Research,* vol. 39, pp. 89–105.

Dominiczak, A. F., Graham, D., McBride, M. W., Brain, N. J., Lee, W. K., Charchar, F. J., Tomaszewski, M., Delles, C., & Hamilton, C. A., 2005, "Corcoran Lecture. Cardiovascular genomics and oxidative stress", *Hypertension*, vol. 45, no. 4, pp. 636-642.

Ducy, P., Zhang, R., Geoffroy, V., Ridall, A. L. & Karsenty, G., 1997, "Osf2/Cbfa1: a transcriptional activator of osteoblast differentiation", *Cell,* vol. 89, no. 1, pp. 747–754.

Errami, M,, Galindo, C. L., Tassa, A. T., Dimaio, J. M., Hill, J. A. & Garner, H. R., 2008, "Doxycycline attenuates isoproterenol- and transverse aortic banding-induced cardiac hypertrophy in mice", *Journal of Pharmacology and Experimental Therapeutics,* vol. 324, no. 3, pp. 1196-1203.

Faustino, N. A. & Cooper, T. A., 2003, "Pre-mRNA splicing and human disease", *Genes & Development,* vol. 17, pp. 419-437.

Feinleib, M., Garrison, R. J., Fabsitz, R., Christian, J. C., Hrubec, Z., Borhani, N. O., Kannel, W. B., Rosenman, R., Schwartz, J. T. & Wagner, J. O., 1977, "The NHLBI twin study of cardiovascular disease risk factors: methodology and summary of results", *American Journal of Epidemiology*, vol. 106, no. 4, pp. 284-285.

Förster, R., Mattis, A. M., Kremmer, E., Wolf, E., Gottfried Brem, G. & Lipp, W., 1996, "A Putative Chemokine Receptor, BLR1, Directs B Cell Migration to Defined Lymphoid Organs and Specific Anatomic Compartments of the Spleen", *Cell,* vol. 87, pp. 1037-1047.

Francia, P., Balla, C., Ricotta, A., Uccellini, A., Frattari, A., Modestino, A., Borro, M., Simmaco, M., Salvati, A., De Biase, L. & Volpe, M., 2010, "Plasma osteopontin reveals left ventricular reverse remodelling following cardiac resynchronization therapy in heart failure", *International Journal of Cardiology*, pp. 1-5.

Friehs, I., Barillas, R., Vasilyev, N. V., Roy, N., McGowan, F. X. & del Nido, P. J., 2006, "Vascular endothelial growth factor prevents apoptosis and preserves contractile function in hypertrophied infant heart", *Circulation,* vol. 114, pp. 290-295.

Funder, J. W., Pearce, P. T., Smith, R. & Smith, A. I., 1988, "Mineralocorticoid action: target tissue specificity is enzyme, not receptor, mediated", *Science*, vol. 242, no. 4878, pp. 583-585.

Garcia-Blanco, M. A., Baraniak, A. P. & Lasda, E. L., 2004, "Alternative splicing in disease and therapy", *Nature Biotechnology,* vol. 22, no. 5, pp. 535-546.

Geller, D. S., Farhi, A., Pinkerton, N., Fradley, M., Moritz, M., Spitzer, A., Meinke, G., Tsai, F. T., Sigler, P. B., & Lifton, R. P. 2000, "Activating mineralocorticoid receptor mutation in hypertension exacerbated by pregnancy", *Science*, vol. 289, no. 5476, pp. 119-123.

Geller, D. S., Zhang, J., Wisgerhof, M. V., Shackleton, C., Kashgarian, M. & Lifton, R. P., 2008, "A Novel Form of Human Mendelian Hypertension Featuring Nonglucocorticoid-Remediable Aldosteronism", *The Journal of Clinical Endocrinology & Metabolism,* vol. 93, no. 8, pp. 3117-3123.

Gibbs, R. A., Weinstock, G. M., Metzker, M. L., Muzny, D. M., Sodergren, E. J., Scherer, S., Scott, G., Steffen, D., Worley, K. C., Burch, P. E., Okwuonu, G., Hines, S., Lewis, L., DeRamo, C., Delgado, O., Dugan-Rocha, S., Miner, G., Morgan, M., Hawes, A., Gill, R., Celera, Holt, R. A., Adams, M. D., Amanatides, P. G., Baden-Tillson, H., Barnstead, M., Chin, S., Evans, C. A., Ferriera, S., Fosler, C., Glodek, A., Gu, Z., Jennings, D., Kraft, C. L., Nguyen, T., Pfannkoch, C. M., Sitter, C., Sutton, G. G., Venter, J. C., Woodage, T., Smith, D., Lee, H. M., Gustafson, E., Cahill, P., Kana, A., Doucette-Stamm, L., Weinstock, K., Fechtel, K., Weiss, R. B., Dunn, D. M., Green, E. D., Blakesley, R. W., Bouffard, G. G., De Jong, P. J., Osoegawa, K., Zhu, B., Marra, M., Schein, J., Bosdet, I., Fjell, C., Jones, S., Krzywinski, M., Mathewson, C., Siddiqui, A., Wye, N., McPherson, J., Zhao, S., Fraser, C. M., Shetty, J., Shatsman, S., Geer, K., Chen, Y., Abramzon, S., Nierman, W. C., Havlak, P. H., Chen, R., Durbin, K. J., Egan, A., Ren, Y., Song, X. Z., Li, B., Liu, Y., Qin, X., Cawley, S., Cooney, A. J., D'Souza, L. M., Martin, K., Wu, J. Q., Gonzalez-Garay, M. L., Jackson, A. R., Kalafus, K. J., McLeod, M. P., Milosavljevic, A., Virk, D., Volkov, A., Wheeler, D. A., Zhang, Z., Bailey, J. A., Eichler, E. E., Tuzun, E., Birney, E., Mongin, E., Ureta-Vidal, A., Woodwark, C., Zdobnov, E., Bork, P., Suyama, M., Torrents, D., Alexandersson, M., Trask, B. J., Young, J. M., Huang, H., Wang, H., Xing, H., Daniels, S., Gietzen, D., Schmidt, J., Stevens, K., Vitt, U., Wingrove, J.,

Camara, F., Mar Alba, M., Abril, J. F., Guigo, R., Smit, A., Dubchak, I., Rubin, E. M., Couronne, O., Poliakov, A., Hubner, N., Ganten, D., Goesele, C., Hummel, O., Kreitler, T., Lee, Y. A., Monti, J., Schulz, H., Zimdahl, H., Himmelbauer, H., Lehrach, H., Jacob, H. J., Bromberg, S., Gullings-Handley, J., Jensen-Seaman, M. I., Kwitek, A. E., Lazar, J., Pasko, D., Tonellato, P. J., Twigger, S., Ponting, C. P., Duarte, J. M., Rice, S., Goodstadt, L., Beatson, S. A., Emes, R. D., Winter, E. E., Webber, C., Brandt, P., Nyakatura, G., Adetobi, M., Chiaromonte, F., Elnitski, L., Eswara, P., Hardison, R. C., Hou, M., Kolbe, D., Makova, K., Miller, W., Nekrutenko, A., Riemer, C., Schwartz, S., Taylor, J., Yang, S., Zhang, Y., Lindpaintner, K., Andrews, T. D., Caccamo, M., Clamp, M., Clarke, L., Curwen, V., Durbin, R., Eyras, E., Searle, S. M., Cooper, G. M., Batzoglou, S., Brudno, M., Sidow, A., Stone, E. A., Payseur, B. A., Bourque, G., Lopez-Otin, C., Puente, X. S., Chakrabarti, K., Chatterji, S., Dewey, C., Pachter, L., Bray, N., Yap, V. B., Caspi, A., Tesler, G., Pevzner, P. A., Haussler, D., Roskin, K. M., Baertsch, R., Clawson, H., Furey, T. S., Hinrichs, A. S., Karolchik, D., Kent, W. J., Rosenbloom, K. R., Trumbower, H., Weirauch, M., Cooper, D. N., Stenson, P. D., Ma, B., Brent, M., Arumugam, M., Shteynberg, D., Copley, R. R., Taylor, M. S., Riethman, H., Mudunuri, U., Peterson, J., Guyer, M., Felsenfeld, A., Old, S., Mockrin, S., & Collins, F., 2004, "Genome sequence of the Brown Norway rat yields insights into mammalian evolution", *Nature*, vol. 428, no. 6982, pp. 493-521.

Ginsberg, M. M. & Busto, R., 1989, "Rodent models of cerebral ischemia", *Stroke,* vol. 20, pp. 1627-1642.

Gong, M. & Hubner, N., 2006, "Molecular genetics of human hypertension", *Clinical Science,* vol. 110, no. 3, pp. 315-326.

Grabner, R., Lotzer, K., Dopping, S., Hildner, M., Radke, D., Beer, M., Spanbroek, R., Lippert, B., Reardon, C. A., Getz, G. S., Fu, Y. X., Hehlgans, T., Mebius, R. E., van der Wall, M., Kruspe, D., Englert, C., Lovas, A., Hu, D., Randolph, G. J., Weih, F. & Habenicht, A. J., 2009, "Lymphotoxin beta receptor signaling promotes tertiary lymphoid organogenesis in the aorta adventitia of aged ApoE_/_ mice", *Journal of Experimental Medicine*, vol. 206, pp. 233–248.

Graf, K., Do, Y. S., Ashizawa, N., Meehan, W. P., Giachelli, C. M., Marboe, C. M., Fleck, E. & Hsueh, W. A., 1997, "Myocardial osteopontin expression is associated with left ventricular hypertrophy", *Circulation,* vol 96, pp. 3063-3071.

Gray, S. D., 1984, "Pressure profiles in neonatal spontaneously hypertensive rats", *Biology of the Neonate,* vol. 45, no. 1, pp. 25-32.

Grossman, W., Jones, D. & McLaurin, L. P., 1975, "Wall stress and patterns of hypertrophy in the human left ventricle", *Journal of Clinical Investigation,* vol. 56, no. 1, pp. 56–64.

Hopcroft, L. E. M., McBride, M .W., Harris, K. J., Sampson, A. K., McClure, J. D., Graham, D., Young, G., Holyoake, T. L., Girolami, M. A. & Dominiczak, A. F., 2010, "Predictive response-relevant clustering of expression data provides insights into disease processes", *Nucleic Acids Research,* vol. 38, no. 20, pp. 6831–6840.

Hu, P., Zhang, D., Swenson, L., Chakrabarti, G., Abel, E. D. & Litwin, S. E., 2003, "Minimally invasive aortic banding in mice: effects of altered cardiomyocyte insulin signaling during pressure overload", *American Journal of Physiology: Heart and Circulatory Physiology,* vol. 285, pp. 1261-1269.

Hubner, N., Wallace, C. A., Zimdahl, H., Petretto, E., Schulz, H., Maciver, F., Mueller, M., Hummel, O., Monti, J., Zidek, V., Musilova, A., Kren, V., Causton, H., Game, L., Born, G., Schmidt, S., Muller, A., Cook, S. A., Kurtz, T. W., Whittaker, J., Pravenec, M. & Aitman, T. J., 2005, "Integrated transcriptional profiling and linkage analysis for identification of genes underlying disease", *Nature Genetics,* vol. 37, no. 3, pp. 243-253

Humphries, S. E., Luong, L. A., Ogg, M. S., Hawe, E. & Miller, G. J., 2001, "The interleukin-6 174 G/C polymorphism is associated with risk of coronary heart disease and systolic blood pressure in healthy men", *European Heart Journal,* vol. 22, pp. 2219–2220.

Jeffs, B., Negrin, C. D., Graham, D., Clark, J. S., Anderson, N. H., Gauguier, D. & Dominiczak, A. F., 2000, "Applicability of a "Speed" Congenic Strategy to Dissect Blood Pressure Quantitative Trait Loci on Rat Chromosome 2", *Hypertension,* vol. 35, pp. 179-187.

Jeske, Y. W., So, A., Kelemen, L., Sukor, N., Willys, C., Bulmer, B., Gordon, R. D., Duffy, D. & Stowasser, M., 2008, "Examination of chromosome 7p22 candidate genes RBaK, PMS2 and GNA12 in familial hyperaldosteronism type II", *Clinical and Experimental Pharmacology and Physiology,* vol. 35, no. 4, pp. 380-385.

Jordan, J., Toka, H. R., Heusser, K., Toka, O., Shannon, J. R., Tank, J., Diedrich, A., Stabroth, C., Stoffels, M., Naraghi, R., Oelkers, W., Schuster, H., Schobel, H. P., Haller, H. & Luft, F. C., 2000, "Severely impaired baroreflex-buffering in patients with monogenic hypertension and neurovascular contact", *Circulation*, vol. 102, no. 21, pp. 2611-2618.

Jurica, M. S. & Moore, M.J., 2003, "Pre-mRNA Splicing: Awash in a Sea of Proteins", *Molecular Cell,* vol. 12, pp. 5–14.

Julius, S., 1993, "Corcoran Lecture. Sympathetic hyperactivity and coronary risk in hypertension", *Hypertension,* vol. 21, pp. 886-893.

Kahan, T., 1998, "The importance of left ventricular hypertrophy in human hypertension" *Journal of Hypertension:Supplement,* vol. 16, no. 7, pp. 23-29.

Kahan, T. & Bergfeldt, L., 2005, "Left ventricular hypertophy in hypertension: It's arrhythmogenic potential", *Heart,* vol.91, pp. 250-256.

Kantor, P. F., Robertson, M. A., Coe, J. Y. & Lopaschuk, G. D., 1999, "Volume Overload Hypertrophy of the Newborn Heart Slows the Maturation of Enzymes Involved in the Regulation of Fatty Acid Metabolism", *Journal of the American College of Cardiology,* vol. 33, No. 6, pp. 1724-1734.

Kapur, K., Xing, Y., Ouyang, Z. & Wong, W. H., 2007, "Exon arrays provide accurate assessments of gene expression", *Genome Biology,* vol. 8, R82, pp. 1-8.

Kasikcioglu, E., Oflaz, H., Akhan, H., Kayserilioglu, A., Mercanoglu, F. & Umman, B., 2004, "Left ventricular remodelling and aortic distensibility in elite power athletes", *Heart Vessels*, vol. 19, pp. 183-188.

Kim, E., Goren, A. & Ast, G., 2007, "Insights into the connection between cancer and alternative splicing", *Trends in Genetics,* vol. 24, no. 1, pp. 7-10.

Kinnula, V. L. & Hassinen, I., 1977, "Effect of hypoxia on mitochondrial mass and cytochrome concentrations in rat heart and liver during postnatal development", *Acta Physiologica Scandinavica,* vol. 99, no. 4, pp. 462-466.

Lander, E. S. & Schork, N. J., 1994, "Genetic dissection of complex traits", *Science*, vol. 265, pp. 2037-2048.

Lenga, Y., Koh, A., Perera, A. S., McCulloch, C. A., Sodek, J. & Zohar, R., 2008, "Osteopontin Expression Is Required for Myofibroblast Differentiation", *Circulation Research, vol*. 102, pp 319-327.

Roselló-Lletí, E., Rivera, M., Martínez-Dolz, L., Juanatey, J. R. G., Cortés, R., Jordán, A., Morillas, P., Lauwers, C., Calabuig, J. R., Antorrena, I., de Rivas, B., Manuel Portolés, M. & Bertomeu, V., 2009, "Inflammatory Activation and Left Ventricular Mass in Essential Hypertension", *American Journal of Hypertension* vol. 22, no. 4, pp. 444–450.

Le Goff, C., Somerville, R. P. T., Kesteloot, F., Powell, K., Birk, D. E., Colige, A. C. & Apte, S. S., 2006, "Regulation of procollagen amino-propeptide processing during mouse embryogenesis by specialization of homologous ADAMTS proteases: insights on collagen biosynthesis and dermatosparaxis", *Development & Disease*, vol. 113, pp. 1587-1596.

Levy, D., Garrison, R. J., Savage, D. D., Kannel, W. B. & Castell, W. P., 1990, "Prognostic implications of echocardiographically determined left ventricular mass in the Framingham heart study", *New England Journal of Medicine,* vol. 322, no. 22, pp. 1561-1566.

Li, L., Shigematsu, Y., Hamada, M., & Hiwada, K., 2001, "Relative wall thickness is an independent predictor of left ventricular systolic and diastolic dysfunctions in essential hypertension", *Hypertension Research,* vol. 24, pp. 493-499.

Lifton, R. P., 1996, "Molecular genetics of human blood pressure variation" *Science*, vol. 272, pp. 676–680.

Livak, K. J. & Schmittgen, T. D., 2001, "Analysis of relative gene expression data using real-time quantitative PCR and the 2(-Delta Delta C(T)) Method", *Methods,* vol. 25, no. 4, pp. 402-408.

Longini, I. M., Jr., Higgins, M. W., Hinton, P. C., Moll, P. P. & Keller, J. B., 1984, "Environmental and genetic sources of familial aggregation of blood pressure in Tecumseh, Michigan", *American Journal of Epidemiology*, vol. 120, no. 1, pp. 131-144.

Lopaschuk, G. D., Collins-Nakai, R. L. & Itoi, T., 1992, "Developmental changes in energy substrate use by the heart", *Cardiovascular Research,* vol. 26, no. 12, pp. 1172-1180.

Lynch, K. W. & Maniatis, T., 1996, "Assembly of specific SR protein complexes on distinct regulatory elements of the Drosophila doublesex splicing enhancer", *Genes and Development,* vol. 10, pp. 2089 – 2101.

MacMahon, S., Peto, R., Cutler, J., Collins, R., Sorlie, P., Neaton, J., Abbott, R., Godwin, J., Dyer, A. & Stamler, J., 1990, "Blood pressure, stroke, and coronary heart disease. Part 1, Prolonged differences in blood pressure: prospective observational studies corrected for the regression dilution bias", *The Lancet*, vol. 335, pp. 765–774.

McBride, M. W., Carr, F. J., Graham, D., Anderson, N. H., Clark, J. S., Lee, W. K., Charchar, F. J., Brosnan, M. J. & Dominiczak, A. F., 2003, "Microarray Analysis of Rat Chromosome 2 Congenic Strains", *Hypertension,* vol. 41, pp. 847-853.

Messerli, F. H., Williams, B. & Ritz, E., 2007, "Essential hypertension", *The Lancet,* vol.370, pp. 591-603.

Mickley, L., Jain, P., Miyake, K., Schriml, L. M., Rao, K., Fojo, T., Bates, S., Dean, M., 2001, "An ATP-binding cassette gene (ABCG3) closely related to the multidrug transporter ABCG2 (MXR/ABCP) has an unusual ATP-binding domain", *Mammalian Genome,* vol. 12, pp. 86–88.

Miura, N. & Tanaka, K., 1993, "Analysis of the rat hepatocyte nuclear factor (HNF) 1 gene promoter: synergistic activation by HNF4 and HNF1 proteins", *Nucleic Acids Research,* vol. 21, no. 16, pp. 3731-3736.

Moatti, D., Faure, S., Fumeron, F., Amara, M. E. W., Seknadji, P., McDermott, D. H., Debré, P., Aumont, M. C., Murphy, P. M., de Prost, D. & Combadière, C., 2001, "Polymorphysm in the fraktalkine receptor CX3CR1 as a genetic risk factor for coronary artery disease", *Blood,* vol. 97, pp. 1925–1928.

Modrek, B. & Lee, C., 2002, "A genomic view of alternative splicing", *Nature Genetics,* vol. 30, pp. 13-19.

Moses, M. A. & del Nido, P. J., 2006, "Vascular endothelial growth factor delays onset of failure in pressure-overload hypertrophy through matrix metalloproteinase activation and angiogenesis", *Basic Research in Cardiology*, vol. 101, pp. 204–213.

Mott, R., Talbot, C. J., Turri, M. G., Collins, A. C. & Flint, J., 2000, "A method for fine mapping quantitative trait loci in outbred animal stocks", *Proceedings of the National Academy of Sciences,* vol. 97, pp. 12649–12654.

Murdoch, C. & Finn, A., 2000, "Chemokine receptors and their role in inflammation and infectious diseases", *Blood,* vol. 95, no. 10, pp. 3032-3043.

Murry, C. E., Giachelli, C. M., Schwartz, S. M. & Vracko, R., 1994, "Macrophages express osteopontin during repair of myocardial necrosis", *American Journal of Pathology*, vol. 145, no. 6, pp. 1450–1462.

Nakashima, K., Zhou, X., Kunkel, G., Zhang, Z., Deng, J. M., Behringer, R. R. & de Crombrugghe, B., 2002, "The novel zinc finger-containing transcription factor osterix is required for osteoblast differentiation and bone formation", *Cell,* vol. 108, no. 1, pp. 17–29.

Nian, M., Lee, P., Khaper, N. & Liu, P., 2004, "Inflammatory cytokines and postmyocardial infarction remodeling", *Circulation Research,* vol. 94, pp. 1543–1553.

Nicol, J. W., Helt, G. A., Blanchard, S. G., Raja, A. & Loraine, A. E., 2009, "The Integrated Genome Browser: free software for distribution and exploration of genome-scale datasets", Bioinformatics, vol. 25, no. 20, pp. 2730-2731.

Oh, Y. B., Gao, S., Shah, A., Kim, J. H., Park, W. H., Kim, S. H., 2010, "Endogenous angiotensin II suppresses stretch-induced ANP secretion via AT1 receptor pathway", *Peptides*

Okamoto, K. & Aoki, K. K., 1963, "Development of a strain of spontaneously hypertensive rats", *Japanese Circulation Journal*, vol. 27, pp. 282-293.

Patrick, D. M., Montgomery, R. L., Qi, X., Obad, S., Kauppinen, S.,
Hill, J. A., Rooij, E. V. & Olson, E. N., 2010, "Stress-dependent cardiac remodeling occurs in the absence of microRNA-21 in mice", *The Journal of Clinical Investigation*, vol. 120, no. 11, pp. 3912- 3916.

Paul, M., Mehr A. P., & Kreutz, R., 2006, "Physiology of Local Renin-Angiotensin Systems", *Physiological Reviews*, vol. 86, no. 3, pp. 747-803.

Petretto, E., Mangion, J., Dickens, N. J., Cook, S. A., Kumaran, M. K., Lu, H., Fischer, J., Maatz, H., Kren, V., Pravenec, M., Hubner, N. & Aitman, T. J., 2006, "Heritability and Tissue Specificity of Expression Quantitative Trait Loci", *PLoS Genetics,* vol. 2, no. 10, pp. 1625-1633.

Proulx, C., El-Helou, V., Gosselin, H., Clement, R., Gillis, M., Villeneuve, L. & Calderone, A., 2007, "Antagonism of stromal cell-derived factor-1 reduces infarct size and improves ventricular function after myocardial infarction", *Pflügers Archiv European Journal of Physiology,* vol. 455, pp. 241–250.

Rafestin-Oblin, M. E., Souque, A., Bocchi, B., Pinon, G., Fagart, J., & Vandewalle, A. 2003, "The severe form of hypertension caused by the activating S810L mutation in the mineralocorticoid receptor is cortisone related", *Endocrinology*, vol. 144, no. 2, pp. 528-533.

Rapp, J. P., 2000, "Genetic analysis of inherited hypertension in the rat", *Physiological Reviews*, vol. 80, no. 1, pp. 135-172.

Renault, M. A., Robbesyn, F., Réant, P., Douin, V., Daret, D., Allières, C., Belloc, I., Couffinhal, T., Arnal, J. F., Klingel, K., Desgranges, C., Santos, P. D., Charpentier, F. & Gadeau, A.P, 2010, "Osteopontin Expression in Cardiomyocytes Induces Dilated Cardiomyopathy" *Circulation Heart Failure,* vol. 3, pp. 431-439.

Rich, G. M., Ulick, S., Cook, S., Wang, J. Z., Lifton, R. P. & Dluhy, R. G., 1992, "Glucocorticoid-remediable aldosteronism in a large kindred: clinical spectrum and diagnosis using a characteristic biochemical phenotype", *Annals of Internal Medicine*, vol. 116, no. 10, pp. 813-820.

Ridinger, H., Rutenberg, C., Lutz, D., Buness, A., Petersen, I., Amann, K. & Maercker, C., 2009, "Expression and tissue localization of ß-catenin, α-actinin and chondroitin sulfate proteoglycan 6 is modulated during rat and human left ventricular hypertrophy", *Experimental and Molecular Pathology,* vol. 86, pp. 23–31.

Rocha, R., Martin-Berger,C. L., Yang, P., Scherrer, R., Delyani, J. & McMahon, E., 2002, "Selective Aldosterone Blockade Prevents Angiotensin II/Salt-Induced Vascular Inflammation in the Rat Heart", *Endocrinology,* vol. 143, no. 12, pp. 4828-4836.

Rooij, E. V., Sutherland, L. B., Qi, X., Richardson, J. A., Hill, J. & Olson, E. N., 2007, "Control of Stress-Dependent Cardiac Growth and Gene Expression by a MicroRNA", *Science,* vol. 316. no. 5824, pp. 575 – 579.

Rozen, S. & Skaletsky, H., 2000, "Primer3 on the WWW for general users and for biologist programmers", *Methods in Molecular Biology*, vol. 132, pp. 365-386. Sammeth, M., Foissac, S. & Roderic Guigo, R., 2008, "A General Definition and Nomenclature for Alternative Splicing Events", *PLoS Computational Biology*, vol. 4, Issue 8, pp. 1-14.

Saar, K., Beck, A., Bihoreau, M., Birney, E., Brocklebank, D., Chen, Y., Cuppen, E., Demonchy, S., Dopazo, J., Flicek, P., Foglio, M., Fujiyama, A., Gut, I. G., Gauguier, D., Guigo, R., Guryev, V., Heinig, M., Hummel, O., Jahn, N., Klages, S., Kren, V., Kube, M., Kuhl, H., Kuramoto, T., Kuroki, Y., Lechner, D., Lee, Y., Lopez-Bigas, N., Lathrop, G. M., Mashimo, T., Medina, I., Mott, R., Patone, G., Perrier-Cornet, J., Platzer, M., Pravenec, M., Reinhardt, R., Sakak, Y., Schilhabel, M., Schulz, H., Serikawa, T., Shikhagaie, M., Tatsumoto, S., Taudien, S., Toyoda, A., Voigt, B., Zelenika, D., Zimdahl, H. & Hubner, N., 2008, "SNP and haplotype mapping for genetic analysis in the rat", *Nature Genetics,* vol. 40, pp. 560 – 566.

Scatena, M., Liaw, L. & Giachelli, C. M., 2007, "Osteopontin: A Multifunctional Molecule Regulating Chronic Inflammation and Vascular Disease", *Arteriosclerosis, Thrombosis, and Vascular Biology,* vol. 27, pp. 2302-2309.

Schiffe, L., Kumper, P., Davalos-Misslitz, A. M., Haubitz, M., Haller, H., Anders, H., Witte, T. & Schiffer, M., 2009, "B-cell-attracting chemokine CXCL13 as a marker of disease activity and renal involvement in systemic lupus erythematosus (SLE)", *Nephrology Dialysis Transplantation,* vol. 24, pp. 3708-3712.

Schuster, H., Wienker, T. E., Bahring, S., Bilginturan, N., Toka, H. R., Neitzel, H., Jeschke, E., Toka, O., Gilbert, D., Lowe, A., Ott, J., Haller, H. & Luft, F. C., 1996, "Severe autosomal dominant hypertension and brachydactyly in a unique Turkish kindred maps to human chromosome 12", *Nature Genetics*, vol. 13, no. 1, pp. 98-100.

Seeland, U., Selejan, S., Engelhardt, S., Muller, P., Lohse, M. J. & Bohm, M., 2007, "Interstitial remodeling in beta1-adrenergic receptor transgenic mice", *Basic Research in Cardiology,* vol. 102, pp. 183–193.

Shimkets, R. A., Warnock, D. G., Bositis, C. M., Nelson-Williams, C., Hansson, J. H., Schambelan, M., Gill, J. R.Jr., Ulick, S., Milora, R. V., Findling, J. W., Canessa, C. M., Rossier, B. C. & Lifton, R. P., 1994, "Liddle's Syndrome: Heritable Human Hypertension Caused by Mutations in the ß Subunit of the Epithelial Sodium Channel", *Cell*, Vol. 79, pp. 407-414.

Shimkets, R. A., Lifton, R. P., & Canessa, C. M., 1997, "The Activity of the Epithelial Sodium Channel Is Regulated by Clathrin-mediated Endocytosis", *The journal of biological chemistry,* vol. 272, pp. 25537–25541.

Singh, K., Sirokman, G., Communal, C., Robinson, G., Conrad, C. H., Brooks, W. W., Bing, O. H. L. & Colucci, W. S., 1999, "Myocardial osteopontin expression coincides with the development of heart failure", *Hypertension,* vol. 33, pp. 663-670.

Snyder, P. M., Price, M. P., McDonald, F. J., Adams, C. M., Volk, K. A., Zeiher, B. G., Stokes, J. B. & Welsh, M .J., 1995, "Mechanism by which Liddle's syndrome mutations increase activity of a human epithelial Na^+ channel", *Cell,* vol. 83, pp. 969-976.

Sodhi, C. P., Phadke, S. A., Batlle, D. & Sahai, A., 2001, "Hypoxia and high glucose cause exaggerated mesangial cell growth and collagen synthesis: role of osteopontin", *American Journal of Physiology: Renal Physiology* vol. 280, no. 1, pp. 667–674.

Solberg, L. C., Valdar, W., Gauguier, D., Nunez, G., Taylor, A., Burnett, S., Arboledas-Hita, C., Hernandez-Pliego, P., Davidson, S., Burns, P., Bhattacharya, S., Hough, T., Higgs, D., Klenerman, P., Cookson, W. O., Zhang, Y., Deacon, R. M., Rawlins, J. N. P., Mott, M. & Flint, J., 2006, "A protocol for high-throughput phenotyping, suitable for quantitative trait analysis in mice", *Mammalian Genome,* vol. 17, no. 2, pp. 129–146.

Stewart, P. M., Wallace, A. M., Valentino, R., Burt, D., Shackleton, C. H., & Edwards, C. R., 1987, "Mineralocorticoid activity of liquorice: 11-beta-hydroxysteroid dehydrogenase deficiency comes of age", *Lancet*, vol. 2, no. 8563, pp. 821-824.

Stowasser, M., Gordon, R. D., Tunny, T. J., Klemm, S. A., Finn, W. L. & Krek, A. L., 1992, "Familial hyperaldosteronism type II: five families with a new variety of primary aldosteronism", *Clinical and Experimental Pharmacology and Physiology*, vol. 19, pp. 319-322.

Sutherland, D. J., Ruse, J. L. & Laidlaw, J. C., 1966, "Hypertension, increased aldosterone secretion and low plasma renin activity relieved by dexamethasone", *Canadian Medical Association Journal*, vol. 95, no. 22, pp. 1109-1119.

Takaba, H., Fukudu, K. & Yao, H., 2004, "Substrain differences, Gender, and Age of Spontaneously Hypertensive Rats Critically Determine Infarct Size Produced by Distal Middle Cerebral Artery Occlusion", *Cellular and Molecular Neurobiology,* vol. 24, no. 5, pp. 589-598.

Tesoriero, A. A., Wong, E. M., Jenkins, M. A., Hopper, J. L., kConFab, Brown, M.A., Chevenix-Trench, G., Spurdle, A. B. & Southey, M. C., 2005, "Molecular Characterization and Cancer Risk Associated With BRCA1 and BRCA2 Splice Site Variants Identified in Multiple-Case Breast Cancer Families", *Human Mutation,* vol. 850, pp. 1-13.

Thum, T., Gross, C., Fiedler, J., Fischer, T., Kissler, S., Bussen, M., Galuppo, P., Just, S., Rottbauer, W., Frantz, S., Castoldi, M., Soutschek, J., Koteliansky, V., Rosenwald, A., Basson, M. A., Licht, J. D., Pena, J. T. R.,Rouhanifard, S. H., Muckenthaler, M. U., Tuschl, T., Martin, G. R., Bauersachs, J. & Engelhardt, S., 2008, "MicroRNA-21 contributes to myocardial disease by stimulating MAP kinase signalling in fibroblasts", *Nature Letters,* vol. 456, pp. 980-986.

Tontonoz, P., Hu, E., & Spiegelman, B. M., 1994, "Stimulation of adipogenesis in fibroblasts by PPAR gamma 2, a lipid-activated transcription factor", *Cell*, vol. 79, no. 7, pp. 1147-1156.

Trueblood, N. A., Xie, Z., Communal, C., Sam, F., Ngoy, S., Liaw, L., Jenkins, A. W., Wang, J., Sawyer, D. B., Bing, O. H., Apstein, C. S., Colucci, W. S. & Singh, K., 2001, "Exaggerated Left Ventricular Dilation and Reduced Collagen Deposition After Myocardial Infarction in Mice Lacking Osteopontin", *Circulation Research,* vol. 88, no. 10, pp. 1080-1087.

Valdar, W., Solberg, L. C., Gauguier, D., Burnett, S., Klenerman, P., Cookson, W. O., Taylor, M. S., Rawlins, J. N., Mott, R. & Flint, J., 2006, "Genome-wide genetic association of complex traits in heterogeneous stock mice", *Nature Genetics,* vol. 38, pp. 879–887.

Verdecchia, P., 2000, "Prognostic Value of Ambulatory Blood Pressure : Current Evidence and Clinical implications", *Hypertension,* vol. 35, pp. 844-851.

Vinereanu, D., Florescu, N., Sculthorpe, N., Tweddel, A. C., Stephens, M. R. & Fraser, A.G., 2002, "Left ventricular long-axis diastolic function is augmented in the hearts of endurance-trained compared with strength-trained athletes". *Clinical Science,* vol. 103, pp. 249-257.

Waterston, R. H., Lindblad-Toh, K., Birney, E., Rogers, J., Abril, J. F., Agarwal, P., Agarwala, R., Ainscough, R., Alexandersson, M., An, P., Antonarakis, S. E., Attwood, J., Baertsch, R., Bailey, J., Barlow, K., Beck, S., Berry, E., Birren, B., Bloom, T., Bork, P., Botcherby, M., Bray, N., Brent, M. R., Brown, D. G., Brown, S. D., Bult, C., Burton, J., Butler, J., Campbell, R. D., Carninci, P., Cawley, S., Chiaromonte, F., Chinwalla, A. T., Church, D. M., Clamp, M., Clee, C., Collins, F. S., Cook, L. L., Copley, R. R., Coulson, A., Couronne, O., Cuff, J., Curwen, V., Cutts, T., Daly, M., David, R., Davies, J., Delehaunty, K. D., Deri, J., Dermitzakis, E. T., Dewey, C., Dickens, N. J., Diekhans, M., Dodge, S., Dubchak, I., Dunn, D. M., Eddy, S. R., Elnitski, L., Emes, R. D., Eswara, P., Eyras, E., Felsenfeld, A., Fewell, G. A., Flicek, P., Foley, K., Frankel, W. N., Fulton, L. A., Fulton, R. S., Furey, T. S., Gage, D., Gibbs, R. A., Glusman, G., Gnerre, S.,

Goldman, N., Goodstadt, L., Grafham, D., Graves, T. A., Green, E. D., Gregory, S., Guigó, R., Guyer, M., Hardison, R. C., Haussler, D., Hayashizaki, Y., Hillier, L. W., Hinrichs, A., Hlavina, W., Holzer, T., Hsu, F., Hua, A., Hubbard, T., Hunt, A., Jackson, I., Jaffe, D. B., Johnson, L. S., Jones, M., Jones, T. A., Joy, A., Kamal, M., Karlsson, E. K., Karolchik, D., Kasprzyk, A., Kawai, J., Keibler, E., Kells, C., Kent, W. J., Kirby, A., Kolbe, D. L., Korf, I., Kucherlapati, R. S., Kulbokas, E. J., Kulp, D., Landers, T., Leger, J. P., Leonard, S., Letunic, I., Levine, R., Li, J., Li, M., Lloyd, C., Lucas, S., Ma, B., Maglott, D. R., Mardis, E. R., Matthews, L., Mauceli, E., Mayer, J. H., McCarthy, M., McCombie, W. R., McLaren, S., McLay, K., McPherson, J. D., Meldrim, J., Meredith, B., Mesirov, J. P., Miller, W., Miner, T. L., Mongin, E., Montgomery, K. T., Morgan, M., Mott, R., Mullikin, J. C., Muzny, D. M., Nash, W. E., Nelson, J. O., Nhan, M. N., Nicol, R., Ning, Z., Nusbaum, C., O'Connor, M. J., Okazaki, Y., Oliver, K., Overton-Larty, E., Pachter, L., Parra, G., Pepin, K. H., Peterson, J., Pevzner, P., Plumb, R., Pohl, C. S., Poliakov, A., Ponce, T. C., Ponting, C. P., Potter, S., Quail, M., Reymond, A., Roe, B. A., Roskin, K. M., Rubin, E. M., Rust, A. G., Santos, R., Sapojnikov, V., Schultz, B., Schultz, J., Schwartz, M. S., Schwartz, S., Scott, C., Seaman, S., Searle, S., Sharpe, T., Sheridan, A., Shownkeen, R., Sims, S., Singer, J. B., Slater, G., Smit, A., Smith, D. R., Spencer, B., Stabenau, A., Stange-Thomann, N., Sugnet, C., Suyama, M., Tesler, G., Thompson, J., Torrents, D., Trevaskis, E., Tromp, J., Ucla, C., Ureta-Vidal, A., Vinson, J. P., Von Niederhausern, A. C., Wade, C. M., Wall, M., Weber, R. J., Weiss, R. B., Wendl, M. C., West, A. P., Wetterstrand, K., Wheeler, R., Whelan, S., Wierzbowski, J., Willey, D., Williams, S., Wilson, R. K., Winter, E., Worley, K. C., Wyman, D., Yang, S., Yang, S. P., Zdobnov, E. M., Zody, M. C.& Lander, E. S., 2002, "Initial sequencing and comparative analysis of the mouse genome" *Nature*, vol. 420, pp. 520-562.

Williams, R.R., Hunt, S. C., Hopkins, P. M., Hasstedt, S. J., Wu, L. L. & Lalouel, J. M., 1994, "Tabulations and expectations regarding the genetics of human hypertension", *Kidney International:Supplement*, vol. 44, pp. 57-64.

Wilson, F. H., Disse-Nicodeme, S., Choate, K. A., Ishikawa, K., Nelson-Williams, C., Desitter, I., Gunel, M., Milford, D. V., Lipkin, G. W., Achard, J. M., Feely, M. P., Dussol, B., Berland, Y., Unwin, R. J., Mayan, H., Simon, D. B., Farfel, Z., Jeunemaitre, X., & Lifton, R. P., 2001, "Human hypertension caused by mutations in WNK kinases", *Science*, vol. 293, no. 5532, pp. 1107-1112.

Wilson, F. H., Kahle, K. T., Sabath, E., Lalioti, M. D., Rapson, A. K., Hoover, R. S., Hebert, S. C., Gamba, G. & Lifton, R. P., 2003, "Molecular pathogenesis of inherited hypertension with hyperkalemia: the Na-Cl cotransporter is inhibited by wild-type but not mutant WNK4", *Proceedings of the National Academy of Sciences of the U.S.A*, vol. 100, no. 2, pp. 680-684.

Wilson, F. H., Hariri, A., Farhi, A., Zhao, H., Petersen, K. F., Toka, H. R., Nelson-Williams, C., Raja, K. M., Kashgarian, M., Shulman, G. I., Scheinman, S. J. & Lifton, R. P., 2004, "A cluster of metabolic defects caused by mutation in a mitochondrial tRNA", *Science*, vol. 306, no. 5699, pp. 1190-1194.

Yamori, Y., 1991, "Overview: studies on spontaneous hypertension-development from animal models toward man", *Clinical and Experimental hypertension. Part A, Theory and practice*, vol. 13, no. 5, pp. 631-644.

Young, M. E., Razeghi, P. & Taegtmeyer, H., 2001, "Clock Genes in the Heart: Characterization and Attenuation With Hypertrophy", Circulation Research, vol. 88, pp. 1142-1150.

Yu, Q., Vazquez, R., Khojeini, E. V., Patel, C., Venkataramani, R., Larson, D. F., 2009, "IL-18 induction of osteopontin mediates cardiac fibrosis and diastolic dysfunction in mice", American Journal of Physiology Heart and Circulaotory Physiology, vol. 297, no. 1, pp. 76-85.

Yucha, C. & Guthrie, D., 2003, "Renal homeostasis of calcium", *Nephrology Nursing Journal*, vol. 30, no. 1, pp. 755–764.

Zhang, Q. Y., Dene, H., Deng, A. Y., Garrett, M. R., Jacob, H. J. & Rapp J. P., '1997', "Interval mapping and congenic strains for a blood pressure QTL on rat Chromosome 13", *Mammalian Genome*, vol. 8, pp. 636-641.

Bibliography

Greenhouse, D. D., Festing, M. F. W., Hasan, S. & Cohen, A. L., 1990, “Genetic Monitoring of Inbred Strains of Rats”, pp. 410-480.

Jolliffe, I. T., 2002, “Principal Component Analysis”, Springer Series in Statistics, 2nd ed.